

Cohort-Based Active Modality Acquisition

Tillmann Rheude^{1†}, Roland Eils^{1,2,3,4†}, Benjamin Wild^{1†}

¹Berlin Institute of Health, Charité - Universitätsmedizin Berlin

²Health Data Science Unit, Heidelberg University Hospital and BioQuant

³Intelligent Medicine Institute, Fudan University

⁴Department of Mathematics and Computer Science, Freie Universität Berlin

[†] Corresponding authors

{benjamin.wild, roland.eils, tillmann.rheude}@bih-charite.de

Abstract

Real-world machine learning applications often involve data from multiple modalities that must be integrated effectively to make robust predictions. However, in many practical settings, not all modalities are available for every sample, and acquiring additional modalities can be costly. This raises the question: which samples should be prioritized for additional modality acquisition when resources are limited? While prior work has explored individual-level acquisition strategies and training-time active learning paradigms, test-time and cohort-based acquisition remain underexplored despite their importance in many real-world settings. We introduce Cohort-based Active Modality Acquisition (CAMA), a novel test-time setting to formalize the challenge of selecting which samples should receive additional modalities. We derive acquisition strategies that leverage a combination of generative imputation and discriminative modeling to estimate the expected benefit of acquiring missing modalities based on common evaluation metrics. We also introduce upper-bound heuristics that provide performance ceilings to benchmark acquisition strategies. Experiments on common multimodal datasets demonstrate that our proposed imputation-based strategies can more effectively guide the acquisition of new samples in comparison to those relying solely on unimodal information, entropy guidance, and random selections. Our work provides an effective solution for optimizing modality acquisition at the cohort level, enabling better utilization of resources in constrained settings.¹

1 Introduction

Consider a clinical healthcare setting where all patients in a cohort might undergo a standard, inexpensive set of initial examinations, such as basic blood tests and anamnesis. However, a more advanced, expensive, or invasive procedure, like genomic sequencing or specialized imaging, could offer crucial diagnostic or prognostic information for a subset of these patients [23]. Given a limited budget or capacity for the more advanced procedure, for which patients should these additional resources be strategically allocated to maximize the overall diagnostic yield or improve treatment outcomes across the entire cohort, rather than deciding on a purely individual-case basis? Balancing potential gains from data modalities against the costs and complexities of acquisition is not unique to healthcare. In remote sensing, for instance, decisions must be made regarding which geographical areas warrant costly high-resolution satellite imagery to supplement widely available, lower-resolution data, aiming to optimize regional environmental monitoring under budget constraints. Likewise, in industrial quality assurance, manufacturers could decide which components from a production batch

¹Code will be published on GitHub.

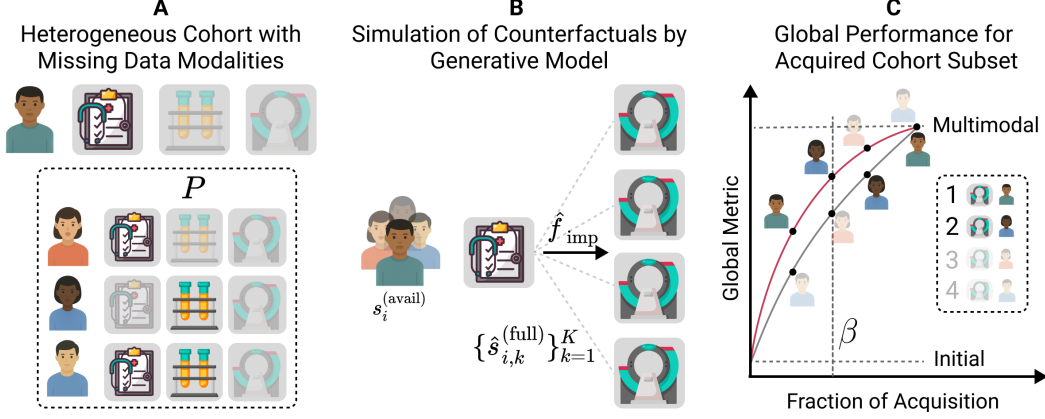


Figure 1: Motivational example for CAMA determining the added value of obtaining the magnetic resonance image (MRI) modality. **(A)** A heterogeneous cohort for which each sample has P distinct modalities. **(B)** Instead of using the initial subset logit scores $s_i^{(avail)}$, a generative model \hat{f}_{imp} imputes one specific missing modality for every patient of the cohort. This leads to full modality logit scores $\{\hat{s}_{i,k}^{(full)}\}_{k=1}^K$. **(C)** An acquisition function (AF) utilizes these scores to rank samples by acquisition priority. The graph demonstrates how the global performance metric improves from the initial baseline towards the performance of a model with access to complete multimodal data, as an increasing fraction of the cohort receives the additional modality. This acquisition process is guided by the proposed strategies operating under the acquisition budget constraint β .

should undergo detailed, time-consuming testing in addition to rapid, standard visual inspections to effectively identify defects at a batch level. This topic of efficient data acquisition has led to several established paradigms in machine learning, such as Active Learning (AL) [22], Active Feature Acquisition (AFA) [50], Active Modality Acquisition (AMA) [28] and multimodal learning with missing data [62]. However, previous research predominantly centers on optimizing acquisition for individual samples or passive patterns of missingness, often not directly addressing test-time budget constraints for an entire cohort. Consequently, the strategic, test-time active acquisition of entire modalities from a cohort perspective is a significant, largely unaddressed gap. This involves deciding, for a given batch of new samples where different subsets of modalities are available, which specific samples should receive an additional, costly modality to best achieve a global objective, *e.g.*, maximizing overall predictive performance or diagnostic accuracy for the cohort, within constraints. We hypothesize that imputation-based Acquisition Functions (AF) can effectively guide resource allocation under cohort-level constraints. The main contributions of this work are as follows:

- We introduce and formalize CAMA - a previously unexplored setting. CAMA addresses the challenge of prioritizing which samples, within a test-time cohort, should undergo additional modality acquisition based on an available subset of modalities.
- We propose a theoretical framework, derived from established evaluation metrics, *e.g.*, Area Under the Receiver Operating Characteristic (AUROC) and Area Under the Precision-Recall Curve (AUPRC), that provides a foundation for developing AFs within the CAMA setting.
- We develop a novel approach for CAMA including a) derivations of AFs by combining generative and discriminative learning and b) the definition of corresponding upper bounds to serve as performance benchmarks.
- We present a comprehensive empirical evaluation of our proposed methods across several multimodal datasets, which vary in their number of modalities and application domains. This includes an analysis of the framework’s key assumptions, boundary conditions, potential performance challenges, and strategies for enhancing robustness.

2 Related Work

In the following, we contextualize our work on CAMA by reviewing key concepts and contributions from several relevant research domains. Given the vast and continually evolving literature in these

areas, this section selectively highlights the work most crucial for understanding the current landscape relevant to our method.

Active Learning (AL) AL traditionally seeks to enhance model training by selecting unlabeled data points for annotation by an oracle [47, 43, 30]. Our methodology draws significantly from AL principles, particularly in the development of an AF to guide the selection process. Consequently, established AL strategies and concepts, such as those rooted in measuring uncertainty [47, 16, 21, 42, 34] or using generative models [56, 67, 66, 34, 40], are central to our work. Existing work on multimodal [45, 7], batch-level [3, 26, 22], or balancing AL [1, 49, 65, 21] is especially relevant to the present work. Our approach, however, diverges from the conventional goals of directly optimizing model training or seeking labels for specific data points. Instead, we aim to identify those samples for which the acquisition of an additional data modality would be most beneficial.

Active Feature Acquisition (AFA) AFA builds upon AL by focusing on selecting the most informative individual features for a given sample, often considering their acquisition costs [41]. Similar to AL approaches, methods for AFA encompass a diverse range of techniques. These include strategies based on measuring uncertainty [21, 4], the use of generative models [31, 32, 14, 64], and Reinforcement Learning (RL) [57, 24, 27, 50, 6]. Other common methodologies involve applying batch-level perspectives [2], leveraging information bottlenecks [38], or employing Kullback-Leibler Divergence (KL-Divergence) [37]. Some AFA techniques rely on calculations of gradients [12], while distinct approaches are manifested as individual, sequential recommender systems [11, 59]. On an application level, even Large Language Models (LLMs), such as Med-PaLM 2 [51], could be employed for AFA, but are explicitly not evaluated in this sense. While sharing the core idea of AFA, our methodology differs significantly: we are not concerned with the selection of individual features, but rather with identifying which entire data modalities to acquire. Furthermore, this decision-making process is applied at the cohort-level, rather than optimizing for individual samples.

Active Modality Acquisition (AMA) AMA can be conceptualized as an extension of AFA, distinguished by its focus on selecting entire data modalities rather than individual features or labels. Prominent related research includes approaches employing RL for multimodal temporal data [28] and methods utilizing submodular optimization in conjunction with Shapley values [48, 18]. However, the former [28] was not evaluated on real-world datasets and differs from our work in its use of RL. The latter [48] primarily investigates the impact of modalities on optimal learning performance. Further studies have explored the use of Gaussian mixtures within Bayesian optimal experimental design, aiming to enhance data acquisition efficiency for model training [33]. This objective differs from ours, as our focus is not on improving the model training process itself, but rather on optimizing performance for a downstream task at test-time. The relative sparsity of existing work for AMA underscores the significance of the research gap that our proposed setting, *i.e.*, CAMA, aims to address.

Multimodal Learning with Missing Data Modalities Research in multimodal learning with missing data modalities offers techniques for robustly handling incomplete datasets. These methods are broadly classified into strategy design aspects, *i.e.*, architecture focus and model combinations, and data processing aspects, *i.e.*, representation focus and modality imputation [62]. Acknowledging the utility of all these approaches, our work emphasizes imputation-based strategies, and thus, this paragraph focuses on these methods. Imputation of missing features is commonly performed using Auto Encoders (AEs) [19], Variational Auto Encoders (VAEs) [25], Generative Adversarial Networks (GANs) [15], or Denoising Diffusion Probabilistic Models (DDPMs) [20, 44]. These methods are naturally extended to multiple modalities, for example, with VAE- [61, 54, 29] and DDPM-based [60] approaches. Notably, the latter, *i.e.*, *IMDer* [60], a multimodal deep learning architecture that imputes missing values with DDPMs in latent spaces, is adapted in our work (section 5). However, this research area does not concern itself with acquiring modalities but only with imputing them.

3 Problem Formulation

Let $\mathcal{D} = \{(\mathbf{x}_i, y_i)\}_{i=1}^N$ be a dataset of N samples, where \mathbf{x}_i denotes the complete set of multimodal features for sample i , and $y_i \in \{0, 1\}$ is the label. We consider two primary settings: first, a simpler scenario involving two modalities, and second, a more generalized multimodal setting.

3.1 Two-Modality Setting

Each sample i is associated with data from two modalities: $\mathbf{x}_i^{(\text{base})}$, the baseline modality that is always observed, and $\mathbf{x}_i^{(\text{add})}$, the additional modality that may be acquired. The baseline modality is assumed to be inexpensive or readily available, while the additional modality might involve higher costs or a more complex acquisition process with global constraints. We assume the existence of two pre-trained models: f_{base} , for the baseline modality, and f_{full} , for both modalities. Let their parameters be denoted by θ_{base} and θ_{full} , respectively. These models compute logit scores s_i^{model} for sample i :

$$s_i^{(\text{base})} = f_{\text{base}}(\mathbf{x}_i^{(\text{base})}, \theta_{\text{base}}) \quad (1)$$

$$s_i^{(\text{full})} = f_{\text{full}}(\mathbf{x}_i^{(\text{base})}, \mathbf{x}_i^{(\text{add})}, \theta_{\text{full}}) \quad (2)$$

The value of $s_i^{(\text{full})}$ is unknown prior to acquiring $\mathbf{x}_i^{(\text{add})}$ and can be conceptualized as an oracle score. The corresponding class probabilities are obtained by applying the sigmoid function. To inform AFs without actually acquiring $\mathbf{x}_i^{(\text{add})}$, we seek to estimate the potential outcome $s_i^{(\text{full})}$. We introduce an imputation model, \hat{f}_{imp} , parameterized by θ_{imp} . This model is designed to approximate the conditional distribution $p(s_i^{(\text{full})} | \mathbf{x}_i^{(\text{base})})$. Specifically, \hat{f}_{imp} takes $\mathbf{x}_i^{(\text{base})}$ as input and generates a set of K plausible logit scores, $\{\hat{s}_{i,k}^{(\text{full})}\}_{k=1}^K$. Each $\hat{s}_{i,k}^{(\text{full})}$ represents a simulated logit score, as if the full set of modalities (including $\mathbf{x}_i^{(\text{add})}$) were available and processed by f_{full} . The imputed probabilities are $\{\hat{p}_{i,k}^{(\text{full})}\}_{k=1}^K$, with $\hat{p}_{i,k}^{(\text{full})} = \sigma(\hat{s}_{i,k}^{(\text{full})})$.

3.2 Generalized Multi-Modality Setting

Extending the two-modality setting, we consider a universe of P distinct modalities, denoted $\mathcal{U} = \{M_0, M_1, \dots, M_{P-1}\}$. For each sample i , a subset of these modalities, $\mathcal{M}_i^{(\text{avail})} \subset \mathcal{U}$, is available at the outset. Modalities in $\mathcal{M}_i^{(\text{avail})}$ are generally easier or cheaper to acquire compared to those in the remaining set $\mathcal{U} \setminus \mathcal{M}_i^{(\text{avail})}$. We denote the features corresponding to the available modalities for sample i as $\mathbf{x}_i^{(\mathcal{M}_i^{(\text{avail})})}$, while \mathbf{x}_i represents the complete set of features for all P modalities for sample i . Our setting is designed to be general, assuming the capability to process any subset of modalities $\mathcal{M} \subseteq \mathcal{U}$. Thus, for a given sample i and any subset \mathcal{M} of its available modalities, a corresponding model $f^{(\mathcal{M})}$, parameterized by $\theta^{(\mathcal{M})}$, can process the features $\mathbf{x}_i^{(\mathcal{M})}$ to compute a logit score $s_i^{(\mathcal{M})}$. This generality is crucial because when multiple modalities are missing for sample i , *i.e.*, the set $\mathcal{M}_i^{(\text{miss})} = \mathcal{U} \setminus \mathcal{M}_i^{(\text{avail})}$ is non-empty and potentially large, an acquisition decision within CAMA might involve obtaining only a specific chosen subset $\mathcal{M}_{\text{acq}} \subseteq \mathcal{M}_i^{(\text{miss})}$ of missing modalities, rather than all of them. Upon such a partial acquisition, the sample i transitions to an updated modality set $\mathcal{M}'_i = \mathcal{M}_i^{(\text{avail})} \cup \mathcal{M}_{\text{acq}}$, and its new score would be $s_i^{(\mathcal{M}'_i)} = f^{(\mathcal{M}'_i)}(\mathbf{x}_i^{(\mathcal{M}'_i)}, \theta^{(\mathcal{M}'_i)})$. We rely on a single, adaptable core model architecture, denoted f , which utilizes a set of parameters θ regardless of the input modality combination. This model is designed to process inputs comprising any subset of the available modalities. The logit score from the initially available modalities, $s_i^{(\text{avail})}$, for a sample i is computed when the model f processes the specific available modality subset $\mathbf{x}_i^{(\mathcal{M}_i^{(\text{avail})})}$:

$$s_i^{(\text{avail})} = f(\mathbf{x}_i^{(\mathcal{M}_i^{(\text{avail})})}, \theta) \quad (3)$$

Similarly, the oracle score, $s_i^{(\text{full})}$, is obtained when the same model f with the same parameters θ utilizes the complete set of P modalities:

$$s_i^{(\text{full})} = f(\mathbf{x}_i, \theta) \quad (4)$$

The score $s_i^{(\text{full})}$ represents the optimal outcome if all P modalities were acquired and is unknown beforehand for samples where $\mathcal{M}_i^{(\text{avail})} \neq \mathcal{U}$. The objective is to strategically acquire modalities from $\mathcal{U} \setminus \mathcal{M}_i^{(\text{avail})}$ for selected samples to enable predictions that approximate the performance achievable with f_{full} . Notably, the scope of the current work is focused on the acquisition of a single, pre-selected modality, simplifying the initial exploration of the task. Again, we employ a generative imputation model, \hat{f}_{imp} , parameterized by θ_{imp} . This model takes the available features $\mathbf{x}_i^{(\mathcal{M}_i^{(\text{avail})})}$ as input and

approximates the conditional distribution $p(s_i^{(\text{full})} | \mathbf{x}_i^{(\mathcal{M}_i^{(\text{avail})})})$. Specifically, \hat{f}_{imp} generates a set of K plausible logit scores, $\{s_{i,k}^{(\text{full})}\}_{k=1}^K$, thereby simulating the oracle score $s_i^{(\text{full})}$ using only the available information. The corresponding imputed probabilities are $\{\hat{p}_{i,k}^{(\text{full})}\}_{k=1}^K$, where $\hat{p}_{i,k}^{(\text{full})} = \sigma(s_{i,k}^{(\text{full})})$. For consistency in defining AFs, we adopt the following unified notation:

- $s_i^{(\text{avail})}$: The logit score derived from the initially available modality or modalities for sample i . This corresponds to $s_i^{(\text{base})}$ in the two-modality setting.
- $s_i^{(\text{full})}$: The true or "oracle" logit score if all relevant modalities are acquired for sample i (where "all relevant" signifies the two modalities in the first setting, or all P modalities in the generalized setting).
- $\{s_{i,k}^{(\text{full})}\}_{k=1}^K$: The set of K imputed logit scores that simulate $s_i^{(\text{full})}$, generated based on the information available for computing $s_i^{(\text{avail})}$.

The probabilities are denoted $p_i^{(\text{avail})}$, $p_i^{(\text{full})}$, and $\{\hat{p}_{i,k}^{(\text{full})}\}_{k=1}^K$, respectively.

3.3 Acquisition and Optimization

An AF selects a subset of samples \mathcal{S} from a cohort of N total samples. This subset $\mathcal{S} \subseteq \{1, \dots, N\}$ has a predetermined size $|\mathcal{S}| = M$, where M is the acquisition budget, *i.e.*, the number of samples for whom additional modalities will be acquired. The final logit $\hat{s}_i(\mathcal{S})$ used for the evaluation of a sample i is then determined by the selection:

$$\hat{s}_i(\mathcal{S}) = \begin{cases} s_i^{(\text{full})} & \text{if } i \in \mathcal{S} \\ s_i^{(\text{avail})} & \text{if } i \notin \mathcal{S} \end{cases} \quad (5)$$

The optimization problem is to find the set \mathcal{S}^* that maximizes a chosen performance metric:

$$\mathcal{S}^* = \arg \max_{\mathcal{S} \subseteq \{1, \dots, N\}: |\mathcal{S}|=M} \text{Metric}(\mathbf{y}, \hat{\mathbf{s}}(\mathcal{S})) \quad (6)$$

where $\mathbf{y} = \{y_i\}_{i=1}^N$ are the true labels, and $\hat{\mathbf{s}}(\mathcal{S}) = \{\hat{s}_i(\mathcal{S})\}_{i=1}^N$ is the vector of resulting logits for all samples in the cohort. Consequently, the task is to identify an optimal, constrained subset for which to acquire additional modalities, while maximizing a performance metric across the entire cohort.

4 Optimizing Metrics and Acquisition Function Strategies

Directly solving the cohort-level optimization problem to identify the optimal sample set \mathcal{S}^* is computationally intractable for large-scale cohorts and budget sizes due to its combinatorial nature. The AFs developed in this work are derived from, and evaluated against, standard metrics of discriminative performance, *i.e.*, AUROC and AUPRC (Appendix B.1).

Normalized Area of Gain We introduce a metric, describing the cumulative performance of an AF, normalized by the total possible gain achievable by transitioning all samples to full multimodal performance. Let $M_{\text{strat}}(f)$ be the performance curve of an AF strategy for a primary metric M with the fraction of the acquisition budget f , M_{uni} be the performance of the unimodal baseline, and M_{multi} the performance of the full multimodal model. The normalized area of gain for the acquisition function AF is

$$G_{\text{full}}^M(\text{AF}) = \frac{\int_0^1 (M_{\text{AF}}(f) - M_{\text{uni}}) df}{M_{\text{multi}} - M_{\text{uni}}}. \quad (7)$$

A higher G_{full}^M indicates capturing a large portion of the achievable performance gain across different acquisition budgets.

Cohort-level Acquisition Function Strategies Our goal is to maximize global metrics for a cohort by strategically selecting samples for modality acquisition. Since direct cohort-level optimization is typically intractable, we employ heuristic AFs selected/adopted from the literature (Section 2) to approximate optimal selection. These strategies are explained in more detail in Appendix B and can be categorized as:

- **Oracle Strategies:** As upper-bound benchmarks, they assume perfect knowledge of outcomes and true labels to greedily select samples yielding the largest immediate gain in the target metric. They are metric-dependent, *i.e.*, there is an AUROC and AUPRC oracle.
- **Upper-Bound Heuristic Strategies:** These heuristics assume knowledge of logit scores under modality completion but are label-agnostic, relying instead on metrics like the true uncertainty reduction, rank change, or KL-Divergence to guide the selection.
- **Baseline Information Strategies:** These AFs make decisions using only baseline information, *i.e.*, from the initially available modality, *e.g.*, maximum unimodal uncertainty or probability.
- **Imputation-Based Strategies:** These strategies are grounded in counterfactual reasoning, addressing the question: How might a sample’s predictive outcome change if a currently missing modality was to be acquired? To explore this, our model architecture facilitates the generation of multiple predicted logit scores under modality completion through imputation of the missing modality, conditioned on all currently available information for that sample.

5 Evaluation

Model Architecture We use an end-to-end late fusion architecture combined with DDPMs operating between latent spaces [60], as illustrated in Figure 2. We employ domain-specific encoders to process the respective modalities: for language inputs, we use a pre-trained BERT model [9], for vision, a Vision Transformer (ViT) [10]. Other data types, *e.g.*, temporal sequences, tabular data, or pre-extracted embeddings, are handled by Transformer encoders [58]. The key architectural design decisions are: a) applying Layer Normalization [5] at the end of each modality’s encoder to stabilize the DDPMs operating between latent spaces, b) calibrating the model with Label Smoothing [55] to produce less overconfident and better-calibrated probability distributions, c) implementing the score models as Diffusion Transformers (DiTs) [39] for improved resource efficiency, and d) employing a Transformer encoder as the final fusion model, as empirical evaluations indicated that more complex fusion architectures did not yield significant performance improvements.

Another key decision involves the handling of missing data modalities. In contrast to previous work [60], we do not pre-train the model on all available data modalities. To control data modality leakage during training, we use a pre-defined, seed-dependent missing modality mask. Unlike batch-dependent masks, which eventually reveal all modalities for every sample across numerous epochs, our static approach ensures that specific modalities remain consistently unavailable for designated samples throughout the entire training process. For designing a classification head that is robust to missing data modalities during validation, we employ two main techniques: missing values are handled by attention masking, and crucially, imputed values from the DDPMs are not passed to the classification head during the training process (represented by dotted lines in Figure 2). For model training, we use the ScheduleFree optimizer [8] across all datasets, determining the model and optimizer hyperparameters through sweeps (Appendix C). The final loss function is defined as $\mathcal{L} = \lambda_1 \cdot \mathcal{L}_{CE} + \sum_{i=1}^P \lambda_2 \cdot \mathcal{L}_{D_i}$, where \mathcal{L}_{CE} denotes the classification loss, \mathcal{L}_{D_i} denotes the DDPM losses, P is the total number of modalities, and λ_i represents the corresponding loss weightings. We find that setting $\lambda_1 = 1.0$ is important for performance on the downstream task.

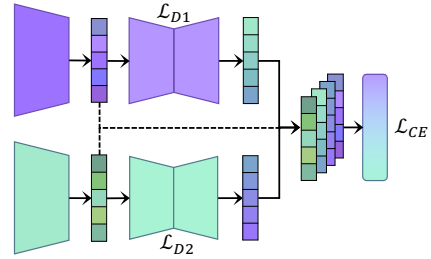


Figure 2: Bi-modal architecture. DDPMs generate the missing embedding(s) for inference only.

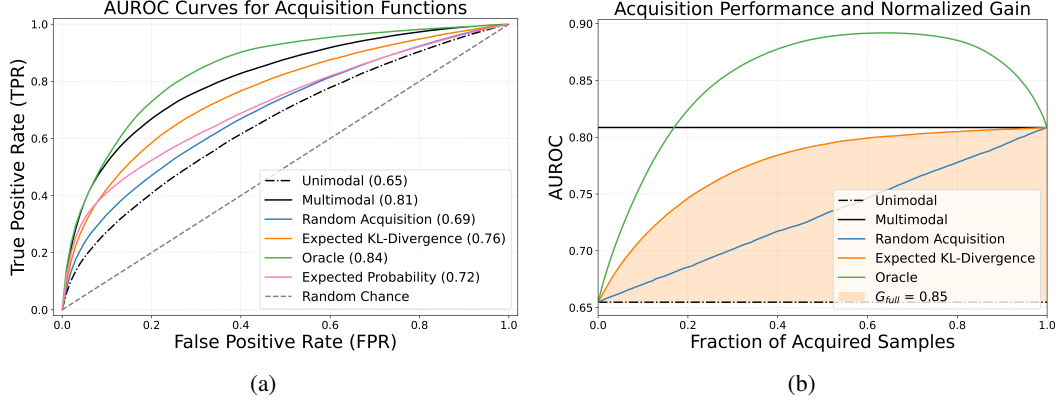


Figure 3: **(a)** AUROC curves for several AFs on the MOSEI dataset [63] at 25% budget. **(b)** Acquisition performance of the best-performing AF from (a) visualizing the gain of the AF during the progressive acquisition of modalities, transitioning the cohort from unimodal states towards full multimodality. Intriguingly, the oracle AF can exceed the full multimodal cohort’s AUROC at certain fractions of acquired modalities, before subsequently declining towards it again.

Datasets We evaluate our methods on three well-known real-world multimodal datasets across different domains. For healthcare applications, MIMIC Symile [46] and MIMIC HAIM [52, 53] are implemented [13].² While the latter contains more samples, it only contains two modalities (results in Appendix F). For emotion recognition, MOSEI [63] is used.³ We design the datasets for binary classification, resulting in ten binary targets for the MIMIC datasets and one binary target for MOSEI. While MOSEI is already class-balanced [63], HAIM and Symile exhibit significant class imbalance [52, 63]. To address this, we employ random oversampling in the training step to tackle this. We find this preprocessing essential to ensure the AFs operate effectively. Importantly, during testing, we retain the original imbalanced distributions.

Model and AF Evaluation For the datasets based on three modalities, we apply five-fold cross validation for the model and downstream evaluations. Due to initial, noisy results for MIMIC HAIM, *i.e.*, the two-modality based dataset, we increased the number of folds for this dataset to ten. Within each cross-validation fold, the predictive model is trained incorporating missing modalities as described above. This approach ensures robust target prediction by the model, even when faced with the complete absence of any modality [36]. Furthermore, a significant advantage is the ability to use a single model across all combinations of available data modalities per fold, thereby obviating the need for multiple models per fold and mitigating potential calibration inconsistencies that could arise from their use. For each sample in the test set, its initial score is established. For the generalized setting, the score is determined based on randomly assigned available modalities, repeated over several runs for robustness. Each AF then calculates scores for test samples using their respective scores and the imputed scores, ranking the samples by priority. We simulate the acquisition by incrementally increasing the budget M . For the splits, we exclude endpoints where the unimodal performance exceeds the multimodal one preventing negative gains. For each budget, the top M ranked samples are considered acquired, and their logits are updated from the initial state to the full-modality state. We report G_{full} for comparisons. Final reported results are aggregated across all cross-validation splits, combinations of missing and available modalities, and random runs to ensure reliable conclusions.

Results Our empirical evaluation demonstrates the efficacy of the proposed CAMA framework. The key results are aggregated in Tables 1 and 2 by averaging over permutations of missing input modalities and multiple random instantiations for each missingness configuration. We benchmarked imputation-based strategies against several baselines: random acquisition, strategies using only unimodal information, label-agnostic upper-bound heuristics, and metric-specific oracles. Oracle strategies, possessing perfect knowledge of true labels and acquisition outcomes, consistently achieve the highest performance. Serving as a theoretical upper bound for a greedy acquisition approach, they

²PhysioNet Credentialed Health Data License 1.5.0

³MIT License

Table 1: Acquisition performance on Symile - results for AUROC/AUPRC. AFs are sorted by their mean. Oracles ‡, upper-bound heuristics † and baselines j. Details in Appendix E.

Strategy	Acquisitions by AUROC, $G_{\text{full}} \uparrow \pm \text{SEM}$			Strategy	Acquisitions by AUPRC, $G_{\text{full}} \uparrow \pm \text{SEM}$		
	Cardiomegaly	Pneumothorax	Mean		Lung Lesion	Pneumothorax	Mean
AUROC ‡	2.787 \pm 0.139	9.461 \pm 1.049	4.580	AUPRC ‡	2.520 \pm 0.250	10.623 \pm 0.708	4.231
KL-Div. †	0.885 \pm 0.011	0.910 \pm 0.054	0.883	KL-Div. †	0.828 \pm 0.073	0.827 \pm 0.043	0.871
KL-Div.	0.747 \pm 0.039	0.773 \pm 0.134	0.833	KL-Div.	0.896 \pm 0.146	0.581 \pm 0.084	0.777
Rank †	0.878 \pm 0.019	0.605 \pm 0.053	0.811	Rank †	0.676 \pm 0.088	0.483 \pm 0.075	0.776
Uncert. †	0.524 \pm 0.025	-0.136 \pm 0.065	0.481	Prob. j	0.756 \pm 0.136	0.811 \pm 0.041	0.550
Uncert. j	0.480 \pm 0.013	0.536 \pm 0.040	0.480	Uncert. †	0.181 \pm 0.067	0.293 \pm 0.052	0.450
Prob. j	0.431 \pm 0.015	0.536 \pm 0.040	0.458	Prob.	0.320 \pm 0.104	0.965 \pm 0.027	0.449
Uncert.	0.450 \pm 0.041	0.055 \pm 0.060	0.440	Uncert.	0.130 \pm 0.053	0.513 \pm 0.066	0.444
Prob.	0.350 \pm 0.053	0.898 \pm 0.061	0.426	Uncert. j	0.215 \pm 0.033	0.811 \pm 0.041	0.443
Rank	0.378 \pm 0.016	0.115 \pm 0.082	0.378	Rank	0.564 \pm 0.086	0.396 \pm 0.054	0.407
Random	0.385 \pm 0.015	0.327 \pm 0.061	0.376	Random	0.503 \pm 0.103	0.527 \pm 0.053	0.388

Table 2: Acquisition performance on MOSEI - results for AUROC/AUPRC. AFs are sorted by their mean. Oracles ‡, upper-bound heuristics † and baselines j. Details in Appendix D.

Acquisitions by AUROC		Acquisitions by AUPRC	
Strategy	$G_{\text{full}} \uparrow \pm \text{SEM}$	Strategy	$G_{\text{full}} \uparrow \pm \text{SEM}$
AUROC ‡	1.478 ± 0.091	AUPRC ‡	1.666 ± 0.161
KL-Divergence †	0.882 ± 0.006	KL-Divergence	0.889 ± 0.052
KL-Divergence	0.855 ± 0.034	Prob.	0.846 ± 0.070
Rank †	0.849 ± 0.008	KL-Divergence †	0.838 ± 0.006
Prob.	0.707 ± 0.037	Rank †	0.806 ± 0.010
Uncert. †	0.663 ± 0.006	Uncert. †	0.708 ± 0.005
Uncert.	0.630 ± 0.015	Uncert.	0.706 ± 0.037
Uncert. j	0.525 ± 0.005	Prob. j	0.543 ± 0.009
Random	0.490 ± 0.004	Uncert. j	0.540 ± 0.006
Prob. j	0.433 ± 0.007	Random	0.525 ± 0.003
Rank	0.432 ± 0.014	Rank	0.457 ± 0.019

are inherently metric-specific, consequently achieving the highest area of gain for the relevant metric. Surprisingly, the global discriminative performance for a mix of baseline and multimodal predictions can sometimes exceed that of a model using only multimodal data. Consequently, performance gains from AFs can exceed the value of one. We employed upper-bound heuristic strategies to benchmark the acquisition logic itself, independent of imputation noise from AFs that approximate the conditional distribution $p(s_i^{(\text{full})} | x_i^{(\mathcal{M}_i^{(\text{avail})})})$. These heuristics are label-agnostic, but access true logit scores post-acquisition, *i.e.*, if a modality was acquired. Among these, strategies based on KL-Divergence (measuring the true per-sample shift from baseline to multimodal distributions) and rank change (evaluating true cohort-level change in sample ranking) demonstrated strong performance. This indicates that prioritizing samples with large expected predictive shifts or significant cohort reordering are effective heuristics for CAMA. Among the imputation-based strategies, which leverage a generative model for counterfactual outcomes ($\{\hat{s}_{i,k}^{(\text{full})}\}_{k=1}^K$), the AF based on expected KL-Divergence consistently and significantly outperformed other imputation methods and simpler baselines like random or baseline uncertainty/probability. Notably, its performance sometimes surpassed certain upper-bound heuristics that use true, *i.e.*, non-imputed, post-acquisition logit scores. This AF effectively identifies samples where acquiring a new modality is predicted via imputation to cause the largest shift in the class probability distribution. Figure 3 (a) illustrates its superiority over unimodal and random baselines at a 25% acquisition budget, and (b) shows it capturing a substantial portion of achievable oracle performance improvement early in the acquisition process. In contrast, while the rank change upper-bound heuristic performed well, its imputation-based counterpart (expected rank change) was considerably weaker. Similarly, AFs based on imputed unimodal uncertainty or expected probability generally underperformed the expected KL-Divergence strategy, suggesting that merely predicting high confidence or uncertainty post-imputation is less effective than quantifying the expected change in predictions. Across different datasets, the relative performance ranking of AFs by gain remained largely consistent, with low SEMs attesting to stability and suggesting the core principles hold in diverse contexts. However, endpoint-specific results on Symile revealed large performance ranges for oracle AFs and some upper-bound heuristics, *e.g.*, rank change- or uncertainty-based AFs. The KL-Divergence-based AF offered a more aligned solution to this variability. Taken together, we

demonstrate the complex landscape of CAMA and affirm the superiority of the imputation-based KL-Divergence strategy for achieving substantial and reliable gains over simpler baselines and several heuristics (additional results in Appendices D to F).

6 Discussion and Conclusion

We introduce CAMA, a novel framework addressing the real-world challenge of optimizing global discriminative performance through strategic test-time acquisition of additional modalities under resource constraints. Motivated by scenarios where obtaining comprehensive multimodal data for every sample is often impractical due to cost, invasiveness, or logistical limitations, CAMA provides an approach to maximizing predictive accuracy across an entire cohort. Our evaluation across multiple multimodal datasets confirms our central hypothesis: Imputation-based AFs can effectively guide resource allocation under cohort-level constraints. The strong performance of imputation-based strategies, especially the KL-Divergence AF, relative to unimodal baselines, random selection, and even some upper-bound heuristics, underscores the effectiveness of counterfactual reasoning. By simulating the potential impact of acquiring a missing modality using existing information, CAMA prioritizes samples where additional data is likely to change predictions. The behavior of oracles, particularly their ability to yield performance exceeding that of a model using complete multimodal data for all samples (Figure 3 (b)), highlights a key aspect of CAMA. This counterintuitive result suggests that an underlying predictive model can achieve better global performance with a strategic curation of samples, some with baseline modalities, others selectively enhanced, rather than uniformly applying all modalities across the cohort. This phenomenon likely occurs because additional modalities may introduce variance, redundancy, or conflicting information that imperfect models cannot optimally reconcile. The oracles circumvent this by selecting only augmentations beneficial to the global metric, allowing a heterogeneous mix of unimodal and multimodal samples to outperform a multimodal dataset. To our surprise, in the MOSEI dataset, the imputation-based KL-Divergence AF was also able to outperform the corresponding Upper-Bound Heuristic that has perfect knowledge of full multimodal data. Conversely, the substantial performance gap between the rank change heuristic and its imputation-based counterpart suggests that global, rank-based metrics may be particularly vulnerable to imputation noise. This highlights that the specific mechanism for deriving utility from imputations is critical for the performance of the AFs. While the KL-Divergence AF demonstrated strong performance, it is important to note that not all imputation-based AFs consistently outperformed simpler strategies across all datasets or endpoints, for instance, those based on expected probabilities or uncertainties often underperformed. This variability, also observed in endpoint-specific analyses, suggests that optimal CAMA strategies can be context-dependent. Crucially, these observations underscore that the specific mechanism for deriving utility from imputations, rather than merely the act of imputation itself, is critical to the performance of the AFs. Despite such context-dependencies, the generally consistent relative ordering of AFs across diverse datasets (with KL-Divergence often leading) and low variance in overall results lend confidence to the robustness of our core findings. The demonstrated ability of the imputation-based KL-Divergence AF to achieve reliable gains by effectively identifying samples where an additional modality is predicted to cause the largest shift in class probability distributions makes this approach particularly valuable. In settings such as healthcare, strategic allocation of costly or invasive diagnostic procedures is essential, and our approach offers a promising direction for these applications. Several avenues for future research emerge from this work. Extending CAMA beyond binary classification to multi-class problems, regression tasks, or more complex prediction scenarios represents a natural progression. Architectural exploration, such as investigating modular two-stage approaches or alternative imputation techniques, *e.g.*, VAEs, could reveal different performance trade-offs. Developing more sophisticated global strategies that directly optimize cohort-level metrics, rather than aggregating individual sample scores, warrants investigation. Recent insights into the relationship between evaluation metrics like AUROC/AUPRC and class imbalance [35], which we found relevant for the effectiveness of AFs, could further refine the AFs. Perhaps most significantly, future work could move beyond selecting which samples should receive a pre-selected modality to dynamically determining which specific modality, from a set of available options, should be acquired for each sample, enabling more granular and resource-efficient approaches at the cohort level.

Acknowledgement We would like to thank Stefan Hegselmann and Lucas Arnoldt for the supportive and insightful discussions throughout the research and development process. The authors

acknowledge the Scientific Computing of the IT Division at the Charité - Universitätsmedizin Berlin for providing computational resources that have contributed to the research results reported in this paper.

References

- [1] Umang Aggarwal, Adrian Popescu, and Céline Hudelot. Active Learning for Imbalanced Datasets. In *IEEE Winter Conference on Applications of Computer Vision, WACV 2020, Snowmass Village, CO, USA, March 1-5, 2020*, pages 1417–1426. IEEE, 2020.
- [2] Vedang Asgaonkar, Aditya Jain, and Abir De. Generator Assisted Mixture of Experts for Feature Acquisition in Batch. In Michael J. Wooldridge, Jennifer G. Dy, and Sriraam Natarajan, editors, *Thirty-Eighth AAAI Conference on Artificial Intelligence, AAAI 2024, Thirty-Sixth Conference on Innovative Applications of Artificial Intelligence, IAAI 2024, Fourteenth Symposium on Educational Advances in Artificial Intelligence, EAAI 2024, February 20-27, 2024, Vancouver, Canada*, pages 10927–10934. AAAI Press, 2024.
- [3] Jordan T. Ash, Chicheng Zhang, Akshay Krishnamurthy, John Langford, and Alekh Agarwal. Deep Batch Active Learning by Diverse, Uncertain Gradient Lower Bounds. In *8th International Conference on Learning Representations, ICLR 2020, Addis Ababa, Ethiopia, April 26-30, 2020*. OpenReview.net, 2020.
- [4] Nicolás Astorga, Tennison Liu, Nabeel Seedat, and Mihaela van der Schaar. Active Learning with LLMs for Partially Observed and Cost-Aware Scenarios. In Amir Globersons, Lester Mackey, Danielle Belgrave, Angela Fan, Ulrich Paquet, Jakub M. Tomczak, and Cheng Zhang, editors, *Advances in Neural Information Processing Systems 38: Annual Conference on Neural Information Processing Systems 2024, NeurIPS 2024, Vancouver, BC, Canada, December 10 - 15, 2024*, 2024.
- [5] Jimmy Lei Ba, Jamie Ryan Kiros, and Geoffrey E. Hinton. Layer Normalization, July 2016. arXiv:1607.06450 [stat].
- [6] Hilmy Baja, Michiel Kallenberg, and Ioannis N. Athanasiadis. To Measure or Not: A Cost-Sensitive, Selective Measuring Environment for Agricultural Management Decisions with Reinforcement Learning, January 2025. arXiv:2501.12823 [cs].
- [7] Gyanendra Das, Xavier Thomas, Anant Raj, and Vikram Gupta. MAViC: Multimodal Active Learning for Video Captioning, December 2022. arXiv:2212.11109 [cs].
- [8] Aaron Defazio, Xingyu Yang, Ahmed Khaled, Konstantin Mishchenko, Harsh Mehta, and Ashok Cutkosky. The Road Less Scheduled. In Amir Globersons, Lester Mackey, Danielle Belgrave, Angela Fan, Ulrich Paquet, Jakub M. Tomczak, and Cheng Zhang, editors, *Advances in Neural Information Processing Systems 38: Annual Conference on Neural Information Processing Systems 2024, NeurIPS 2024, Vancouver, BC, Canada, December 10 - 15, 2024*, 2024.
- [9] Jacob Devlin, Ming-Wei Chang, Kenton Lee, and Kristina Toutanova. BERT: Pre-training of Deep Bidirectional Transformers for Language Understanding. In Jill Burstein, Christy Doran, and Thamar Solorio, editors, *Proceedings of the 2019 Conference of the North American Chapter of the Association for Computational Linguistics: Human Language Technologies, NAACL-HLT 2019, Minneapolis, MN, USA, June 2-7, 2019, Volume 1 (Long and Short Papers)*, pages 4171–4186. Association for Computational Linguistics, 2019.
- [10] Alexey Dosovitskiy, Lucas Beyer, Alexander Kolesnikov, Dirk Weissenborn, Xiaohua Zhai, Thomas Unterthiner, Mostafa Dehghani, Matthias Minderer, Georg Heigold, Sylvain Gelly, Jakob Uszkoreit, and Neil Houlsby. An Image is Worth 16x16 Words: Transformers for Image Recognition at Scale. *9th International Conference on Learning Representations, ICLR 2021*, 2021.
- [11] Jan Freyberg, Abhijit Guha Roy, Terry Spitz, Beverly Freeman, Mike Schaekermann, Patricia Strachan, Eva Schnider, Renee Wong, Dale R. Webster, Alan Karthikesalingam, Yun Liu, Krishnamurthy Dvijotham, and Umesh Telang. MINT: A wrapper to make multi-modal and multi-image AI models interactive, January 2024. arXiv:2401.12032 [cs].

- [12] Aritra Ghosh and Andrew S. Lan. DiFA: Differentiable Feature Acquisition. In Brian Williams, Yiling Chen, and Jennifer Neville, editors, *Thirty-Seventh AAAI Conference on Artificial Intelligence, AAAI 2023, Thirty-Fifth Conference on Innovative Applications of Artificial Intelligence, IAAI 2023, Thirteenth Symposium on Educational Advances in Artificial Intelligence, EAAI 2023, Washington, DC, USA, February 7-14, 2023*, pages 7705–7713. AAAI Press, 2023.
- [13] Ary L. Goldberger, Luis A. N. Amaral, Leon Glass, Jeffrey M. Hausdorff, Plamen Ch. Ivanov, Roger G. Mark, Joseph E. Mietus, George B. Moody, Chung-Kang Peng, and H. Eugene Stanley. PhysioBank, PhysioToolkit, and PhysioNet: Components of a New Research Resource for Complex Physiologic Signals. *Circulation*, 101(23), June 2000.
- [14] Wenbo Gong, Sebastian Tschitschek, Sebastian Nowozin, Richard E Turner, José Miguel Hernández-Lobato, and Cheng Zhang. Icebreaker: Element-wise Efficient Information Acquisition with a Bayesian Deep Latent Gaussian Model. In H. Wallach, H. Larochelle, A. Beygelzimer, F. d’Alché-Buc, E. Fox, and R. Garnett, editors, *Advances in Neural Information Processing Systems*, volume 32. Curran Associates, Inc., 2019.
- [15] Ian J. Goodfellow, Jean Pouget-Abadie, Mehdi Mirza, Bing Xu, David Warde-Farley, Sherjil Ozair, Aaron C. Courville, and Yoshua Bengio. Generative Adversarial Nets. In Zoubin Ghahramani, Max Welling, Corinna Cortes, Neil D. Lawrence, and Kilian Q. Weinberger, editors, *Advances in Neural Information Processing Systems 27: Annual Conference on Neural Information Processing Systems 2014, December 8-13 2014, Montreal, Quebec, Canada*, pages 2672–2680, 2014.
- [16] Jongmin Han and Seokho Kang. Active learning with missing values considering imputation uncertainty. *Knowledge-Based Systems*, 224:107079, July 2021.
- [17] Kaiming He, Xiangyu Zhang, Shaoqing Ren, and Jian Sun. Delving Deep into Rectifiers: Surpassing Human-Level Performance on ImageNet Classification. In *2015 IEEE International Conference on Computer Vision, ICCV 2015, Santiago, Chile, December 7-13, 2015*, pages 1026–1034. IEEE Computer Society, 2015.
- [18] Yifei He, Runxiang Cheng, Gargi Balasubramaniam, Yao-Hung Hubert Tsai, and Han Zhao. Efficient Modality Selection in Multimodal Learning. *Journal of Machine Learning Research*, 25(47):1–39, 2024.
- [19] Geoffrey E. Hinton and Richard S. Zemel. Autoencoders, Minimum Description Length and Helmholtz Free Energy. In Jack D. Cowan, Gerald Tesauro, and Joshua Alspector, editors, *Advances in Neural Information Processing Systems 6, [7th NIPS Conference, Denver, Colorado, USA, 1993]*, pages 3–10. Morgan Kaufmann, 1993.
- [20] Jonathan Ho, Ajay Jain, and Pieter Abbeel. Denoising Diffusion Probabilistic Models. In Hugo Larochelle, Marc’Aurelio Ranzato, Raia Hadsell, Maria-Florina Balcan, and Hsuan-Tien Lin, editors, *Advances in Neural Information Processing Systems 34: Annual Conference on Neural Information Processing Systems 2020, NeurIPS 2020, December 6-12, 2020, virtual*, 2020.
- [21] Arthur Hoarau, Benjamin Quost, Sébastien Destercke, and Willem Waegeman. Reducing Aleatoric and Epistemic Uncertainty through Multi-modal Data Acquisition, January 2025. arXiv:2501.18268 [cs].
- [22] David Holzmüller, Viktor Zaverkin, Johannes Kästner, and Ingo Steinwart. A Framework and Benchmark for Deep Batch Active Learning for Regression. *J. Mach. Learn. Res.*, 24:164:1–164:81, 2023.
- [23] Yu Huang, Chenzhuang Du, Zihui Xue, Xuanyao Chen, Hang Zhao, and Longbo Huang. What Makes Multi-Modal Learning Better than Single (Provably). In Marc’Aurelio Ranzato, Alina Beygelzimer, Yann N. Dauphin, Percy Liang, and Jennifer Wortman Vaughan, editors, *Advances in Neural Information Processing Systems 34: Annual Conference on Neural Information Processing Systems 2021, NeurIPS 2021, December 6-14, 2021, virtual*, pages 10944–10956, 2021.
- [24] Jaromír Janisch, Tomáš Pevný, and Viliam Lisý. Classification with costly features as a sequential decision-making problem. *Machine Learning*, 109(8):1587–1615, August 2020.

- [25] Diederik P. Kingma and Max Welling. Auto-Encoding Variational Bayes. In Yoshua Bengio and Yann LeCun, editors, *2nd International Conference on Learning Representations, ICLR 2014, Banff, AB, Canada, April 14-16, 2014, Conference Track Proceedings*, 2014.
- [26] Andreas Kirsch, Joost van Amersfoort, and Yarin Gal. BatchBALD: Efficient and Diverse Batch Acquisition for Deep Bayesian Active Learning. In Hanna M. Wallach, Hugo Larochelle, Alina Beygelzimer, Florence d’Alché Buc, Emily B. Fox, and Roman Garnett, editors, *Advances in Neural Information Processing Systems 32: Annual Conference on Neural Information Processing Systems 2019, NeurIPS 2019, December 8-14, 2019, Vancouver, BC, Canada*, pages 7024–7035, 2019.
- [27] Henrik von Kleist, Alireza Zamanian, Ilya Shpitser, and Narges Ahmidi. Evaluation of Active Feature Acquisition Methods for Time-varying Feature Settings. *Journal of Machine Learning Research*, 26(60):1–84, 2025.
- [28] Jannik Kossen, Cătălina Cangea, Eszter Vértés, Andrew Jaegle, Viorica Patraucean, Ira Ktena, Nenad Tomasev, and Danielle Belgrave. Active Acquisition for Multimodal Temporal Data: A Challenging Decision-Making Task. *Transactions on Machine Learning Research*, 2023.
- [29] Sarah Lewis, Tatiana Matejovicova, Yingzhen Li, Angus Lamb, Yordan Zaykov, Miltiadis Allamanis, and Cheng Zhang. Accurate Imputation and Efficient Data Acquisition with Transformer-based VAEs. In *Advances in Neural Information Processing Systems 35: Annual Conference on Neural Information Processing Systems 2021, NeurIPS 2021, December 6-14, 2021, 2021*.
- [30] Dongyuan Li, Zhen Wang, Yankai Chen, Renhe Jiang, Weiping Ding, and Manabu Okumura. A Survey on Deep Active Learning: Recent Advances and New Frontiers. *IEEE Trans. Neural Networks Learn. Syst.*, 36(4):5879–5899, 2025.
- [31] Yang Li and Junier Oliva. Active Feature Acquisition with Generative Surrogate Models. In Marina Meila and Tong Zhang, editors, *Proceedings of the 38th International Conference on Machine Learning, ICML 2021, 18-24 July 2021, Virtual Event*, volume 139 of *Proceedings of Machine Learning Research*, pages 6450–6459. PMLR, 2021.
- [32] Yang Li and Junier Oliva. Distribution Guided Active Feature Acquisition, October 2024. arXiv:2410.03915 [cs].
- [33] Quan Long. Multimodal information gain in Bayesian design of experiments. *Comput. Stat.*, 37(2):865–885, 2022.
- [34] Chao Ma, Sebastian Tschiatschek, Konstantina Palla, José Miguel Hernández-Lobato, Sebastian Nowozin, and Cheng Zhang. EDDI: Efficient Dynamic Discovery of High-Value Information with Partial VAE. In Kamalika Chaudhuri and Ruslan Salakhutdinov, editors, *Proceedings of the 36th International Conference on Machine Learning, ICML 2019, 9-15 June 2019, Long Beach, California, USA*, volume 97 of *Proceedings of Machine Learning Research*, pages 4234–4243. PMLR, 2019.
- [35] Matthew B. A. McDermott, Haoran Zhang, Lasse Hyldig Hansen, Giovanni Angelotti, and Jack Gallifant. A Closer Look at AUROC and AUPRC under Class Imbalance. In Amir Globersons, Lester Mackey, Danielle Belgrave, Angela Fan, Ulrich Paquet, Jakub M. Tomczak, and Cheng Zhang, editors, *Advances in Neural Information Processing Systems 38: Annual Conference on Neural Information Processing Systems 2024, NeurIPS 2024, Vancouver, BC, Canada, December 10 - 15, 2024*, 2024.
- [36] Marius Memmel, Roman Bachmann, and Amir Zamir. Modality-invariant Visual Odometry for Embodied Vision. In *IEEE/CVF Conference on Computer Vision and Pattern Recognition, CVPR 2023, Vancouver, BC, Canada, June 17-24, 2023*, pages 21549–21559. IEEE, 2023.
- [37] Sriraam Natarajan, Srijita Das, Nandini Ramanan, Gautam Kunapuli, and Predrag Radivojac. On Whom Should I Perform this Lab Test Next? An Active Feature Elicitation Approach. In *Proceedings of the Twenty-Seventh International Joint Conference on Artificial Intelligence*, pages 3498–3505, Stockholm, Sweden, July 2018. International Joint Conferences on Artificial Intelligence Organization.

- [38] Alexander Luke Ian Norcliffe, Changhee Lee, Fergus Imrie, Mihaela van der Schaar, and Pietro Lio. Information Bottleneck for Active Feature Acquisition, 2025.
- [39] William Peebles and Saining Xie. Scalable Diffusion Models with Transformers. In *IEEE/CVF International Conference on Computer Vision, ICCV 2023, Paris, France, October 1-6, 2023*, pages 4172–4182. IEEE, 2023.
- [40] Ignacio Peis, Chao Ma, and José Miguel Hernández-Lobato. Missing Data Imputation and Acquisition with Deep Hierarchical Models and Hamiltonian Monte Carlo. In Sanmi Koyejo, S. Mohamed, A. Agarwal, Danielle Belgrave, K. Cho, and A. Oh, editors, *Advances in Neural Information Processing Systems 35: Annual Conference on Neural Information Processing Systems 2022, NeurIPS 2022, New Orleans, LA, USA, November 28 - December 9, 2022*, 2022.
- [41] Arman Rahbar, Linus Aronsson, and Morteza Haghir Chehreghani. A Survey on Active Feature Acquisition Strategies, February 2025. arXiv:2502.11067 [cs].
- [42] Anant Raj and Francis R. Bach. Convergence of Uncertainty Sampling for Active Learning. In Kamalika Chaudhuri, Stefanie Jegelka, Le Song, Csaba Szepesvári, Gang Niu, and Sivan Sabato, editors, *International Conference on Machine Learning, ICML 2022, 17-23 July 2022, Baltimore, Maryland, USA*, volume 162 of *Proceedings of Machine Learning Research*, pages 18310–18331. PMLR, 2022.
- [43] Pengzhen Ren, Yun Xiao, Xiaojun Chang, Po-Yao Huang, Zhihui Li, Brij B. Gupta, Xiaojiang Chen, and Xin Wang. A Survey of Deep Active Learning. *ACM Computing Surveys*, 54(9):1–40, December 2022.
- [44] Robin Rombach, Andreas Blattmann, Dominik Lorenz, Patrick Esser, and Björn Ommer. High-Resolution Image Synthesis with Latent Diffusion Models. In *IEEE/CVF Conference on Computer Vision and Pattern Recognition, CVPR 2022, New Orleans, LA, USA, June 18-24, 2022*, pages 10674–10685. IEEE, 2022.
- [45] Ognjen Rudovic, Meiru Zhang, Björn W. Schuller, and Rosalind W. Picard. Multi-modal Active Learning From Human Data: A Deep Reinforcement Learning Approach. In Wen Gao, Helen Mei-Ling Meng, Matthew Turk, Susan R. Fussell, Björn W. Schuller, Yale Song, and Kai Yu, editors, *International Conference on Multimodal Interaction, ICMI 2019, Suzhou, China, October 14-18, 2019*, pages 6–15. ACM, 2019.
- [46] Adriel Saporta, Aahlad Puli, Mark Goldstein, and Rajesh Ranganath. Contrasting with Symile: Simple Model-Agnostic Representation Learning for Unlimited Modalities. In *Advances in Neural Information Processing Systems*, 2024.
- [47] Burr Settles. *Active Learning*. Synthesis Lectures on Artificial Intelligence and Machine Learning. Springer International Publishing, Cham, 2012.
- [48] L. S. Shapley. A Value for n-Person Games. In Harold William Kuhn and Albert William Tucker, editors, *Contributions to the Theory of Games (AM-28), Volume II*, pages 307–318. Princeton University Press, December 1953.
- [49] Meng Shen, Yizheng Huang, Jianxiong Yin, Heqing Zou, Deepu Rajan, and Simon See. Towards Balanced Active Learning for Multimodal Classification. In *Proceedings of the 31st ACM International Conference on Multimedia*, pages 3434–3445, October 2023.
- [50] Hajin Shim, Sung Ju Hwang, and Eunho Yang. Joint Active Feature Acquisition and Classification with Variable-Size Set Encoding. In S. Bengio, H. Wallach, H. Larochelle, K. Grauman, N. Cesa-Bianchi, and R. Garnett, editors, *Advances in Neural Information Processing Systems*, volume 31. Curran Associates, Inc., 2018.
- [51] Karan Singhal, Tao Tu, Juraj Gottweis, Rory Sayres, Ellery Wulczyn, Mohamed Amin, Le Hou, Kevin Clark, Stephen R. Pfohl, Heather Cole-Lewis, Darlene Neal, Qazi Mamunur Rashid, Mike Schaekermann, Amy Wang, Dev Dash, Jonathan H. Chen, Nigam H. Shah, Sami Lachgar, Philip Andrew Mansfield, Sushant Prakash, Bradley Green, Ewa Dominowska, Blaise Agüera Y Arcas, Nenad Tomašev, Yun Liu, Renee Wong, Christopher Semturs, S. Sara Mahdavi, Joelle K. Barral, Dale R. Webster, Greg S. Corrado, Yossi Matias, Shekoofeh Azizi, Alan

- Karthikesalingam, and Vivek Natarajan. Toward expert-level medical question answering with large language models. *Nature Medicine*, January 2025.
- [52] Luis R. Soenksen, Yu Ma, Cynthia Zeng, Leonard Boussieux, Kimberly Villalobos Carballo, Liangyuan Na, Holly M. Wiberg, Michael L. Li, Ignacio Fuentes, and Dimitris Bertsimas. Integrated multimodal artificial intelligence framework for healthcare applications. *npj Digital Medicine*, 5(1):149, September 2022.
 - [53] Luis R Soenksen, Yu Ma, Cynthia Zeng, Leonard David Jean Boussieux, Kimberly Villalobos Carballo, Liangyuan Na, Holly Wiberg, Michael Li, Ignacio Fuentes, and Dimitris Bertsimas. Code for generating the HAIM multimodal dataset of MIMIC-IV clinical data and x-rays.
 - [54] Thomas M. Sutter, Imant Daunhawer, and Julia E. Vogt. Generalized Multimodal ELBO. In *9th International Conference on Learning Representations, ICLR 2021, Virtual Event, Austria, May 3-7, 2021*. OpenReview.net, 2021.
 - [55] Christian Szegedy, Vincent Vanhoucke, Sergey Ioffe, Jon Shlens, and Zbigniew Wojna. Rethinking the Inception Architecture for Computer Vision. In *Proceedings of the IEEE Conference on Computer Vision and Pattern Recognition (CVPR)*, June 2016.
 - [56] Toan Tran, Thanh-Toan Do, Ian Reid, and Gustavo Carneiro. Bayesian Generative Active Deep Learning. In Kamalika Chaudhuri and Ruslan Salakhutdinov, editors, *Proceedings of the 36th International Conference on Machine Learning*, volume 97 of *Proceedings of Machine Learning Research*, pages 6295–6304. PMLR, June 2019.
 - [57] Michael Valancius, Max Lennon, and Junier Oliva. Acquisition Conditioned Oracle for Non-greedy Active Feature Acquisition. In *Forty-first International Conference on Machine Learning, ICML 2024, Vienna, Austria, July 21-27, 2024*. OpenReview.net, 2024.
 - [58] Ashish Vaswani, Noam Shazeer, Niki Parmar, Jakob Uszkoreit, Llion Jones, Aidan N. Gomez, Lukasz Kaiser, and Illia Polosukhin. Attention is All you Need. In Isabelle Guyon, Ulrike von Luxburg, Samy Bengio, Hanna M. Wallach, Rob Fergus, S. V. N. Vishwanathan, and Roman Garnett, editors, *Advances in Neural Information Processing Systems 30: Annual Conference on Neural Information Processing Systems 2017, December 4-9, 2017, Long Beach, CA, USA*, pages 5998–6008, 2017.
 - [59] Gerome Vivar, Kamilia Mullakaeva, Andreas Zwergal, Nassir Navab, and Seyed-Ahmad Ahmadi. Peri-Diagnostic Decision Support Through Cost-Efficient Feature Acquisition at Test-Time. In Anne L. Martel, Purang Abolmaesumi, Danail Stoyanov, Diana Mateus, Maria A. Zuluaga, S. Kevin Zhou, Daniel Racoceanu, and Leo Joskowicz, editors, *Medical Image Computing and Computer Assisted Intervention - MICCAI 2020*, volume 12262, pages 572–581. Springer International Publishing, Cham, 2020. Series Title: Lecture Notes in Computer Science.
 - [60] Yuanzhi Wang, Yong Li, and Zhen Cui. Incomplete Multimodality-Diffused Emotion Recognition. In Alice Oh, Tristan Naumann, Amir Globerson, Kate Saenko, Moritz Hardt, and Sergey Levine, editors, *Advances in Neural Information Processing Systems 36: Annual Conference on Neural Information Processing Systems 2023, NeurIPS 2023, New Orleans, LA, USA, December 10 - 16, 2023*, 2023.
 - [61] Daniel Wesego and Pedram Rooshenas. Score-Based Multimodal Autoencoder. *Transactions on Machine Learning Research*, 2024.
 - [62] Renjie Wu, Hu Wang, Hsiang-Ting Chen, and Gustavo Carneiro. Deep Multimodal Learning with Missing Modality: A Survey, October 2024. arXiv:2409.07825 [cs].
 - [63] Amir Zadeh, Paul Pu Liang, Soujanya Poria, E. Cambria, and Louis-Philippe Morency. Multimodal Language Analysis in the Wild: CMU-MOSEI Dataset and Interpretable Dynamic Fusion Graph. In *Annual Meeting of the Association for Computational Linguistics*, 2018.
 - [64] Sara Zannone, Jose Miguel Hernandez Lobato, Cheng Zhang, and Konstantina Palla. ODIN: Optimal Discovery of High-value INformation Using Model-based Deep Reinforcement Learning. In *Real-world Sequential Decision Making Workshop, ICML*, June 2019.

- [65] Jifan Zhang, Shuai Shao, Saurabh Verma, and Robert D. Nowak. Algorithm Selection for Deep Active Learning with Imbalanced Datasets. In Alice Oh, Tristan Naumann, Amir Globerson, Kate Saenko, Moritz Hardt, and Sergey Levine, editors, *Advances in Neural Information Processing Systems 36: Annual Conference on Neural Information Processing Systems 2023, NeurIPS 2023, New Orleans, LA, USA, December 10 - 16, 2023*, 2023.
- [66] Xulu Zhang, Wengyu Zhang, Xiaoyong Wei, Jinlin Wu, Zhaoxiang Zhang, Zhen Lei, and Qing Li. Generative active learning for image synthesis personalization. In *ACM Multimedia 2024*, 2024.
- [67] Jia-Jie Zhu and José Bento. Generative Adversarial Active Learning, November 2017. arXiv:1702.07956 [cs].

A Broader Impact and Ethics

The CAMA setting introduced in this paper offers potential for positive broader impacts, primarily by enabling more efficient use of resources in multimodal machine learning. In resource-constrained fields like healthcare, this could facilitate access to more robust and comprehensive model performance by strategically guiding the acquisition of costly or limited additional data modalities. This could translate to improved diagnostic accuracy where such data is critical but not uniformly available for all samples in a cohort. However, the deployment of CAMA, particularly its core function of ranking and prioritizing samples for modality acquisition, necessitates careful ethical consideration. This raises concerns about equity and fairness, especially if the downstream application impacts critical decisions. A significant risk is the potential to introduce biases, including racial, socioeconomic, or other demographic biases. Therefore, the development and application of CAMA must be approached with a strong commitment to ethical principles.

B Details about Acquisition Function Strategies

B.1 AUROC and AUPRC

To derive the proposed acquisition strategies, we briefly explain the metrics used in the following paragraphs.

AUROC The Area Under the Receiver Operating Characteristic (AUROC) measures the model’s ability to discriminate between positive and negative classes and is defined as

$$\text{AUROC}(\mathbf{y}, \mathbf{s}) = \frac{1}{N_+ N_-} \sum_{i: y_i=1} \sum_{j: y_j=0} \left(\mathbb{I}(s_i > s_j) + \frac{1}{2} \mathbb{I}(s_i = s_j) \right) \quad (8)$$

where $N_+ = |\{i | y_i = 1\}|$ and $N_- = |\{j | y_j = 0\}|$.

AUPRC The Area Under the Precision-Recall Curve (AUPRC) summarizes the trade-off between precision (P_t) and recall (R_t) across different decision thresholds t and is defined as

$$\text{AUPRC}(\mathbf{y}, \mathbf{p}) = \sum_{k=1}^{N'} (R_k - R_{k-1}) P_k \quad (9)$$

where points (R_k, P_k) are ordered by threshold from the PR curve, N' is the number of unique thresholds, and $\mathbf{p} = \sigma(\mathbf{s})$.

B.2 Oracle Acquisition Strategies: Exact Gain Calculation

Oracle acquisition strategies serve as theoretical upper limits for the performance of greedy acquisition approaches. They operate under the ideal assumption that the true labels y_i and the outcome scores $s_i^{(\text{full})}$ are known for all samples $i \in \{1, \dots, N\}$. While not implementable in practice, these oracle strategies provide benchmarks by selecting samples based on their exact marginal contribution to the global evaluation metric. The general principle is to iteratively select M samples. At each step, among the samples for which the additional modality has not yet been acquired, the oracle picks the one that provides the largest true immediate gain to the chosen global metric.

AUROC Oracle The AUROC oracle strategy aims to maximize the cohort’s AUROC by identifying, at each step, the sample i that yields the largest immediate increase in this metric if its additional modality were acquired (changing its score from $s_i^{(\text{avail})}$ to $s_i^{(\text{full})}$), *i.e.*, a greedy selection. This prospective increase is quantified by the marginal gain g_i^{AUROC} . The components of this gain, $g_i^{\text{AUROC}}(y_i = 1)$ (for positive samples) and $g_i^{\text{AUROC}}(y_i = 0)$ (for negative samples), reflect the net change in favorable pairwise score comparisons relative to samples of the other class. Recall the definition of AUROC from eq. (8):

$$\text{AUROC}(\mathbf{y}, \mathbf{s}) = \frac{1}{N_+ N_-} \sum_{i: y_i=1} \sum_{j: y_j=0} \left(\mathbb{I}(s_i > s_j) + \frac{1}{2} \mathbb{I}(s_i = s_j) \right).$$

The total marginal gain for sample i , representing the exact change in the cohort’s AUROC value, is then, by considering positive and negative samples and neglecting the normalization factor:

$$g_i^{\text{AUROC}}(y_i = 1) = \sum_{j: y_j=0} \left(\mathbb{I}(s_i^{(\text{full})} > s_j^{(\text{avail})}) - \mathbb{I}(s_i^{(\text{avail})} > s_j^{(\text{avail})}) + \frac{1}{2} \left[\mathbb{I}(s_i^{(\text{full})} = s_j^{(\text{avail})}) - \mathbb{I}(s_i^{(\text{avail})} = s_j^{(\text{avail})}) \right] \right) \quad (10)$$

$$g_i^{\text{AUROC}}(y_i = 0) = \sum_{j: y_j=1} \left(\mathbb{I}(s_j^{(\text{avail})} > s_i^{(\text{full})}) - \mathbb{I}(s_j^{(\text{avail})} > s_i^{(\text{avail})}) + \frac{1}{2} \left[\mathbb{I}(s_j^{(\text{avail})} = s_i^{(\text{full})}) - \mathbb{I}(s_j^{(\text{avail})} = s_i^{(\text{avail})}) \right] \right) \quad (11)$$

$$g_i^{\text{AUROC}} = \frac{1}{N_+ N_-} (g_i^{\text{AUROC}}(y_i = 1) \cdot \mathbb{I}(y_i = 1) + g_i^{\text{AUROC}}(y_i = 0) \cdot \mathbb{I}(y_i = 0)) \quad (12)$$

AUPRC Oracle The AUPRC oracle strategy seeks to maximize the cohort’s AUPRC. It operates by identifying, at each step, the sample i which, if its additional modality were acquired (changing its score from $s_i^{(\text{avail})}$ to $s_i^{(\text{full})}$), would yield the largest immediate increase in the global AUPRC value, *i.e.*, a greedy selection. This marginal gain, g_i^{AUPRC} , represents the exact change in the cohort’s AUPRC. Let $\mathbf{s}^{(\text{avail})}$ be the vector of scores where all samples k have score $s_k^{(\text{full})}$. Let $\mathbf{s}^{(1 \setminus i, 2_i)}$ denote the score vector that is identical to $\mathbf{s}^{(\text{avail})}$ except that for sample i , the score $s_i^{(\text{avail})}$ is replaced by $s_i^{(\text{full})}$. The marginal gain for sample i is then defined as:

$$g_i^{\text{AUPRC}} = \text{AUPRC}(\mathbf{y}, \mathbf{s}^{(1 \setminus i, 2_i)}) - \text{AUPRC}(\mathbf{y}, \mathbf{s}^{(\text{avail})}) \quad (13)$$

B.3 Upper-Bound Heuristic Strategies

The preceding oracle strategies take the assumption of perfect foresight into both the true labels y_i and the exact outcome scores $s_i^{(\text{full})}$. We now introduce a distinct class of upper-bound heuristic strategies. These strategies still presume access to the true future scores $s_i^{(\text{full})}$ for any sample i if its additional modality were acquired. However, the following upper-bound heuristics are label-agnostic, *i.e.*, the true label y_i of a candidate sample is not used when determining its priority for acquisition. Consequently, the selection principle for these strategies must rely on how the known change from an initial score $s_i^{(\text{avail})}$ to the future score $s_i^{(\text{full})}$ is expected to influence the global evaluation metric, without direct reference to the sample’s ground truth label.

Maximum True Uncertainty Reduction The uncertainty reduction strategy prioritizes acquiring the additional modality for samples where doing so is expected to yield the largest decrease in predictive uncertainty. For each sample i , uncertainty is quantified using the binary entropy $\mathcal{H}(p_i)$ of its predicted probability p_i for the positive class, defined as:

$$\mathcal{H}(p_i) = -p_i \log_2 p_i - (1 - p_i) \log_2 (1 - p_i), \quad (14)$$

The acquisition strategy operates with knowledge of the initial probability $p_i^{(\text{avail})} = \sigma(s_i^{(\text{avail})})$ derived from the available modalities, and crucially, the true future probability $p_i^{(\text{full}, \text{true})} = \sigma(s_i^{(\text{full}, \text{true})})$ that would be obtained if the additional modality were acquired (where $s_i^{(\text{full}, \text{true})}$ is the oracle score). The acquisition score g_i^{UR} for sample i is then the exact reduction in entropy:

$$g_i^{\text{UR}} = \mathcal{H}(p_i^{(\text{avail})}) - \mathcal{H}(p_i^{(\text{full}, \text{true})}). \quad (15)$$

Samples with higher g_i^{UR} values, indicating a greater expected reduction in uncertainty, are prioritized for modality acquisition.

Maximum True Rank Change This rank change strategy prioritizes samples whose relative standing within the cohort, based on predicted probability of belonging to the positive class, would change most significantly if the additional modality were acquired. For each sample i , we consider its rank $R(p_i)$ when all N samples in the cohort are ordered by their respective probabilities p_i . The acquisition score g_i^{RC} for sample i is defined as the absolute magnitude of this change in rank:

$$g_i^{\text{RC}} = |R(p_i^{(\text{full}, \text{true})}) - R(p_i^{(\text{avail})})|. \quad (16)$$

Samples exhibiting a higher g_i^{RC} are prioritized for modality acquisition, since they are expected to cause the largest shift in the sample's rank-ordered position relative to its peers.

KL-Divergence The KL-Divergence acquisition strategy aims to identify samples for which acquiring the additional modality would lead to the largest change in the predicted probability distribution. Specifically, it quantifies the divergence from the predicted probability distribution based on the true future score, $P_i^{(\text{full}, \text{true})} \sim \text{Bernoulli}(p_i^{(\text{full}, \text{true})})$, back to the initial distribution based on baseline data, $P_i^{(\text{avail})} \sim \text{Bernoulli}(p_i^{(\text{avail})})$. This is measured by the KL-Divergence $D_{\text{KL}}(P_i^{(\text{avail})} \| P_i^{(\text{full}, \text{true})})$ and can be defined as follows for an acquisition function:

$$g_i^{\text{KLD}} = D_{\text{KL}}(P_i^{(\text{avail})} \| P_i^{(\text{full}, \text{true})}) \quad (17)$$

$$= p_i^{(\text{avail})} \log_2 \frac{p_i^{(\text{avail})}}{p_i^{(\text{full}, \text{true})}} + (1 - p_i^{(\text{avail})}) \log_2 \frac{1 - p_i^{(\text{avail})}}{1 - p_i^{(\text{full}, \text{true})}} \quad (18)$$

Samples with a higher g_i^{KLD} are prioritized, as this indicates a greater discrepancy between the prediction based on available data and the prediction that would be made with the additional modality.

B.4 Baseline Information Strategies

Shifting from approaches that leverage oracle knowledge of future scores ($s_i^{(\text{full})}$), the present section details methods serving as practical, label-agnostic baselines. They make acquisition decisions based exclusively on information derived from the initially available modality ($s_i^{(\text{avail})}$). A Random Acquisition strategy serves as a fundamental baseline.

Maximum Baseline Uncertainty The Maximum Baseline Uncertainty strategy is a baseline that prioritizes samples for which the prediction based on the initially available modality is most uncertain. The acquisition score for sample i is directly the binary entropy $\mathcal{H}(p_i^{(\text{avail})})$, as defined in eq. (14):

$$g_i^{\text{UU}} = \mathcal{H}(p_i^{(\text{avail})}). \quad (19)$$

Samples with a higher g_i^{UU} , *i.e.*, $p_i^{(\text{avail})}$ closer to 0.5, since the entropy $H(p_i^{(\text{avail})})$ is symmetric around $p_i^{(\text{avail})} = 0.5$, are selected first.

Maximum Baseline Probability This approach prioritizes acquiring the additional modality for samples that the baseline model already predicts as belonging to the positive class with high confidence. The acquisition score g_i^{UP} for sample i is simply its initial probability $p_i^{(\text{avail})}$ based on the available modality:

$$g_i^{\text{UP}} = p_i^{(\text{avail})}, \quad (20)$$

Samples with a higher g_i^{UP} are prioritized for acquisition.

B.5 Imputation-Based Strategies

Having explored strategies that assume perfect knowledge of the true labels y_i and/or future scores $s_i^{(\text{full})}$, and simpler baselines relying only on current information $s_i^{(\text{avail})}$, we now introduce methods aiming to bridge the gap by offering a practical and label-agnostic pathway to modality acquisition. They operate by utilizing an imputation model, f_{imp} , to generate a set of K plausible future scores, denoted $\{s_{i,k}^{(\text{full})}\}_{k=1}^K$, conditioned on the initially available data $s_i^{(\text{avail})}$. The core principle of these strategies is to then derive acquisition scores from statistics of this imputed score distribution, with the goal of emulating the decision-making process, but without requiring true future knowledge at test time.

Maximum Expected Probability The Maximum Expected Probability strategy prioritizes samples which have the highest average probability of belonging to the positive class after modality acquisition. It relies on the set of K imputed future probabilities $\{\hat{p}_{i,k}^{(\text{full})}\}_{k=1}^K$, where each $\hat{p}_{i,k}^{(\text{full})} = \sigma(\hat{s}_{i,k}^{(\text{full})})$ is derived from an imputed future score $\hat{s}_{i,k}^{(\text{full})}$. The acquisition score g_i^{eP} for sample i is the mean of these imputed probabilities:

$$g_i^{\text{eP}} = \frac{1}{K} \sum_{k=1}^K \hat{p}_{i,k}^{(\text{full})}. \quad (21)$$

Samples with a higher g_i^{eP} are selected, representing instances where the imputation model, on average, predicts a high likelihood of being positive if the additional modality were acquired.

Maximum Expected Uncertainty Reduction The Maximum Expected Uncertainty Reduction strategy aims to select samples for which the acquisition of the additional modality is anticipated to yield the largest average decrease in predictive uncertainty (eq. (14)). This strategy considers the initial entropy $\mathcal{H}(p_i^{(\text{avail})})$, and the distribution of entropies $\{\mathcal{H}(\hat{p}_{i,k}^{(\text{full})})\}_{k=1}^K$. The acquisition score g_i^{eUR} is the difference between the initial entropy and the mean of the imputed future entropies:

$$g_i^{\text{eUR}} = \mathcal{H}(p_i^{(\text{avail})}) - \frac{1}{K} \sum_{k=1}^K \mathcal{H}(\hat{p}_{i,k}^{(\text{full})}). \quad (22)$$

Samples with higher g_i^{eUR} are prioritized, indicating a greater expected clarification of the prediction upon acquiring the new modality.

Expected Rank Change The Maximum Expected Rank Change strategy prioritizes samples for which the acquisition of the additional modality is anticipated to cause the largest change in their rank, relative to the initial ranking based on $p_i^{(\text{avail})}$. It aims to mirror the "Maximum True Rank Change" strategy by using imputed future probabilities. Let $R(p_i^{(\text{avail})})$ denote the rank of sample i when all N samples in the cohort are ordered by their initial probabilities $p_j^{(\text{avail})}$ (for $j = 1, \dots, N$). For each of the K imputed future probabilities $\hat{p}_{i,k}^{(\text{full})}$ for sample i , let $R(\hat{p}_{i,k}^{(\text{full})})$ denote the rank of sample i if its probability were $\hat{p}_{i,k}^{(\text{full})}$ while all other samples $j \neq i$ retain their initial probabilities $p_j^{(\text{avail})}$. The acquisition score g_i^{eRC} is then the mean of the absolute differences between these imputed future ranks and the initial rank:

$$g_i^{\text{eRC}} = \frac{1}{K} \sum_{k=1}^K |R(\hat{p}_{i,k}^{(\text{full})}) - R(p_i^{(\text{avail})})|. \quad (23)$$

Samples with a higher g_i^{eRC} are selected, as they are expected to experience the largest shift in their rank-ordered position relative to other samples in the cohort upon modality acquisition.

Expected KL-Divergence The Expected KL-Divergence strategy selects samples where the initial probability distribution is expected to diverge most significantly from the future probability distributions derived from the K imputed scores. The acquisition score g_i^{eKLD} is the average KL-Divergence $D_{\text{KL}}(P_i^{(\text{avail})} \parallel \hat{P}_i^{(\text{full}, k)})$ over the K imputations:

$$g_i^{\text{eKLD}} = \frac{1}{K} \sum_{k=1}^K D_{\text{KL}} \left(P_i^{(\text{avail})} \parallel \hat{P}_i^{(\text{full}, k)} \right). \quad (24)$$

A higher g_i^{eKLD} indicates that, on average, the imputed future predictions substantially differ from the initial baseline prediction, suggesting a significant informational update from acquiring the additional modality.

C Hyperparameters, Model Details and Compute Environment

We use well established hyperparameters from the literatur for the modality specific encoders and only optimize the remaining parameters. Notably, our experiments compared three approaches for normalizing the encoder output: No Normalization, Batch Normalization, and Layer Normalization. We found Layer Normalization to be particularly advantageous, as it both stabilized training convergence and significantly enhanced the performance of the DDPMs. We also evaluated the impact of using only the CLS token representation from the encoder versus leveraging the full output sequence. This comparison revealed no substantial effect on performance, suggesting the sufficiency of the CLS token representation for our task. Layers in the network are initialized using He initialization [17] if they were not pre-initialized by the specific encoder architecture. We find this important for stabilizing the DDPMs during earlier epochs of the end-to-end model training especially.

We perform hyperparameter sweeps for the remaining parts of the designed model in the following ranges:

- Transformer Head
 - Embedding dimension: [32, 64, 128, 256, 512, 1024]
 - Feed-Forward network: [128, 256, 512, 1024, 2048]
 - Dropout: [0, 0.1, 0.2]
 - Number of heads: [4, 8, 16]
 - Number of layers: [2, 4, 6, 8]
- DDPMs
 - Embedding dimension: analogous to Transformer head
 - Hidden dimension: [32, 64, 128, 256, 512, 1024]
 - Dropout: [0, 0.1, 0.2]
 - Number of heads: [4, 8, 16]
 - Number of layers: [2, 4, 6, 8]
 - Number of steps: [10, 25, 50, 100, 250, 500]
- ScheduleFree Optimizer
 - Learning rate: [1e-1, 1e-2, 1e-3, 3e-4, 1e-4, 1e-5]
 - Warmup steps: [0, 100, 200]
 - Weight decay: [0, 0.01, 0.001]

The models are trained with early stopping but without any maximum number of epochs. For the imputation based acquisition functions, 100 DDPM samples are used during inference of the model.

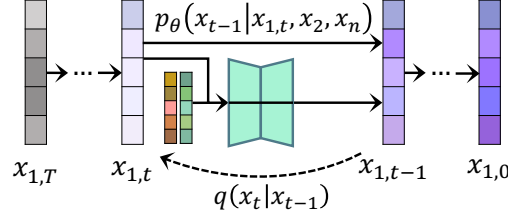


Figure 4: The latent DDPM with its (de)noising functions. Coloring represents less noise in the latent space, starting with pure noise in $X_{i,T} = X_{1,T}$ with T steps and modality i . The DDPM is conditioned with two non-missing latent spaces, each from one remaining modality respectively.

Our experiments are conducted on a High-Performance Cluster (HPC) with the following environment:

1. 21 Dell PowerEdge R7525 compute nodes, each with:
 - 64 AMD Epyc cores (Rome)
 - 512GB RAM
 - 1 NVIDIA A100 40G GPU
2. 2 Dell PowerEdge XE8545 compute nodes, each with:
 - 128 AMD Epyc cores (Milan)
 - 512GB RAM
 - 4 NVIDIA A100 40G GPUs (NVLink-connected)

D Detailed Results for MOSEI

Table 3: Acquisition performance on MOSEI, presenting results for AUROC strategies. For each metric, strategies are sorted by their descending $G_{\text{full}} \uparrow$ values. Oracle strategies are marked with ‡, upper-bound heuristics with † and unimodal baselines with ¡.

Strategy	Target	Mean
AUROC ‡	1.478 \pm 0.091	1.478
AUPRC ‡	1.422 \pm 0.085	1.422
KL-Div. †	0.882 \pm 0.006	0.882
KL-Div.	0.855 \pm 0.034	0.855
Rank †	0.849 \pm 0.008	0.849
Prob.	0.707 \pm 0.037	0.707
Uncert. †	0.663 \pm 0.006	0.663
Uncert.	0.630 \pm 0.015	0.630
Uncert. ¡	0.525 \pm 0.005	0.525
Random	0.490 \pm 0.004	0.490
Prob. ¡	0.433 \pm 0.007	0.433
Rank	0.432 \pm 0.014	0.432

Table 4: Acquisition performance on MOSEI, presenting results for AUPRC strategies. For each metric, strategies are sorted by their descending $G_{\text{full}} \uparrow$ values. Oracle strategies are marked with ‡, upper-bound heuristics with † and unimodal baselines with ¡.

Strategy	Target	Mean
AUPRC ‡	1.666 \pm 0.161	1.666
AUROC ‡	1.557 \pm 0.147	1.557
KL-Div.	0.889 \pm 0.052	0.889
Prob.	0.846 \pm 0.070	0.846
KL-Div. †	0.838 \pm 0.006	0.838
Rank †	0.806 \pm 0.010	0.806
Uncert. †	0.708 \pm 0.005	0.708
Uncert.	0.706 \pm 0.037	0.706
Prob. ¡	0.543 \pm 0.009	0.543
Uncert. ¡	0.540 \pm 0.006	0.540
Random	0.525 \pm 0.003	0.525
Rank	0.457 \pm 0.019	0.457

Table 5: Acquisition performance on MOSEI, presenting results for AUROC strategies. For each metric, strategies are sorted by their descending $G_{\text{full}} \uparrow$ values. Oracle strategies are marked with ‡, upper-bound heuristics with † and unimodal baselines with ¡. Here, Image is imputed by Text.

Strategy	Target	Mean
AUROC ‡	0.995 \pm 0.006	0.995
AUPRC ‡	0.912 \pm 0.016	0.912
KL-Div. †	0.777 \pm 0.005	0.777
Rank †	0.763 \pm 0.012	0.763
Uncert. †	0.599 \pm 0.015	0.599
KL-Div.	0.551 \pm 0.012	0.551
Rank	0.524 \pm 0.012	0.524
Random	0.521 \pm 0.006	0.521
Uncert. ¡	0.507 \pm 0.015	0.507
Uncert.	0.500 \pm 0.021	0.500
Prob.	0.473 \pm 0.010	0.473
Prob. ¡	0.451 \pm 0.013	0.451

Table 6: Acquisition performance on MOSEI, presenting results for AUPRC strategies. For each metric, strategies are sorted by their descending $G_{\text{full}} \uparrow$ values. Oracle strategies are marked with ‡, upper-bound heuristics with † and unimodal baselines with j. Here, Image is imputed by Text.

Strategy	Target	Mean
AUPRC ‡	0.995 \pm 0.012	0.995
AUROC ‡	0.966 \pm 0.008	0.966
KL-Div. †	0.790 \pm 0.015	0.790
Rank †	0.781 \pm 0.014	0.781
Uncert. †	0.673 \pm 0.019	0.673
Prob.	0.598 \pm 0.006	0.598
KL-Div.	0.590 \pm 0.009	0.590
Prob. j	0.578 \pm 0.009	0.578
Random	0.575 \pm 0.008	0.575
Uncert.	0.567 \pm 0.009	0.567
Uncert. j	0.565 \pm 0.018	0.565
Rank	0.560 \pm 0.012	0.560

Table 7: Acquisition performance on MOSEI, presenting results for AUROC strategies. For each metric, strategies are sorted by their descending $G_{\text{full}} \uparrow$ values. Oracle strategies are marked with ‡, upper-bound heuristics with † and unimodal baselines with j. Here, Image is imputed by Audio.

Strategy	Target	Mean
AUROC ‡	1.052 \pm 0.007	1.052
AUPRC ‡	0.947 \pm 0.012	0.947
KL-Div. †	0.785 \pm 0.009	0.785
Rank †	0.783 \pm 0.010	0.783
Uncert. †	0.672 \pm 0.007	0.672
Rank	0.576 \pm 0.013	0.576
KL-Div.	0.566 \pm 0.011	0.566
Random	0.553 \pm 0.008	0.553
Prob.	0.547 \pm 0.002	0.547
Uncert.	0.545 \pm 0.009	0.545
Uncert. j	0.545 \pm 0.009	0.545
Prob. j	0.526 \pm 0.014	0.526

Table 8: Acquisition performance on MOSEI, presenting results for AUPRC strategies. For each metric, strategies are sorted by their descending $G_{\text{full}} \uparrow$ values. Oracle strategies are marked with ‡, upper-bound heuristics with † and unimodal baselines with j. Here, Image is imputed by Audio.

Strategy	Target	Mean
AUROC ‡	1.053 \pm 0.008	1.053
AUPRC ‡	1.011 \pm 0.010	1.011
KL-Div. †	0.803 \pm 0.005	0.803
Rank †	0.802 \pm 0.012	0.802
Uncert. †	0.742 \pm 0.006	0.742
Prob.	0.629 \pm 0.004	0.629
Prob. j	0.616 \pm 0.008	0.616
Rank	0.614 \pm 0.007	0.614
Random	0.603 \pm 0.005	0.603
KL-Div.	0.601 \pm 0.009	0.601
Uncert. j	0.601 \pm 0.014	0.601
Uncert.	0.586 \pm 0.007	0.586

Table 9: Acquisition performance on MOSEI, presenting results for AUROC strategies. For each metric, strategies are sorted by their descending $G_{\text{full}} \uparrow$ values. Oracle strategies are marked with ‡, upper-bound heuristics with † and unimodal baselines with ¶. Here, Image is imputed by Text and Audio.

Strategy	Target	Mean
AUROC ‡	1.321 \pm 0.009	1.321
AUPRC ‡	1.263 \pm 0.010	1.263
KL-Div. †	0.979 \pm 0.006	0.979
Rank †	0.960 \pm 0.005	0.960
Uncert. †	0.716 \pm 0.004	0.716
KL-Div.	0.603 \pm 0.007	0.603
Prob. ¶	0.534 \pm 0.008	0.534
Uncert. ¶	0.513 \pm 0.004	0.513
Prob.	0.513 \pm 0.002	0.513
Uncert.	0.499 \pm 0.004	0.499
Random	0.489 \pm 0.002	0.489
Rank	0.463 \pm 0.005	0.463

Table 10: Acquisition performance on MOSEI, presenting results for AUPRC strategies. For each metric, strategies are sorted by their descending $G_{\text{full}} \uparrow$ values. Oracle strategies are marked with ‡, upper-bound heuristics with † and unimodal baselines with ¶. Here, Image is imputed by Text and Audio.

Strategy	Target	Mean
AUPRC ‡	1.315 \pm 0.012	1.315
AUROC ‡	1.154 \pm 0.011	1.154
KL-Div. †	0.862 \pm 0.006	0.862
Rank †	0.811 \pm 0.006	0.811
Uncert. †	0.750 \pm 0.004	0.750
Prob. ¶	0.676 \pm 0.007	0.676
KL-Div.	0.627 \pm 0.009	0.627
Prob.	0.610 \pm 0.003	0.610
Random	0.527 \pm 0.002	0.527
Rank	0.491 \pm 0.005	0.491
Uncert. ¶	0.480 \pm 0.005	0.480
Uncert.	0.452 \pm 0.004	0.452

Table 11: Acquisition performance on MOSEI, presenting results for AUROC strategies. For each metric, strategies are sorted by their descending $G_{\text{full}} \uparrow$ values. Oracle strategies are marked with ‡, upper-bound heuristics with † and unimodal baselines with ¶. Here, Text is imputed by Image.

Strategy	Target	Mean
AUROC ‡	1.613 \pm 0.269	1.613
AUPRC ‡	1.535 \pm 0.253	1.535
KL-Div.	0.900 \pm 0.023	0.900
KL-Div. †	0.845 \pm 0.018	0.845
Prob.	0.806 \pm 0.022	0.806
Rank †	0.772 \pm 0.024	0.772
Uncert.	0.651 \pm 0.049	0.651
Uncert. †	0.633 \pm 0.060	0.633
Uncert. ¶	0.466 \pm 0.045	0.466
Prob. ¶	0.418 \pm 0.055	0.418
Random	0.417 \pm 0.061	0.417
Rank	0.309 \pm 0.089	0.309

Table 12: Acquisition performance on MOSEI, presenting results for AUPRC strategies. For each metric, strategies are sorted by their descending $G_{\text{full}} \uparrow$ values. Oracle strategies are marked with ‡, upper-bound heuristics with † and unimodal baselines with ¡. Here, Text is imputed by Image.

Strategy	Target	Mean
AUPRC ‡	1.493 \pm 0.166	1.493
AUROC ‡	1.473 \pm 0.164	1.473
KL-Div.	0.896 \pm 0.022	0.896
Prob.	0.861 \pm 0.023	0.861
KL-Div. †	0.843 \pm 0.010	0.843
Rank †	0.784 \pm 0.025	0.784
Uncert.	0.747 \pm 0.030	0.747
Uncert. †	0.697 \pm 0.030	0.697
Uncert. ¡	0.537 \pm 0.014	0.537
Prob. ¡	0.532 \pm 0.045	0.532
Random	0.489 \pm 0.051	0.489
Rank	0.420 \pm 0.065	0.420

Table 13: Acquisition performance on MOSEI, presenting results for AUROC strategies. For each metric, strategies are sorted by their descending $G_{\text{full}} \uparrow$ values. Oracle strategies are marked with ‡, upper-bound heuristics with † and unimodal baselines with ¡. Here, Text is imputed by Audio.

Strategy	Target	Mean
AUROC ‡	8.867 \pm 1.712	8.867
AUPRC ‡	8.253 \pm 1.671	8.253
Prob.	3.157 \pm 1.229	3.157
KL-Div.	2.962 \pm 0.925	2.962
Uncert.	1.592 \pm 0.350	1.592
Uncert. †	0.913 \pm 0.121	0.913
Prob. ¡	0.662 \pm 0.071	0.662
KL-Div. †	0.645 \pm 0.051	0.645
Uncert. ¡	0.591 \pm 0.147	0.591
Rank †	0.494 \pm 0.147	0.494
Random	0.316 \pm 0.059	0.316
Rank	-0.413 \pm 0.421	-0.413

Table 14: Acquisition performance on MOSEI, presenting results for AUPRC strategies. For each metric, strategies are sorted by their descending $G_{\text{full}} \uparrow$ values. Oracle strategies are marked with ‡, upper-bound heuristics with † and unimodal baselines with ¡. Here, Text is imputed by Audio.

Strategy	Target	Mean
AUPRC ‡	16.066 \pm 2.592	16.066
AUROC ‡	14.996 \pm 2.362	14.996
Prob.	6.861 \pm 1.806	6.861
KL-Div.	4.582 \pm 1.938	4.582
Uncert.	3.844 \pm 0.806	3.844
Prob. ¡	0.971 \pm 0.014	0.971
Uncert. †	0.893 \pm 0.141	0.893
Uncert. ¡	0.473 \pm 0.204	0.473
KL-Div. †	0.387 \pm 0.136	0.387
Random	0.376 \pm 0.086	0.376
Rank †	0.015 \pm 0.262	0.015
Rank	-1.134 \pm 0.463	-1.134

Table 15: Acquisition performance on MOSEI, presenting results for AUROC strategies. For each metric, strategies are sorted by their descending $G_{\text{full}} \uparrow$ values. Oracle strategies are marked with ‡, upper-bound heuristics with † and unimodal baselines with j. Here, Text is imputed by Image and Audio.

Strategy	Target	Mean
AUROC ‡	1.207 \pm 0.012	1.207
AUPRC ‡	1.176 \pm 0.013	1.176
KL-Div.	0.892 \pm 0.002	0.892
KL-Div. †	0.851 \pm 0.002	0.851
Rank †	0.836 \pm 0.004	0.836
Prob.	0.665 \pm 0.004	0.665
Uncert.	0.662 \pm 0.008	0.662
Uncert. †	0.649 \pm 0.009	0.649
Uncert. j	0.538 \pm 0.009	0.538
Random	0.512 \pm 0.002	0.512
Rank	0.489 \pm 0.003	0.489
Prob. j	0.379 \pm 0.003	0.379

Table 16: Acquisition performance on MOSEI, presenting results for AUPRC strategies. For each metric, strategies are sorted by their descending $G_{\text{full}} \uparrow$ values. Oracle strategies are marked with ‡, upper-bound heuristics with † and unimodal baselines with j. Here, Text is imputed by Image and Audio.

Strategy	Target	Mean
AUPRC ‡	1.280 \pm 0.013	1.280
AUROC ‡	1.259 \pm 0.013	1.259
KL-Div.	0.894 \pm 0.004	0.894
KL-Div. †	0.842 \pm 0.004	0.842
Rank †	0.840 \pm 0.005	0.840
Prob.	0.727 \pm 0.003	0.727
Uncert.	0.720 \pm 0.007	0.720
Uncert. †	0.691 \pm 0.009	0.691
Uncert. j	0.567 \pm 0.009	0.567
Random	0.531 \pm 0.003	0.531
Rank	0.520 \pm 0.003	0.520
Prob. j	0.462 \pm 0.004	0.462

Table 17: Acquisition performance on MOSEI, presenting results for AUROC strategies. For each metric, strategies are sorted by their descending $G_{\text{full}} \uparrow$ values. Oracle strategies are marked with ‡, upper-bound heuristics with † and unimodal baselines with j. Here, Audio is imputed by Image.

Strategy	Target	Mean
AUROC ‡	1.238 \pm 0.124	1.238
AUPRC ‡	1.192 \pm 0.121	1.192
KL-Div. †	0.826 \pm 0.014	0.826
KL-Div.	0.800 \pm 0.012	0.800
Rank †	0.752 \pm 0.030	0.752
Prob.	0.684 \pm 0.020	0.684
Uncert.	0.552 \pm 0.035	0.552
Uncert. †	0.544 \pm 0.034	0.544
Uncert. j	0.436 \pm 0.043	0.436
Random	0.397 \pm 0.052	0.397
Prob. j	0.374 \pm 0.034	0.374
Rank	0.326 \pm 0.072	0.326

Table 18: Acquisition performance on MOSEI, presenting results for AUPRC strategies. For each metric, strategies are sorted by their descending $G_{\text{full}} \uparrow$ values. Oracle strategies are marked with ‡, upper-bound heuristics with † and unimodal baselines with ¡. Here, Audio is imputed by Image.

Strategy	Target	Mean
AUPRC ‡	1.207 \pm 0.093	1.207
AUROC ‡	1.178 \pm 0.091	1.178
KL-Div. †	0.821 \pm 0.019	0.821
KL-Div.	0.803 \pm 0.017	0.803
Rank †	0.780 \pm 0.025	0.780
Prob.	0.737 \pm 0.024	0.737
Uncert. †	0.627 \pm 0.023	0.627
Uncert.	0.625 \pm 0.023	0.625
Prob. ¡	0.510 \pm 0.034	0.510
Uncert. ¡	0.502 \pm 0.016	0.502
Random	0.478 \pm 0.039	0.478
Rank	0.445 \pm 0.052	0.445

Table 19: Acquisition performance on MOSEI, presenting results for AUROC strategies. For each metric, strategies are sorted by their descending $G_{\text{full}} \uparrow$ values. Oracle strategies are marked with ‡, upper-bound heuristics with † and unimodal baselines with ¡. Here, Audio is imputed by Text.

Strategy	Target	Mean
AUROC ‡	4.955 \pm 0.417	4.955
AUPRC ‡	4.760 \pm 0.414	4.760
Prob.	2.306 \pm 0.259	2.306
KL-Div.	2.305 \pm 0.360	2.305
Uncert.	1.154 \pm 0.141	1.154
KL-Div. †	0.815 \pm 0.043	0.815
Rank †	0.563 \pm 0.073	0.563
Uncert. †	0.520 \pm 0.026	0.520
Uncert. ¡	0.519 \pm 0.023	0.519
Prob. ¡	0.416 \pm 0.007	0.416
Random	0.326 \pm 0.024	0.326
Rank	-0.210 \pm 0.123	-0.210

Table 20: Acquisition performance on MOSEI, presenting results for AUPRC strategies. For each metric, strategies are sorted by their descending $G_{\text{full}} \uparrow$ values. Oracle strategies are marked with ‡, upper-bound heuristics with † and unimodal baselines with ¡. Here, Audio is imputed by Text.

Strategy	Target	Mean
AUPRC ‡	6.275 \pm 0.948	6.275
AUROC ‡	5.337 \pm 0.797	5.337
Prob.	2.571 \pm 0.483	2.571
KL-Div.	2.335 \pm 0.499	2.335
Uncert.	1.626 \pm 0.303	1.626
KL-Div. †	0.817 \pm 0.057	0.817
Rank †	0.645 \pm 0.098	0.645
Uncert. ¡	0.604 \pm 0.044	0.604
Uncert. †	0.604 \pm 0.059	0.604
Prob. ¡	0.511 \pm 0.018	0.511
Random	0.439 \pm 0.023	0.439
Rank	-0.093 \pm 0.135	-0.093

Table 21: Acquisition performance on MOSEI, presenting results for AUROC strategies. For each metric, strategies are sorted by their descending $G_{\text{full}} \uparrow$ values. Oracle strategies are marked with ‡, upper-bound heuristics with † and unimodal baselines with ¶. Here, Audio is imputed by Image and Text.

Strategy	Target	Mean
AUROC ‡	1.215 \pm 0.010	1.215
AUPRC ‡	1.194 \pm 0.010	1.194
KL-Div. †	0.865 \pm 0.002	0.865
KL-Div.	0.857 \pm 0.002	0.857
Rank †	0.833 \pm 0.004	0.833
Prob.	0.667 \pm 0.003	0.667
Uncert.	0.646 \pm 0.007	0.646
Uncert. †	0.645 \pm 0.007	0.645
Uncert. ¶	0.536 \pm 0.008	0.536
Random	0.503 \pm 0.003	0.503
Rank	0.459 \pm 0.004	0.459
Prob. ¶	0.368 \pm 0.005	0.368

Table 22: Acquisition performance on MOSEI, presenting results for AUPRC strategies. For each metric, strategies are sorted by their descending $G_{\text{full}} \uparrow$ values. Oracle strategies are marked with ‡, upper-bound heuristics with † and unimodal baselines with ¶. Here, Audio is imputed by Image and Text.

Strategy	Target	Mean
AUPRC ‡	1.275 \pm 0.011	1.275
AUROC ‡	1.230 \pm 0.011	1.230
KL-Div. †	0.850 \pm 0.004	0.850
KL-Div.	0.846 \pm 0.004	0.846
Rank †	0.837 \pm 0.005	0.837
Prob.	0.725 \pm 0.003	0.725
Uncert.	0.694 \pm 0.007	0.694
Uncert. †	0.693 \pm 0.006	0.693
Uncert. ¶	0.566 \pm 0.008	0.566
Random	0.530 \pm 0.003	0.530
Rank	0.489 \pm 0.004	0.489
Prob. ¶	0.462 \pm 0.005	0.462

E Detailed Results for MIMIC Symile

Table 23: Acquisition performance on MIMIC Symile, presenting results for AUROC strategies. For each metric, strategies are sorted by their descending $G_{\text{full}} \uparrow$ values. Oracle strategies are marked with ‡, upper-bound heuristics with † and unimodal baselines with j.

Strategy	Fracture	Enl. Card.	Consolidation	Atelectasis	Edema	Mean
AUROC ‡	2.876 ± 0.368	3.722 ± 0.370	2.856 ± 0.147	4.862 ± 0.356	2.793 ± 0.324	4.580
AUPRC ‡	2.845 ± 0.362	3.622 ± 0.361	2.766 ± 0.143	4.711 ± 0.343	2.639 ± 0.298	4.502
KL-Div. †	1.029 ± 0.165	1.019 ± 0.051	0.885 ± 0.025	0.841 ± 0.045	0.920 ± 0.011	0.883
KL-Div.	0.838 ± 0.164	0.882 ± 0.064	0.706 ± 0.021	0.779 ± 0.114	0.893 ± 0.080	0.833
Rank †	0.963 ± 0.153	0.924 ± 0.058	0.946 ± 0.025	0.802 ± 0.068	0.887 ± 0.022	0.811
Uncert. †	0.915 ± 0.138	0.763 ± 0.052	0.749 ± 0.031	0.152 ± 0.052	0.648 ± 0.012	0.481
Uncert. j	0.616 ± 0.100	0.482 ± 0.033	0.543 ± 0.024	0.380 ± 0.031	0.539 ± 0.010	0.480
Prob. j	0.153 ± 0.086	0.519 ± 0.035	0.464 ± 0.020	0.446 ± 0.068	0.421 ± 0.010	0.458
Uncert.	0.851 ± 0.138	0.686 ± 0.051	0.701 ± 0.029	0.188 ± 0.094	0.588 ± 0.018	0.440
Prob.	0.861 ± 0.118	0.638 ± 0.046	0.610 ± 0.021	0.099 ± 0.107	0.514 ± 0.099	0.426
Rank	0.123 ± 0.155	0.331 ± 0.043	0.434 ± 0.026	0.371 ± 0.083	0.352 ± 0.030	0.378
Random	0.241 ± 0.121	0.399 ± 0.044	0.479 ± 0.020	0.250 ± 0.080	0.425 ± 0.017	0.376

Strategy	Cardiomegaly	Lung Lesion	Lung Opacity	Pneumonia	Pneumothorax	Mean
AUROC ‡	2.787 ± 0.139	4.974 ± 0.581	6.657 ± 0.649	4.817 ± 0.430	9.461 ± 1.049	4.580
AUPRC ‡	2.672 ± 0.133	4.873 ± 0.570	6.391 ± 0.625	4.510 ± 0.398	9.992 ± 1.087	4.502
KL-Div. †	0.885 ± 0.011	0.753 ± 0.179	0.750 ± 0.087	0.837 ± 0.043	0.910 ± 0.054	0.883
KL-Div.	0.747 ± 0.039	1.266 ± 0.258	0.683 ± 0.106	0.761 ± 0.060	0.773 ± 0.134	0.833
Rank †	0.878 ± 0.019	0.411 ± 0.216	0.793 ± 0.056	0.902 ± 0.029	0.605 ± 0.053	0.811
Uncert. †	0.524 ± 0.025	0.251 ± 0.177	0.212 ± 0.054	0.728 ± 0.023	-0.136 ± 0.065	0.481
Uncert. j	0.480 ± 0.013	0.201 ± 0.179	0.406 ± 0.041	0.615 ± 0.019	0.536 ± 0.040	0.480
Prob. j	0.431 ± 0.015	0.778 ± 0.212	0.417 ± 0.065	0.416 ± 0.055	0.536 ± 0.040	0.458
Uncert.	0.450 ± 0.041	0.022 ± 0.173	0.199 ± 0.057	0.658 ± 0.045	0.055 ± 0.060	0.440
Prob.	0.350 ± 0.053	0.190 ± 0.223	-0.075 ± 0.077	0.172 ± 0.142	0.898 ± 0.061	0.426
Rank	0.378 ± 0.016	0.607 ± 0.150	0.635 ± 0.080	0.437 ± 0.054	0.115 ± 0.082	0.378
Random	0.385 ± 0.015	0.365 ± 0.225	0.381 ± 0.057	0.505 ± 0.038	0.327 ± 0.061	0.376

Table 24: Acquisition performance on MIMIC Symile, presenting results for AUPRC strategies. For each metric, strategies are sorted by their descending $G_{\text{full}} \uparrow$ values. Oracle strategies are marked with ‡, upper-bound heuristics with † and unimodal baselines with j.

Strategy	Fracture	Enl. Card.	Consolidation	Atelectasis	Edema	Mean
AUPRC ‡	2.579 ± 0.343	2.964 ± 0.201	4.784 ± 1.130	3.093 ± 0.201	3.015 ± 0.141	4.231
AUROC ‡	2.563 ± 0.330	2.772 ± 0.182	4.448 ± 1.044	3.127 ± 0.204	2.869 ± 0.137	3.820
KL-Div. †	0.883 ± 0.094	0.970 ± 0.038	0.933 ± 0.057	0.781 ± 0.038	0.939 ± 0.013	0.871
KL-Div.	0.770 ± 0.210	0.899 ± 0.044	0.895 ± 0.159	0.684 ± 0.063	0.832 ± 0.039	0.777
Rank †	0.659 ± 0.176	0.858 ± 0.033	0.903 ± 0.090	0.720 ± 0.064	0.897 ± 0.022	0.776
Prob. j	0.242 ± 0.068	0.523 ± 0.026	0.546 ± 0.030	0.512 ± 0.064	0.533 ± 0.013	0.550
Uncert. †	0.604 ± 0.073	0.812 ± 0.044	0.709 ± 0.036	0.050 ± 0.039	0.645 ± 0.015	0.450
Prob.	0.631 ± 0.073	0.673 ± 0.036	0.503 ± 0.106	0.028 ± 0.069	0.624 ± 0.049	0.449
Uncert.	0.663 ± 0.108	0.744 ± 0.046	0.611 ± 0.073	0.118 ± 0.034	0.569 ± 0.017	0.444
Uncert. j	0.428 ± 0.155	0.524 ± 0.031	0.509 ± 0.036	0.246 ± 0.018	0.519 ± 0.011	0.443
Rank	0.461 ± 0.188	0.388 ± 0.034	0.421 ± 0.064	0.318 ± 0.053	0.351 ± 0.022	0.407
Random	0.149 ± 0.103	0.423 ± 0.032	0.429 ± 0.097	0.222 ± 0.094	0.448 ± 0.012	0.388

Strategy	Cardiomegaly	Lung Lesion	Lung Opacity	Pneumonia	Pneumothorax	Mean
AUPRC ‡	2.746 ± 0.110	2.520 ± 0.250	4.092 ± 0.259	5.895 ± 0.406	10.623 ± 0.708	4.231
AUROC ‡	2.683 ± 0.105	2.534 ± 0.249	4.138 ± 0.259	5.407 ± 0.385	7.657 ± 0.496	3.820
KL-Div. †	0.853 ± 0.010	0.828 ± 0.073	0.792 ± 0.037	0.906 ± 0.032	0.827 ± 0.043	0.871
KL-Div.	0.729 ± 0.034	0.896 ± 0.146	0.722 ± 0.043	0.763 ± 0.059	0.581 ± 0.084	0.777
Rank †	0.882 ± 0.018	0.676 ± 0.088	0.771 ± 0.045	0.911 ± 0.030	0.483 ± 0.075	0.776
Prob. j	0.479 ± 0.017	0.756 ± 0.136	0.555 ± 0.037	0.541 ± 0.029	0.811 ± 0.041	0.550
Uncert. †	0.473 ± 0.029	0.181 ± 0.067	0.140 ± 0.029	0.595 ± 0.024	0.293 ± 0.052	0.450
Prob.	0.366 ± 0.047	0.320 ± 0.104	0.041 ± 0.065	0.339 ± 0.079	0.965 ± 0.027	0.449
Uncert.	0.424 ± 0.038	0.130 ± 0.053	0.149 ± 0.034	0.519 ± 0.033	0.513 ± 0.066	0.444
Uncert. j	0.434 ± 0.018	0.215 ± 0.033	0.260 ± 0.023	0.482 ± 0.019	0.811 ± 0.041	0.443
Rank	0.384 ± 0.014	0.564 ± 0.086	0.402 ± 0.050	0.389 ± 0.034	0.396 ± 0.054	0.407
Random	0.386 ± 0.013	0.503 ± 0.103	0.354 ± 0.053	0.435 ± 0.033	0.527 ± 0.053	0.388

Table 25: Acquisition performance on MIMIC Symile, presenting results for AUROC strategies. For each metric, strategies are sorted by their descending $G_{\text{full}} \uparrow$ values. Oracle strategies are marked with \ddagger , upper-bound heuristics with \dagger and unimodal baselines with \mathfrak{j} . Here, Image is imputed by Lab.

Strategy	Fracture	Enl. Card.	Consolidation	Atelectasis	Edema	Mean
AUROC \ddagger	4.144 \pm 2.172	2.120 \pm 0.465	2.803 \pm 0.306	2.381 \pm 0.215	1.684 \pm 0.070	4.104
AUPRC \ddagger	4.130 \pm 2.196	2.063 \pm 0.487	2.524 \pm 0.233	2.279 \pm 0.203	1.564 \pm 0.063	4.019
KL-Div. \dagger	0.728 \pm 0.137	0.816 \pm 0.011	0.611 \pm 0.084	0.837 \pm 0.028	0.813 \pm 0.009	0.825
Rank \dagger	1.062 \pm 0.643	0.614 \pm 0.111	0.591 \pm 0.157	0.816 \pm 0.065	0.765 \pm 0.024	0.707
Uncert. \dagger	0.686 \pm 0.374	0.606 \pm 0.068	0.637 \pm 0.140	0.496 \pm 0.148	0.619 \pm 0.024	0.601
Uncert.	0.168 \pm 0.317	0.400 \pm 0.025	0.620 \pm 0.179	0.422 \pm 0.130	0.493 \pm 0.019	0.448
Prob. \mathfrak{j}	0.129 \pm 0.339	0.515 \pm 0.057	0.530 \pm 0.049	0.601 \pm 0.101	0.477 \pm 0.018	0.444
Uncert. \mathfrak{j}	0.129 \pm 0.339	0.332 \pm 0.069	0.423 \pm 0.201	0.456 \pm 0.106	0.503 \pm 0.020	0.433
Prob.	0.231 \pm 0.288	0.498 \pm 0.036	0.514 \pm 0.060	0.503 \pm 0.056	0.454 \pm 0.020	0.379
Random	-0.509 \pm 0.041	0.356 \pm 0.070	0.503 \pm 0.163	0.609 \pm 0.091	0.492 \pm 0.023	0.307
KL-Div.	-1.410 \pm 0.037	0.477 \pm 0.108	0.282 \pm 0.146	0.626 \pm 0.137	0.503 \pm 0.022	0.247
Rank	-0.725 \pm 0.858	0.190 \pm 0.201	0.520 \pm 0.018	0.403 \pm 0.085	0.527 \pm 0.032	0.225

Strategy	Cardiomegaly	Lung Lesion	Lung Opacity	Pneumonia	Pneumothorax	Mean
AUROC \ddagger	1.793 \pm 0.077	5.417 \pm 4.001	7.073 \pm 2.202	4.743 \pm 1.268	8.881 \pm 1.894	4.104
AUPRC \ddagger	1.719 \pm 0.068	5.363 \pm 3.950	6.585 \pm 2.017	4.433 \pm 1.187	9.530 \pm 2.017	4.019
KL-Div. \dagger	0.822 \pm 0.010	1.543 \pm 0.689	0.663 \pm 0.095	0.884 \pm 0.063	0.530 \pm 0.109	0.825
Rank \dagger	0.663 \pm 0.042	1.291 \pm 0.557	0.530 \pm 0.154	0.705 \pm 0.170	0.035 \pm 0.068	0.707
Uncert. \dagger	0.272 \pm 0.091	1.128 \pm 0.870	0.622 \pm 0.187	0.687 \pm 0.038	0.254 \pm 0.213	0.601
Uncert.	0.395 \pm 0.020	0.574 \pm 0.327	0.400 \pm 0.126	0.395 \pm 0.040	0.608 \pm 0.201	0.448
Prob. \mathfrak{j}	0.419 \pm 0.065	0.505 \pm 0.108	0.263 \pm 0.254	0.417 \pm 0.228	0.587 \pm 0.180	0.444
Uncert. \mathfrak{j}	0.433 \pm 0.015	0.490 \pm 0.096	0.558 \pm 0.358	0.424 \pm 0.053	0.587 \pm 0.180	0.433
Prob.	0.301 \pm 0.081	0.418 \pm 0.193	0.034 \pm 0.303	0.372 \pm 0.256	0.461 \pm 0.128	0.379
Random	0.420 \pm 0.063	0.384 \pm 0.068	0.200 \pm 0.455	0.444 \pm 0.085	0.169 \pm 0.359	0.307
KL-Div.	0.492 \pm 0.030	0.847 \pm 0.033	0.459 \pm 0.146	0.481 \pm 0.158	-0.285 \pm 0.221	0.247
Rank	0.434 \pm 0.045	-0.219 \pm 0.837	0.956 \pm 0.383	0.363 \pm 0.080	-0.201 \pm 0.261	0.225

Table 26: Acquisition performance on MIMIC Symile, presenting results for AUPRC strategies. For each metric, strategies are sorted by their descending $G_{\text{full}} \uparrow$ values. Oracle strategies are marked with \ddagger , upper-bound heuristics with \dagger and unimodal baselines with \mathfrak{j} . Here, Image is imputed by Lab.

Strategy	Fracture	Enl. Card.	Consolidation	Atelectasis	Edema	Mean
AUPRC \ddagger	3.844 \pm 2.595	1.792 \pm 0.288	2.826 \pm 0.677	1.930 \pm 0.221	1.778 \pm 0.101	4.862
AUROC \ddagger	3.844 \pm 2.592	1.743 \pm 0.263	2.776 \pm 0.672	1.929 \pm 0.225	1.723 \pm 0.097	4.070
KL-Div. \dagger	0.869 \pm 0.023	0.827 \pm 0.021	0.620 \pm 0.156	0.812 \pm 0.024	0.775 \pm 0.013	0.770
Prob. \mathfrak{j}	0.132 \pm 0.484	0.592 \pm 0.029	0.754 \pm 0.084	0.632 \pm 0.071	0.612 \pm 0.012	0.621
Rank \dagger	1.398 \pm 0.874	0.566 \pm 0.140	0.492 \pm 0.345	0.827 \pm 0.034	0.759 \pm 0.024	0.575
Prob.	0.210 \pm 0.451	0.575 \pm 0.018	0.735 \pm 0.084	0.591 \pm 0.035	0.598 \pm 0.016	0.568
Uncert. \dagger	0.712 \pm 0.210	0.650 \pm 0.111	0.655 \pm 0.118	0.538 \pm 0.165	0.579 \pm 0.041	0.498
Uncert.	0.157 \pm 0.477	0.456 \pm 0.075	0.516 \pm 0.245	0.477 \pm 0.170	0.358 \pm 0.021	0.441
Random	-0.110 \pm 0.296	0.408 \pm 0.060	0.420 \pm 0.208	0.599 \pm 0.156	0.489 \pm 0.037	0.440
Uncert. \mathfrak{j}	0.132 \pm 0.484	0.369 \pm 0.094	0.199 \pm 0.387	0.466 \pm 0.152	0.368 \pm 0.022	0.401
Rank	-0.777 \pm 1.263	0.261 \pm 0.185	0.548 \pm 0.051	0.438 \pm 0.134	0.480 \pm 0.042	0.290
KL-Div.	-1.450 \pm 1.121	0.464 \pm 0.132	0.149 \pm 0.370	0.652 \pm 0.149	0.610 \pm 0.010	0.131

Strategy	Cardiomegaly	Lung Lesion	Lung Opacity	Pneumonia	Pneumothorax	Mean
AUPRC \ddagger	1.749 \pm 0.092	2.456 \pm 1.140	7.505 \pm 3.891	4.470 \pm 1.249	20.270 \pm 6.707	4.862
AUROC \ddagger	1.765 \pm 0.093	2.410 \pm 1.120	7.446 \pm 3.823	4.188 \pm 1.199	12.878 \pm 4.427	4.070
KL-Div. \dagger	0.774 \pm 0.017	1.035 \pm 0.214	0.413 \pm 0.176	0.793 \pm 0.046	0.781 \pm 0.044	0.770
Prob. \mathfrak{j}	0.452 \pm 0.103	0.528 \pm 0.184	0.497 \pm 0.287	0.664 \pm 0.107	1.352 \pm 0.410	0.621
Rank \dagger	0.667 \pm 0.037	0.888 \pm 0.274	0.326 \pm 0.248	0.669 \pm 0.058	-0.837 \pm 0.865	0.575
Prob.	0.327 \pm 0.126	0.398 \pm 0.274	0.407 \pm 0.140	0.659 \pm 0.129	1.176 \pm 0.314	0.568
Uncert. \dagger	0.269 \pm 0.134	0.598 \pm 0.430	0.291 \pm 0.099	0.562 \pm 0.027	0.129 \pm 0.407	0.498
Uncert.	0.321 \pm 0.042	0.317 \pm 0.186	0.176 \pm 0.196	0.242 \pm 0.030	1.390 \pm 0.419	0.441
Random	0.369 \pm 0.101	0.478 \pm 0.117	0.810 \pm 0.961	0.449 \pm 0.051	0.484 \pm 0.166	0.440
Uncert. \mathfrak{j}	0.343 \pm 0.033	0.372 \pm 0.120	0.142 \pm 0.320	0.265 \pm 0.044	1.352 \pm 0.410	0.401
Rank	0.390 \pm 0.068	0.069 \pm 0.552	1.071 \pm 0.611	0.469 \pm 0.059	-0.047 \pm 0.555	0.290
KL-Div.	0.507 \pm 0.059	0.742 \pm 0.101	0.382 \pm 0.251	0.639 \pm 0.066	-1.388 \pm 1.198	0.131

Table 27: Acquisition performance on MIMIC Symile, presenting results for AUROC strategies. For each metric, strategies are sorted by their descending $G_{\text{full}} \uparrow$ values. Oracle strategies are marked with \ddagger , upper-bound heuristics with \dagger and unimodal baselines with \jmath . Here, Image is imputed by ECG.

Strategy	Fracture	Enl. Card.	Consolidation	Atelectasis	Edema	Mean
AUROC \ddagger	4.028 \pm 2.600	1.959 \pm 0.358	1.960 \pm 0.164	3.526 \pm 0.947	1.639 \pm 0.050	3.892
AUPRC \ddagger	4.027 \pm 2.600	1.882 \pm 0.323	1.891 \pm 0.153	3.527 \pm 0.951	1.650 \pm 0.044	3.858
KL-Div. \dagger	0.963 \pm 0.224	0.852 \pm 0.051	0.725 \pm 0.030	0.614 \pm 0.152	0.777 \pm 0.003	0.874
KL-Div.	0.425 \pm 0.323	0.561 \pm 0.079	0.769 \pm 0.096	-0.353 \pm 0.827	0.621 \pm 0.030	0.669
Prob. \jmath	0.133 \pm 0.291	0.442 \pm 0.050	0.500 \pm 0.028	-0.684 \pm 0.967	0.427 \pm 0.022	0.650
Prob.	0.650 \pm 0.024	0.538 \pm 0.107	0.709 \pm 0.095	0.162 \pm 0.130	0.591 \pm 0.024	0.443
Rank	0.411 \pm 0.193	0.337 \pm 0.122	0.538 \pm 0.050	-0.165 \pm 0.412	0.445 \pm 0.038	0.380
Rank \dagger	0.192 \pm 0.075	0.559 \pm 0.101	0.753 \pm 0.013	-0.784 \pm 1.091	0.719 \pm 0.043	0.327
Random	-0.803 \pm 0.529	0.482 \pm 0.038	0.647 \pm 0.019	0.227 \pm 0.307	0.513 \pm 0.018	0.263
Uncert.	0.750 \pm 0.011	0.527 \pm 0.112	0.720 \pm 0.083	0.466 \pm 0.229	0.431 \pm 0.026	0.167
Uncert. \dagger	0.934 \pm 0.189	0.700 \pm 0.131	0.717 \pm 0.039	-0.853 \pm 0.584	0.658 \pm 0.050	0.024
Uncert. \jmath	-0.962 \pm 1.403	0.380 \pm 0.050	0.567 \pm 0.064	0.591 \pm 0.180	0.427 \pm 0.022	-0.055

Strategy	Cardiomegaly	Lung Lesion	Lung Opacity	Pneumonia	Pneumothorax	Mean
AUROC \ddagger	2.263 \pm 0.151	9.495 \pm 7.441	4.112 \pm 0.961	2.196 \pm 0.132	7.745 \pm 2.386	3.892
AUPRC \ddagger	2.286 \pm 0.146	9.374 \pm 7.273	4.008 \pm 0.897	2.080 \pm 0.132	7.852 \pm 2.437	3.858
KL-Div. \dagger	0.777 \pm 0.016	1.758 \pm 1.206	0.881 \pm 0.085	0.725 \pm 0.019	0.664 \pm 0.088	0.874
KL-Div.	0.271 \pm 0.065	2.123 \pm 1.791	0.776 \pm 0.125	0.571 \pm 0.018	0.924 \pm 0.134	0.669
Prob. \jmath	0.336 \pm 0.018	3.511 \pm 2.928	0.632 \pm 0.027	0.575 \pm 0.048	0.625 \pm 0.086	0.650
Prob.	0.374 \pm 0.034	-0.235 \pm 0.921	0.122 \pm 0.178	0.568 \pm 0.030	0.952 \pm 0.095	0.443
Rank	0.201 \pm 0.072	0.764 \pm 0.047	0.272 \pm 0.153	0.639 \pm 0.029	0.363 \pm 0.307	0.380
Rank \dagger	0.560 \pm 0.050	-0.731 \pm 0.850	0.808 \pm 0.103	0.777 \pm 0.022	0.416 \pm 0.209	0.327
Random	0.222 \pm 0.044	0.102 \pm 0.610	0.485 \pm 0.131	0.515 \pm 0.036	0.240 \pm 0.153	0.263
Uncert.	0.382 \pm 0.028	-2.196 \pm 2.882	0.086 \pm 0.165	0.630 \pm 0.021	-0.129 \pm 0.190	0.167
Uncert. \dagger	0.741 \pm 0.021	-3.450 \pm 3.932	-0.150 \pm 0.160	0.727 \pm 0.010	0.213 \pm 0.412	0.024
Uncert. \jmath	0.307 \pm 0.038	-3.361 \pm 3.790	0.231 \pm 0.070	0.649 \pm 0.017	0.625 \pm 0.086	-0.055

Table 28: Acquisition performance on MIMIC Symile, presenting results for AUPRC strategies. For each metric, strategies are sorted by their descending $G_{\text{full}} \uparrow$ values. Oracle strategies are marked with \ddagger , upper-bound heuristics with \dagger and unimodal baselines with \jmath . Here, Image is imputed by ECG.

Strategy	Fracture	Enl. Card.	Consolidation	Atelectasis	Edema	Mean
AUPRC \ddagger	6.343 \pm 5.165	1.593 \pm 0.113	1.950 \pm 0.162	2.785 \pm 0.530	1.832 \pm 0.041	4.085
AUROC \ddagger	6.343 \pm 5.165	1.583 \pm 0.124	1.899 \pm 0.146	2.785 \pm 0.528	1.745 \pm 0.041	3.830
KL-Div. \dagger	1.358 \pm 0.553	0.818 \pm 0.060	0.776 \pm 0.039	0.526 \pm 0.206	0.855 \pm 0.004	0.814
Prob.	0.498 \pm 0.210	0.552 \pm 0.123	0.868 \pm 0.103	0.136 \pm 0.118	0.722 \pm 0.027	0.590
Uncert. \dagger	1.331 \pm 0.520	0.699 \pm 0.124	0.790 \pm 0.026	-0.640 \pm 0.325	0.745 \pm 0.040	0.489
Uncert.	0.642 \pm 0.147	0.553 \pm 0.129	0.874 \pm 0.099	0.297 \pm 0.183	0.553 \pm 0.015	0.462
KL-Div.	-0.784 \pm 1.571	0.613 \pm 0.082	0.870 \pm 0.127	-0.203 \pm 0.570	0.737 \pm 0.035	0.434
Rank \dagger	-0.157 \pm 0.576	0.643 \pm 0.064	0.808 \pm 0.008	-0.477 \pm 0.824	0.741 \pm 0.031	0.420
Rank	0.116 \pm 0.576	0.468 \pm 0.033	0.652 \pm 0.045	-0.068 \pm 0.285	0.524 \pm 0.027	0.419
Prob. \jmath	-0.190 \pm 0.747	0.496 \pm 0.049	0.578 \pm 0.027	-0.626 \pm 0.854	0.534 \pm 0.013	0.382
Random	-3.009 \pm 2.890	0.530 \pm 0.060	0.715 \pm 0.037	-0.038 \pm 0.461	0.591 \pm 0.012	0.098
Uncert. \jmath	-4.523 \pm 5.002	0.451 \pm 0.068	0.668 \pm 0.070	0.360 \pm 0.105	0.534 \pm 0.013	-0.049

Strategy	Cardiomegaly	Lung Lesion	Lung Opacity	Pneumonia	Pneumothorax	Mean
AUPRC \ddagger	2.458 \pm 0.268	2.158 \pm 0.482	2.735 \pm 0.464	3.162 \pm 0.383	15.830 \pm 5.601	4.085
AUROC \ddagger	2.378 \pm 0.251	2.138 \pm 0.469	2.745 \pm 0.470	2.848 \pm 0.316	13.842 \pm 4.585	3.830
KL-Div. \dagger	0.827 \pm 0.009	0.679 \pm 0.250	0.711 \pm 0.063	0.727 \pm 0.026	0.861 \pm 0.024	0.814
Prob.	0.471 \pm 0.038	0.519 \pm 0.046	0.173 \pm 0.148	0.712 \pm 0.048	1.249 \pm 0.094	0.590
Uncert. \dagger	0.803 \pm 0.012	0.184 \pm 0.270	-0.069 \pm 0.111	0.723 \pm 0.046	0.326 \pm 0.207	0.489
Uncert.	0.477 \pm 0.035	0.224 \pm 0.340	0.181 \pm 0.070	0.625 \pm 0.030	0.192 \pm 0.082	0.462
KL-Div.	0.288 \pm 0.055	0.468 \pm 0.419	0.466 \pm 0.061	0.595 \pm 0.049	1.285 \pm 0.172	0.434
Rank \dagger	0.555 \pm 0.041	-0.005 \pm 0.389	0.715 \pm 0.109	0.809 \pm 0.034	0.573 \pm 0.150	0.420
Rank	0.234 \pm 0.057	0.554 \pm 0.118	0.214 \pm 0.099	0.688 \pm 0.053	0.810 \pm 0.388	0.419
Prob. \jmath	0.427 \pm 0.037	0.704 \pm 0.458	0.524 \pm 0.057	0.574 \pm 0.072	0.801 \pm 0.041	0.382
Random	0.227 \pm 0.042	0.518 \pm 0.037	0.362 \pm 0.020	0.505 \pm 0.048	0.584 \pm 0.155	0.098
Uncert. \jmath	0.304 \pm 0.125	0.033 \pm 0.364	0.225 \pm 0.012	0.659 \pm 0.046	0.801 \pm 0.041	-0.049

Table 29: Acquisition performance on MIMIC Symile, presenting results for AUROC strategies. For each metric, strategies are sorted by their descending $G_{\text{full}} \uparrow$ values. Oracle strategies are marked with ‡, upper-bound heuristics with † and unimodal baselines with j. Here, Image is imputed by Lab and ECG.

Strategy	Fracture	Enl. Card.	Consolidation	Atelectasis	Edema	Mean
AUROC ‡	2.679 ±0.496	3.081 ±0.257	2.539 ±0.150	5.098 ±0.624	2.119 ±0.086	3.911
AUPRC ‡	2.677 ±0.497	2.998 ±0.252	2.497 ±0.157	5.004 ±0.610	1.955 ±0.077	3.879
KL-Div. †	1.006 ±0.111	1.105 ±0.082	0.880 ±0.033	0.703 ±0.095	1.017 ±0.023	0.922
Rank †	0.760 ±0.142	1.076 ±0.073	0.993 ±0.052	0.930 ±0.136	1.036 ±0.023	0.884
Prob.	0.883 ±0.111	0.563 ±0.062	0.620 ±0.034	0.706 ±0.096	0.593 ±0.010	0.628
KL-Div.	0.770 ±0.122	0.736 ±0.077	0.711 ±0.031	0.049 ±0.191	0.535 ±0.015	0.512
Uncert.	0.785 ±0.085	0.535 ±0.064	0.728 ±0.050	0.545 ±0.088	0.556 ±0.015	0.505
Uncert. †	0.975 ±0.140	0.877 ±0.083	0.886 ±0.065	0.300 ±0.043	0.634 ±0.018	0.494
Uncert. j	0.514 ±0.151	0.495 ±0.038	0.529 ±0.045	0.466 ±0.056	0.545 ±0.014	0.474
Random	0.005 ±0.204	0.386 ±0.047	0.467 ±0.031	0.373 ±0.145	0.472 ±0.014	0.425
Prob. j	0.265 ±0.046	0.463 ±0.035	0.461 ±0.037	0.268 ±0.136	0.401 ±0.009	0.421
Rank	0.594 ±0.082	0.335 ±0.079	0.423 ±0.070	0.130 ±0.226	0.466 ±0.012	0.392

Strategy	Cardiomegaly	Lung Lesion	Lung Opacity	Pneumonia	Pneumothorax	Mean
AUROC ‡	2.552 ±0.116	3.249 ±0.605	4.964 ±0.431	3.736 ±0.369	9.096 ±1.223	3.911
AUPRC ‡	2.346 ±0.107	3.207 ±0.582	4.794 ±0.405	3.500 ±0.354	9.812 ±1.335	3.879
KL-Div. †	0.910 ±0.030	0.517 ±0.243	0.811 ±0.052	0.967 ±0.061	1.298 ±0.121	0.922
Rank †	1.047 ±0.032	0.545 ±0.093	0.839 ±0.055	1.010 ±0.056	0.607 ±0.109	0.884
Prob.	0.453 ±0.016	0.680 ±0.352	0.391 ±0.064	0.443 ±0.042	0.950 ±0.096	0.628
KL-Div.	0.374 ±0.016	0.403 ±0.210	0.457 ±0.079	0.518 ±0.036	0.565 ±0.103	0.512
Uncert.	0.476 ±0.011	0.289 ±0.162	0.366 ±0.052	0.599 ±0.031	0.171 ±0.078	0.505
Uncert. †	0.514 ±0.027	0.200 ±0.151	0.293 ±0.058	0.729 ±0.044	-0.468 ±0.155	0.494
Uncert. j	0.457 ±0.013	0.241 ±0.261	0.381 ±0.040	0.588 ±0.023	0.520 ±0.055	0.474
Random	0.418 ±0.015	0.739 ±0.256	0.530 ±0.100	0.493 ±0.051	0.362 ±0.101	0.425
Prob. j	0.437 ±0.011	0.448 ±0.230	0.496 ±0.057	0.449 ±0.027	0.519 ±0.055	0.421
Rank	0.408 ±0.017	0.581 ±0.211	0.493 ±0.063	0.487 ±0.054	-0.000 ±0.092	0.392

Table 30: Acquisition performance on MIMIC Symile, presenting results for AUPRC strategies. For each metric, strategies are sorted by their descending $G_{\text{full}} \uparrow$ values. Oracle strategies are marked with ‡, upper-bound heuristics with † and unimodal baselines with j. Here, Image is imputed by Lab and ECG.

Strategy	Fracture	Enl. Card.	Consolidation	Atelectasis	Edema	Mean
AUPRC ‡	3.244 ±0.899	2.660 ±0.365	3.290 ±0.320	3.756 ±0.538	2.484 ±0.159	4.063
AUROC ‡	3.171 ±0.850	2.463 ±0.315	2.940 ±0.288	3.790 ±0.546	2.347 ±0.154	3.588
KL-Div. †	1.111 ±0.223	0.983 ±0.104	0.998 ±0.079	0.674 ±0.088	1.014 ±0.034	0.939
Rank †	0.503 ±0.538	0.727 ±0.084	1.063 ±0.108	0.762 ±0.088	1.014 ±0.036	0.822
Prob.	0.821 ±0.184	0.581 ±0.048	0.714 ±0.055	0.478 ±0.083	0.648 ±0.012	0.610
KL-Div.	1.238 ±0.634	0.636 ±0.075	0.754 ±0.075	0.330 ±0.146	0.467 ±0.020	0.585
Prob. j	0.196 ±0.143	0.567 ±0.044	0.520 ±0.042	0.442 ±0.111	0.572 ±0.014	0.515
Uncert.	1.018 ±0.316	0.516 ±0.058	0.783 ±0.081	0.285 ±0.039	0.505 ±0.015	0.500
Uncert. †	0.826 ±0.166	0.950 ±0.103	0.923 ±0.060	0.143 ±0.041	0.636 ±0.029	0.493
Rank	1.133 ±0.543	0.375 ±0.081	0.582 ±0.103	0.139 ±0.174	0.469 ±0.018	0.491
Uncert. j	0.843 ±0.289	0.410 ±0.050	0.562 ±0.061	0.275 ±0.038	0.521 ±0.019	0.467
Random	-0.073 ±0.199	0.397 ±0.084	0.556 ±0.053	0.411 ±0.100	0.470 ±0.013	0.406

Strategy	Cardiomegaly	Lung Lesion	Lung Opacity	Pneumonia	Pneumothorax	Mean
AUPRC ‡	2.494 ±0.181	2.376 ±0.472	4.061 ±0.416	4.964 ±0.520	11.303 ±0.974	4.063
AUROC ‡	2.526 ±0.178	2.362 ±0.461	4.092 ±0.418	4.454 ±0.466	7.738 ±0.631	3.588
KL-Div. †	0.823 ±0.022	0.809 ±0.139	0.873 ±0.081	1.002 ±0.049	1.105 ±0.058	0.939
Rank †	1.012 ±0.039	0.573 ±0.099	0.952 ±0.093	1.027 ±0.058	0.591 ±0.077	0.822
Prob.	0.448 ±0.029	0.569 ±0.185	0.404 ±0.073	0.481 ±0.039	0.959 ±0.048	0.610
KL-Div.	0.346 ±0.023	0.560 ±0.075	0.524 ±0.074	0.441 ±0.037	0.551 ±0.075	0.585
Prob. j	0.555 ±0.015	0.448 ±0.096	0.607 ±0.062	0.528 ±0.032	0.715 ±0.033	0.515
Uncert.	0.346 ±0.019	0.323 ±0.061	0.279 ±0.041	0.466 ±0.034	0.475 ±0.062	0.500
Uncert. †	0.394 ±0.037	0.201 ±0.029	0.184 ±0.050	0.624 ±0.044	0.054 ±0.058	0.493
Rank	0.390 ±0.023	0.523 ±0.091	0.359 ±0.088	0.449 ±0.034	0.492 ±0.045	0.491
Uncert. j	0.334 ±0.018	0.257 ±0.049	0.262 ±0.035	0.491 ±0.029	0.715 ±0.033	0.467
Random	0.415 ±0.015	0.575 ±0.228	0.368 ±0.069	0.432 ±0.057	0.510 ±0.090	0.406

Table 31: Acquisition performance on MIMIC Symile, presenting results for AUROC strategies. For each metric, strategies are sorted by their descending $G_{\text{full}} \uparrow$ values. Oracle strategies are marked with \ddagger , upper-bound heuristics with \dagger and unimodal baselines with \jmath . Here, Lab is imputed by Image .

Strategy	Fracture	Enl. Card.	Consolidation	Atelectasis	Edema	Mean
AUROC \ddagger	2.404 \pm 0.448	5.403 \pm 1.547	2.446 \pm 0.350	4.261	4.715 \pm 0.988	6.306
AUPRC \ddagger	2.201 \pm 0.321	5.125 \pm 1.430	2.293 \pm 0.316	3.979	4.385 \pm 0.925	6.096
KL-Div.	0.443 \pm 0.028	0.503 \pm 0.316	0.523 \pm 0.078	0.383	0.193 \pm 0.090	0.684
KL-Div. \dagger	0.901 \pm 0.104	0.727 \pm 0.113	0.874 \pm 0.045	0.807	0.670 \pm 0.093	0.634
Rank \dagger	0.490 \pm 0.208	0.872 \pm 0.019	0.873 \pm 0.081	1.691	0.627 \pm 0.148	0.604
Uncert. \jmath	0.515 \pm 0.062	0.781 \pm 0.101	0.394 \pm 0.106	0.310	0.636 \pm 0.041	0.487
Random	0.366 \pm 0.519	0.662 \pm 0.085	0.504 \pm 0.111	0.087	0.229 \pm 0.142	0.419
Rank \jmath	0.105 \pm 0.251	0.444 \pm 0.144	0.567 \pm 0.112	0.267	0.449 \pm 0.055	0.390
Prob.	0.087 \pm 0.217	0.428 \pm 0.155	0.574 \pm 0.117	0.221	0.457 \pm 0.056	0.380
Uncert.	0.074 \pm 0.187	0.593 \pm 0.168	0.415 \pm 0.107	0.278	0.624 \pm 0.029	0.311
Uncert. \dagger	-0.204 \pm 0.122	0.690 \pm 0.193	0.319 \pm 0.084	-0.511	0.507 \pm 0.100	0.154
Rank	0.848 \pm 0.131	-0.103 \pm 0.100	0.309 \pm 0.073	-0.390	0.463 \pm 0.125	-0.139

Strategy	Cardiomegaly	Lung Lesion	Lung Opacity	Pneumonia	Pneumothorax	Mean
AUROC \ddagger	11.461	9.175 \pm 4.619	10.440 \pm 4.341	4.058 \pm 0.233	8.693 \pm 2.295	6.306
AUPRC \ddagger	11.109	9.165 \pm 4.679	9.894 \pm 4.024	3.780 \pm 0.189	9.031 \pm 2.515	6.096
KL-Div.	0.477	3.593 \pm 0.801	0.055 \pm 1.005	0.630 \pm 0.024	0.037 \pm 0.291	0.684
KL-Div. \dagger	0.359	0.043 \pm 1.152	0.608 \pm 0.141	0.793 \pm 0.054	0.561 \pm 0.157	0.634
Rank \dagger	0.396	0.640 \pm 1.426	-0.637 \pm 0.091	0.797 \pm 0.031	0.296 \pm 0.208	0.604
Uncert. \jmath	0.277	0.172 \pm 0.139	0.706 \pm 0.448	0.501 \pm 0.107	0.575 \pm 0.126	0.487
Random	-0.872	2.030 \pm 1.179	0.329 \pm 0.460	0.490 \pm 0.124	0.365 \pm 0.137	0.419
Prob. \jmath	0.471	1.854 \pm 1.407	-1.445 \pm 0.962	0.615 \pm 0.016	0.575 \pm 0.126	0.390
Prob.	0.551	2.347 \pm 0.438	-2.017 \pm 0.592	0.581 \pm 0.030	0.575 \pm 0.116	0.380
Uncert.	0.646	0.200 \pm 0.174	-0.684 \pm 0.697	0.401 \pm 0.073	0.566 \pm 0.142	0.311
Uncert. \dagger	0.507	1.296 \pm 0.137	-1.510 \pm 0.311	0.320 \pm 0.119	0.128 \pm 0.257	0.154
Rank	-0.413	-1.673 \pm 4.164	-0.741 \pm 0.142	0.398 \pm 0.150	-0.084 \pm 0.300	-0.139

Table 32: Acquisition performance on MIMIC Symile, presenting results for AUPRC strategies. For each metric, strategies are sorted by their descending $G_{\text{full}} \uparrow$ values. Oracle strategies are marked with \ddagger , upper-bound heuristics with \dagger and unimodal baselines with \jmath . Here, Lab is imputed by Image .

Strategy	Fracture	Enl. Card.	Consolidation	Atelectasis	Edema	Mean
AUPRC \ddagger	2.142 \pm 0.360	3.772 \pm 0.624	4.042 \pm 1.747	—	5.560 \pm 1.093	4.751
AUROC \ddagger	2.329 \pm 0.461	3.452 \pm 0.513	3.960 \pm 1.724	—	5.110 \pm 0.828	4.207
KL-Div. \dagger	0.916 \pm 0.056	0.648 \pm 0.079	0.997 \pm 0.160	—	0.568 \pm 0.132	0.699
KL-Div.	0.499 \pm 0.117	0.481 \pm 0.203	0.413 \pm 0.187	—	0.269 \pm 0.189	0.680
Rank \dagger	0.400 \pm 0.206	0.686 \pm 0.095	1.106 \pm 0.342	—	0.603 \pm 0.139	0.590
Prob. \jmath	-0.362 \pm 0.445	0.629 \pm 0.007	0.325 \pm 0.326	—	0.672 \pm 0.112	0.572
Prob.	-0.381 \pm 0.441	0.618 \pm 0.008	0.339 \pm 0.318	—	0.681 \pm 0.114	0.442
Uncert. \jmath	0.455 \pm 0.060	0.484 \pm 0.099	0.537 \pm 0.231	—	0.585 \pm 0.160	0.440
Random	0.283 \pm 0.513	0.635 \pm 0.001	0.303 \pm 0.231	—	0.253 \pm 0.115	0.356
Rank	0.824 \pm 0.103	-0.157 \pm 0.006	-0.044 \pm 0.404	—	0.246 \pm 0.115	0.186
Uncert. \dagger	-1.106 \pm 0.446	0.506 \pm 0.100	0.258 \pm 0.136	—	0.477 \pm 0.270	0.153
Uncert.	-0.429 \pm 0.473	0.415 \pm 0.161	0.541 \pm 0.220	—	0.570 \pm 0.164	0.124

Strategy	Cardiomegaly	Lung Lesion	Lung Opacity	Pneumonia	Pneumothorax	Mean
AUPRC \ddagger	—	3.615 \pm 0.753	3.868	4.819 \pm 0.587	10.192 \pm 4.607	4.751
AUROC \ddagger	—	3.623 \pm 0.745	3.977	4.465 \pm 0.417	6.742 \pm 2.483	4.207
KL-Div. \dagger	—	0.503 \pm 0.458	0.513	0.865 \pm 0.112	0.585 \pm 0.087	0.699
KL-Div.	—	1.905 \pm 0.140	0.987	0.723 \pm 0.115	0.162 \pm 0.123	0.680
Rank \dagger	—	0.974 \pm 0.661	-0.184	0.709 \pm 0.066	0.426 \pm 0.076	0.590
Prob. \jmath	—	1.363 \pm 0.660	0.282	0.708 \pm 0.061	0.963 \pm 0.071	0.572
Prob.	—	1.133 \pm 0.483	-0.486	0.659 \pm 0.050	0.976 \pm 0.085	0.442
Uncert. \jmath	—	0.053 \pm 0.070	0.109	0.330 \pm 0.055	0.963 \pm 0.071	0.440
Random	—	0.088 \pm 0.319	0.534	0.455 \pm 0.187	0.296 \pm 0.199	0.356
Rank	—	0.274 \pm 1.456	-0.263	0.304 \pm 0.238	0.301 \pm 0.113	0.186
Uncert. \dagger	—	0.621 \pm 0.157	-0.406	0.202 \pm 0.069	0.674 \pm 0.151	0.153
Uncert.	—	-0.397 \pm 0.271	-0.893	0.261 \pm 0.024	0.925 \pm 0.045	0.124

Table 33: Acquisition performance on MIMIC Symile, presenting results for AUROC strategies. For each metric, strategies are sorted by their descending $G_{\text{full}} \uparrow$ values. Oracle strategies are marked with ‡, upper-bound heuristics with † and unimodal baselines with j. Here, Lab is imputed by ECG.

Strategy	Fracture	Enl. Card.	Consolidation	Atelectasis	Edema	Mean
AUROC ‡	2.830 ± 1.006	6.507 ± 2.813	1.993 ± 0.252	13.751 ± 3.349	5.706 ± 1.964	7.637
AUPRC ‡	2.812 ± 1.015	6.130 ± 2.582	1.926 ± 0.224	13.739 ± 3.350	5.766 ± 1.941	7.595
KL-Div.	0.735 ± 0.130	1.221 ± 0.208	0.670 ± 0.136	4.739 ± 1.683	2.234 ± 0.684	2.096
KL-Div. †	0.807 ± 0.072	1.043 ± 0.176	0.855 ± 0.056	0.933 ± 0.345	0.841 ± 0.028	0.727
Rank	0.395 ± 0.117	0.160 ± 0.439	0.298 ± 0.039	1.303 ± 1.170	-1.119 ± 0.726	0.619
Uncert. j	0.421 ± 0.290	0.544 ± 0.303	0.456 ± 0.081	0.431 ± 0.170	0.324 ± 0.024	0.574
Prob. j	0.069 ± 0.066	0.372 ± 0.420	0.505 ± 0.102	0.161 ± 0.787	0.324 ± 0.024	0.521
Uncert. †	0.665 ± 0.104	0.273 ± 0.305	0.688 ± 0.056	-0.218 ± 1.149	0.568 ± 0.041	0.437
Rank †	0.454 ± 0.258	0.880 ± 0.255	0.756 ± 0.027	0.462 ± 0.641	0.398 ± 0.151	0.290
Random	0.117 ± 0.418	0.737 ± 0.338	0.531 ± 0.041	-0.400 ± 1.001	0.107 ± 0.142	0.189
Prob.	0.569 ± 0.115	0.126 ± 0.370	0.775 ± 0.075	-4.498 ± 1.913	2.255 ± 0.646	-0.333
Uncert.	0.612 ± 0.125	0.499 ± 0.346	0.773 ± 0.078	-4.102 ± 1.614	0.071 ± 0.175	-0.744

Strategy	Cardiomegaly	Lung Lesion	Lung Opacity	Pneumonia	Pneumothorax	Mean
AUROC ‡	—	13.135 ± 7.362	9.638 ± 2.483	3.075 ± 0.250	12.098 ± 2.848	7.637
AUPRC ‡	—	13.203 ± 7.497	9.552 ± 2.486	2.943 ± 0.186	12.285 ± 2.892	7.595
KL-Div.	—	4.580 ± 1.600	2.539 ± 0.511	0.646 ± 0.117	1.494 ± 0.303	2.096
KL-Div. †	—	-0.560 ± 1.556	0.982 ± 0.050	0.761 ± 0.031	0.884 ± 0.076	0.727
Rank	—	2.305 ± 0.688	1.567 ± 0.771	0.642 ± 0.053	0.017 ± 0.983	0.619
Uncert. j	—	1.397 ± 1.699	0.190 ± 0.028	0.541 ± 0.082	0.867 ± 0.198	0.574
Prob. j	—	0.657 ± 2.145	1.107 ± 0.654	0.626 ± 0.050	0.867 ± 0.198	0.521
Uncert. †	—	2.300 ± 1.585	0.157 ± 0.299	0.563 ± 0.120	-1.060 ± 0.540	0.437
Rank †	—	-2.847 ± 4.746	1.545 ± 0.340	0.776 ± 0.020	0.185 ± 0.511	0.290
Random	—	-0.793 ± 3.159	0.931 ± 0.196	0.555 ± 0.085	-0.086 ± 0.456	0.189
Prob.	—	-2.903 ± 3.257	-1.391 ± 0.383	0.455 ± 0.124	1.617 ± 0.337	-0.333
Uncert.	—	-2.336 ± 1.344	-1.290 ± 0.341	0.494 ± 0.140	-1.416 ± 0.454	-0.744

Table 34: Acquisition performance on MIMIC Symile, presenting results for AUPRC strategies. For each metric, strategies are sorted by their descending $G_{\text{full}} \uparrow$ values. Oracle strategies are marked with ‡, upper-bound heuristics with † and unimodal baselines with j. Here, Lab is imputed by ECG.

Strategy	Fracture	Enl. Card.	Consolidation	Atelectasis	Edema	Mean
AUPRC ‡	4.231 ± 2.318	4.018 ± 1.224	2.093 ± 0.267	6.269 ± 0.383	5.741 ± 1.374	6.317
AUROC ‡	4.202 ± 2.309	3.797 ± 1.010	2.025 ± 0.267	6.278 ± 0.382	5.522 ± 1.430	6.043
KL-Div.	0.721 ± 0.166	1.292 ± 0.411	0.780 ± 0.157	1.533 ± 0.215	2.267 ± 0.487	1.779
Prob. j	-0.282 ± 0.309	0.672 ± 0.126	0.594 ± 0.102	0.769 ± 0.144	0.645 ± 0.093	1.112
KL-Div. †	0.924 ± 0.069	0.825 ± 0.017	0.883 ± 0.030	0.717 ± 0.570	0.897 ± 0.019	0.972
Rank †	0.030 ± 0.698	0.643 ± 0.103	0.846 ± 0.041	0.619 ± 1.260	0.351 ± 0.208	0.900
Prob.	0.532 ± 0.179	1.116 ± 0.598	0.920 ± 0.086	-0.332 ± 0.041	2.300 ± 0.464	0.751
Random	-0.458 ± 0.636	0.631 ± 0.184	0.659 ± 0.051	0.925 ± 0.146	0.264 ± 0.154	0.556
Uncert. †	0.730 ± 0.109	0.793 ± 0.209	0.784 ± 0.034	0.030 ± 0.615	0.740 ± 0.024	0.550
Rank	0.092 ± 0.485	0.353 ± 0.268	0.372 ± 0.058	-0.032 ± 0.027	-0.641 ± 0.441	0.458
Uncert. j	-1.088 ± 1.658	0.451 ± 0.118	0.605 ± 0.085	0.152 ± 0.036	0.645 ± 0.093	0.260
Uncert.	0.580 ± 0.189	1.080 ± 0.651	0.930 ± 0.088	-0.549 ± 0.088	0.351 ± 0.131	0.145

Strategy	Cardiomegaly	Lung Lesion	Lung Opacity	Pneumonia	Pneumothorax	Mean
AUPRC ‡	—	8.610 ± 6.961	5.951 ± 0.522	7.534 ± 2.031	12.402 ± 2.525	6.317
AUROC ‡	—	8.593 ± 6.932	5.993 ± 0.479	6.573 ± 1.760	11.403 ± 2.388	6.043
KL-Div.	—	5.709 ± 4.716	1.662 ± 0.095	0.667 ± 0.138	1.378 ± 0.274	1.779
Prob. j	—	5.083 ± 4.111	0.941 ± 0.112	0.581 ± 0.069	1.005 ± 0.151	1.112
KL-Div. †	—	2.009 ± 1.288	0.811 ± 0.344	0.772 ± 0.111	0.910 ± 0.021	0.972
Rank †	—	3.099 ± 2.419	1.137 ± 0.603	0.812 ± 0.056	0.561 ± 0.207	0.900
Prob.	—	0.927 ± 0.497	-0.770 ± 0.192	0.647 ± 0.140	1.420 ± 0.260	0.751
Random	—	1.804 ± 0.871	0.053 ± 0.419	0.510 ± 0.130	0.616 ± 0.097	0.556
Uncert. †	—	1.431 ± 1.304	-0.150 ± 0.288	0.555 ± 0.159	0.032 ± 0.114	0.550
Rank	—	1.988 ± 1.092	0.643 ± 0.448	0.564 ± 0.136	0.788 ± 0.367	0.458
Uncert. j	—	-0.023 ± 0.028	0.078 ± 0.073	0.516 ± 0.137	1.005 ± 0.151	0.260
Uncert.	—	-0.954 ± 0.761	-0.714 ± 0.206	0.591 ± 0.192	-0.013 ± 0.125	0.145

Table 35: Acquisition performance on MIMIC Symile, presenting results for AUROC strategies. For each metric, strategies are sorted by their descending $G_{\text{full}} \uparrow$ values. Oracle strategies are marked with \ddagger , upper-bound heuristics with \dagger and unimodal baselines with . . Here, Lab is imputed by Image and ECG.

Strategy	Fracture	Enl. Card.	Consolidation	Atelectasis	Edema	Mean
AUROC \ddagger	2.416 \pm 0.727	2.670 \pm 0.218	3.090 \pm 0.355	3.712 \pm 0.446	2.174 \pm 0.050	4.233
AUPRC \ddagger	2.373 \pm 0.691	2.609 \pm 0.213	3.018 \pm 0.347	3.613 \pm 0.428	2.127 \pm 0.050	4.174
KL-Div.	1.088 \pm 0.224	0.875 \pm 0.022	0.667 \pm 0.039	1.193 \pm 0.091	0.885 \pm 0.008	1.035
KL-Div. \dagger	1.165 \pm 0.267	0.883 \pm 0.024	1.050 \pm 0.058	1.092 \pm 0.080	0.925 \pm 0.006	0.981
Rank \dagger	1.373 \pm 0.427	0.811 \pm 0.024	1.076 \pm 0.050	0.904 \pm 0.066	0.888 \pm 0.008	0.883
Prob. .	0.088 \pm 0.147	0.529 \pm 0.030	0.376 \pm 0.025	0.804 \pm 0.069	0.324 \pm 0.007	0.521
Uncert. \dagger	1.008 \pm 0.213	0.720 \pm 0.056	0.781 \pm 0.030	-0.092 \pm 0.044	0.675 \pm 0.027	0.494
Uncert. .	0.772 \pm 0.126	0.492 \pm 0.034	0.627 \pm 0.033	0.183 \pm 0.030	0.506 \pm 0.019	0.469
Uncert. \ddagger	0.981 \pm 0.208	0.718 \pm 0.054	0.736 \pm 0.028	-0.143 \pm 0.044	0.636 \pm 0.027	0.448
Prob.	1.084 \pm 0.241	0.647 \pm 0.048	0.657 \pm 0.039	-0.270 \pm 0.085	0.767 \pm 0.008	0.390
Rank	-0.190 \pm 0.547	0.273 \pm 0.051	0.415 \pm 0.044	0.448 \pm 0.088	0.192 \pm 0.017	0.350
Random	0.212 \pm 0.278	0.404 \pm 0.030	0.503 \pm 0.030	0.247 \pm 0.113	0.439 \pm 0.014	0.268

Strategy	Cardiomegaly	Lung Lesion	Lung Opacity	Pneumonia	Pneumothorax	Mean
AUROC \ddagger	2.438 \pm 0.113	6.864 \pm 1.482	6.398 \pm 0.783	4.889 \pm 0.635	7.680 \pm 0.820	4.233
AUPRC \ddagger	2.430 \pm 0.113	6.687 \pm 1.431	6.099 \pm 0.731	4.629 \pm 0.591	8.157 \pm 0.892	4.174
KL-Div.	0.887 \pm 0.006	2.529 \pm 0.817	0.914 \pm 0.102	0.661 \pm 0.036	0.651 \pm 0.058	1.035
KL-Div. \dagger	0.887 \pm 0.007	1.245 \pm 0.526	0.863 \pm 0.089	0.809 \pm 0.032	0.892 \pm 0.057	0.981
Rank \dagger	0.777 \pm 0.012	0.383 \pm 0.609	0.822 \pm 0.095	0.940 \pm 0.026	0.855 \pm 0.073	0.883
Prob. .	0.260 \pm 0.006	1.476 \pm 0.565	0.538 \pm 0.131	0.387 \pm 0.044	0.425 \pm 0.039	0.521
Uncert. \dagger	0.878 \pm 0.008	0.148 \pm 0.198	0.045 \pm 0.084	0.831 \pm 0.047	-0.059 \pm 0.078	0.494
Uncert. .	0.693 \pm 0.009	-0.022 \pm 0.318	0.281 \pm 0.070	0.730 \pm 0.044	0.425 \pm 0.039	0.469
Uncert. \ddagger	0.882 \pm 0.007	-0.351 \pm 0.366	0.040 \pm 0.080	0.838 \pm 0.047	0.141 \pm 0.068	0.448
Prob.	0.718 \pm 0.008	-0.467 \pm 0.520	-0.425 \pm 0.153	0.445 \pm 0.063	0.743 \pm 0.056	0.390
Rank	0.326 \pm 0.026	0.909 \pm 0.407	0.492 \pm 0.087	0.561 \pm 0.035	0.079 \pm 0.133	0.350
Random	0.334 \pm 0.016	-0.383 \pm 0.692	0.212 \pm 0.120	0.492 \pm 0.033	0.216 \pm 0.078	0.268

Table 36: Acquisition performance on MIMIC Symile, presenting results for AUPRC strategies. For each metric, strategies are sorted by their descending $G_{\text{full}} \uparrow$ values. Oracle strategies are marked with \ddagger , upper-bound heuristics with \dagger and unimodal baselines with . . Here, Lab is imputed by Image and ECG.

Strategy	Fracture	Enl. Card.	Consolidation	Atelectasis	Edema	Mean
AUPRC \ddagger	1.965 \pm 0.497	2.573 \pm 0.236	3.714 \pm 0.473	2.444 \pm 0.174	2.962 \pm 0.166	3.748
AUROC \ddagger	1.958 \pm 0.488	2.455 \pm 0.211	3.425 \pm 0.436	2.481 \pm 0.176	2.778 \pm 0.157	3.328
KL-Div. \dagger	0.961 \pm 0.228	0.918 \pm 0.033	1.042 \pm 0.082	0.985 \pm 0.053	0.954 \pm 0.013	0.878
KL-Div.	0.914 \pm 0.236	0.921 \pm 0.039	0.587 \pm 0.056	1.038 \pm 0.046	0.925 \pm 0.011	0.835
Rank \dagger	0.899 \pm 0.233	0.896 \pm 0.037	1.138 \pm 0.112	0.886 \pm 0.051	0.922 \pm 0.019	0.820
Prob. .	0.265 \pm 0.173	0.475 \pm 0.038	0.424 \pm 0.060	0.712 \pm 0.038	0.344 \pm 0.012	0.518
Uncert. .	0.573 \pm 0.099	0.564 \pm 0.041	0.601 \pm 0.074	0.152 \pm 0.016	0.527 \pm 0.023	0.485
Uncert. \dagger	0.610 \pm 0.076	0.741 \pm 0.066	0.736 \pm 0.075	-0.096 \pm 0.042	0.718 \pm 0.030	0.482
Uncert.	0.662 \pm 0.086	0.759 \pm 0.070	0.723 \pm 0.084	-0.131 \pm 0.030	0.691 \pm 0.028	0.482
Prob.	0.811 \pm 0.100	0.619 \pm 0.048	0.677 \pm 0.026	-0.376 \pm 0.097	0.848 \pm 0.014	0.469
Random	0.504 \pm 0.107	0.449 \pm 0.031	0.612 \pm 0.063	0.242 \pm 0.096	0.471 \pm 0.024	0.431
Rank	0.516 \pm 0.085	0.343 \pm 0.047	0.412 \pm 0.046	0.355 \pm 0.050	0.202 \pm 0.019	0.370

Strategy	Cardiomegaly	Lung Lesion	Lung Opacity	Pneumonia	Pneumothorax	Mean
AUPRC \ddagger	3.070 \pm 0.202	2.036 \pm 0.167	3.622 \pm 0.323	5.602 \pm 0.520	9.490 \pm 1.511	3.748
AUROC \ddagger	2.907 \pm 0.188	2.050 \pm 0.170	3.696 \pm 0.332	4.856 \pm 0.452	6.677 \pm 0.867	3.328
KL-Div. \dagger	0.890 \pm 0.014	0.761 \pm 0.095	0.815 \pm 0.055	0.824 \pm 0.051	0.629 \pm 0.127	0.878
KL-Div.	0.938 \pm 0.017	0.964 \pm 0.166	0.923 \pm 0.067	0.675 \pm 0.045	0.466 \pm 0.230	0.835
Rank \dagger	0.807 \pm 0.020	0.452 \pm 0.119	0.721 \pm 0.057	0.920 \pm 0.047	0.560 \pm 0.254	0.820
Prob. .	0.266 \pm 0.012	0.860 \pm 0.124	0.576 \pm 0.066	0.479 \pm 0.048	0.781 \pm 0.148	0.518
Uncert. .	0.720 \pm 0.018	0.158 \pm 0.050	0.219 \pm 0.024	0.560 \pm 0.038	0.781 \pm 0.148	0.485
Uncert. \dagger	0.880 \pm 0.018	0.171 \pm 0.115	0.034 \pm 0.040	0.616 \pm 0.032	0.411 \pm 0.168	0.482
Uncert.	0.932 \pm 0.018	0.020 \pm 0.100	-0.017 \pm 0.041	0.606 \pm 0.037	0.573 \pm 0.244	0.482
Prob.	0.756 \pm 0.008	0.182 \pm 0.257	-0.400 \pm 0.112	0.669 \pm 0.034	0.906 \pm 0.035	0.469
Random	0.375 \pm 0.027	0.362 \pm 0.172	0.296 \pm 0.055	0.464 \pm 0.057	0.539 \pm 0.133	0.431
Rank	0.368 \pm 0.036	0.486 \pm 0.142	0.363 \pm 0.070	0.418 \pm 0.039	0.234 \pm 0.154	0.370

Table 37: Acquisition performance on MIMIC Symile, presenting results for AUROC strategies. For each metric, strategies are sorted by their descending $G_{\text{full}} \uparrow$ values. Oracle strategies are marked with \ddagger , upper-bound heuristics with \dagger and unimodal baselines with \jmath . Here, ECG is imputed by Image

Strategy	Fracture	Enl. Card.	Consolidation	Atelectasis	Edema	Mean
AUPRC \ddagger	3.471 \pm 1.673	20.672 \pm 5.891	—	—	36.396	29.159
AUROC \ddagger	3.489 \pm 1.656	21.015 \pm 5.247	—	—	37.701	28.964
KL-Div.	0.084 \pm 0.465	-1.318 \pm 0.868	—	—	6.736	3.317
Uncert. \jmath	0.637 \pm 0.113	-0.592 \pm 0.877	—	—	0.868	0.515
Prob.	0.542 \pm 0.247	0.096 \pm 0.156	—	—	-0.629	0.507
Random	0.440 \pm 0.455	0.389 \pm 1.478	—	—	-1.424	0.484
Uncert. \dagger	0.648 \pm 0.497	-0.099 \pm 0.724	—	—	0.379	0.135
Rank \dagger	0.550 \pm 0.379	-2.342 \pm 1.928	—	—	-1.276	0.122
Rank	-0.355 \pm 0.092	-1.669 \pm 0.386	—	—	1.017	0.062
KL-Div. \dagger	0.546 \pm 0.073	0.036 \pm 0.994	—	—	0.028	0.032
Prob. \jmath	0.507 \pm 0.072	0.236 \pm 0.361	—	—	-0.431	-0.192
Uncert.	0.672 \pm 0.578	0.131 \pm 0.351	—	—	-1.407	-0.817

Strategy	Cardiomegaly	Lung Lesion	Lung Opacity	Pneumonia	Pneumothorax	Mean
AUPRC \ddagger	9.842 \pm 4.172	3.063 \pm 1.274	7.269	—	123.400	29.159
AUROC \ddagger	10.077 \pm 4.361	2.979 \pm 1.139	7.291	—	120.197	28.964
KL-Div.	0.564 \pm 0.077	-0.078 \pm 0.298	0.510	—	16.719	3.317
Uncert. \jmath	0.530 \pm 0.132	0.704 \pm 0.031	0.307	—	1.149	0.515
Prob.	0.450 \pm 0.024	-0.870 \pm 0.334	-2.693	—	6.656	0.507
Random	0.379 \pm 0.012	-1.139 \pm 0.014	-0.550	—	5.293	0.484
Uncert. \dagger	0.804 \pm 0.006	-0.572 \pm 0.283	-1.485	—	1.267	0.135
Rank \dagger	0.645 \pm 0.055	1.070 \pm 0.717	0.008	—	2.199	0.122
Rank	-0.519 \pm 0.529	0.730 \pm 1.632	-0.053	—	1.286	0.062
KL-Div. \dagger	0.834 \pm 0.029	0.528 \pm 0.682	-0.013	—	-1.737	0.032
Prob. \jmath	0.371 \pm 0.024	-1.503 \pm 0.841	-1.676	—	1.149	-0.192
Uncert.	0.762 \pm 0.061	-0.322 \pm 0.369	-1.467	—	-4.089	-0.817

Table 38: Acquisition performance on MIMIC Symile, presenting results for AUPRC strategies. For each metric, strategies are sorted by their descending $G_{\text{full}} \uparrow$ values. Oracle strategies are marked with \ddagger , upper-bound heuristics with \dagger and unimodal baselines with \jmath . Here, ECG is imputed by Image

Strategy	Fracture	Enl. Card.	Consolidation	Atelectasis	Edema	Mean
AUPRC \ddagger	1.631	—	100.646 \pm 71.555	—	—	33.428
AUROC \ddagger	1.570	—	94.376 \pm 64.277	—	—	30.463
KL-Div.	0.600	—	15.994 \pm 7.400	—	—	4.721
KL-Div. \dagger	0.635	—	2.975 \pm 3.762	—	—	1.163
Uncert. \jmath	0.456	—	0.652 \pm 0.902	—	—	0.692
Prob. \jmath	0.408	—	0.503 \pm 0.861	—	—	0.567
Uncert. \dagger	-0.027	—	0.199 \pm 0.327	—	—	0.542
Rank	-1.052	—	-0.692 \pm 4.909	—	—	-0.467
Uncert.	-0.225	—	-5.787 \pm 1.743	—	—	-0.999
Rank \dagger	0.943	—	-7.003 \pm 1.999	—	—	-1.214
Random	-0.336	—	-7.531 \pm 5.766	—	—	-1.297
Prob.	0.075	—	-10.442 \pm 1.040	—	—	-2.263

Strategy	Cardiomegaly	Lung Lesion	Lung Opacity	Pneumonia	Pneumothorax	Mean
AUPRC \ddagger	5.642	—	—	—	25.793 \pm 2.491	33.428
AUROC \ddagger	5.266	—	—	—	20.640 \pm 0.100	30.463
KL-Div.	0.419	—	—	—	1.872 \pm 0.563	4.721
KL-Div. \dagger	0.855	—	—	—	0.187 \pm 0.187	1.163
Uncert. \jmath	0.685	—	—	—	0.975 \pm 0.304	0.692
Prob. \jmath	0.383	—	—	—	0.975 \pm 0.304	0.567
Uncert. \dagger	0.919	—	—	—	1.080 \pm 0.443	0.542
Rank	0.340	—	—	—	-0.463 \pm 1.077	-0.467
Uncert.	0.880	—	—	—	1.136 \pm 0.162	-0.999
Rank \dagger	0.784	—	—	—	0.421 \pm 0.150	-1.214
Random	0.360	—	—	—	2.318 \pm 0.166	-1.297
Prob.	0.491	—	—	—	0.824 \pm 0.321	-2.263

Table 39: Acquisition performance on MIMIC Symile, presenting results for AUROC strategies. For each metric, strategies are sorted by their descending $G_{\text{full}} \uparrow$ values. Oracle strategies are marked with \ddagger , upper-bound heuristics with \dagger and unimodal baselines with \mathfrak{j} . Here, ECG is imputed by Lab.

Strategy	Fracture	Enl. Card.	Consolidation	Atelectasis	Edema	Mean
AUROC \ddagger	9.961 \pm 1.805	7.528 \pm 1.743	7.425	9.429 \pm 3.404	42.327	14.888
AUPRC \ddagger	9.983 \pm 1.802	7.193 \pm 1.464	6.817	8.641 \pm 3.071	36.997	14.203
KL-Div.	-0.756 \pm 0.967	0.491 \pm 1.880	1.805	1.782 \pm 0.998	12.001	2.649
KL-Div. \dagger	-0.137 \pm 1.838	0.978 \pm 0.072	0.178	0.356 \pm 0.377	0.288	0.405
Uncert. \dagger	0.271 \pm 0.133	0.892 \pm 0.394	1.249	0.377 \pm 0.354	-0.143	0.399
Random	1.112 \pm 1.486	0.492 \pm 0.457	-0.650	0.656 \pm 0.102	-1.051	0.387
Uncert. \mathfrak{j}	0.201 \pm 0.098	0.537 \pm 0.099	0.628	0.023 \pm 0.305	-0.118	0.384
Uncert.	0.078 \pm 0.296	1.509 \pm 0.221	1.945	1.538 \pm 1.059	1.277	0.335
Rank \dagger	-0.183 \pm 0.795	0.976 \pm 0.600	0.012	0.962 \pm 0.193	-1.285	0.308
Rank \mathfrak{j}	0.201 \pm 0.098	0.474 \pm 0.027	0.760	0.650 \pm 0.152	0.394	0.074
Rank	-2.489 \pm 1.558	0.182 \pm 0.173	-0.177	0.630 \pm 0.303	0.104	-0.312
Prob.	0.203 \pm 0.341	2.386 \pm 0.784	1.834	1.222 \pm 0.693	-15.313	-1.990

Strategy	Cardiomegaly	Lung Lesion	Lung Opacity	Pneumonia	Pneumothorax	Mean
AUROC \ddagger	6.604 \pm 1.266	2.091 \pm 0.714	16.140 \pm 11.342	32.694 \pm 13.014	14.683	14.888
AUPRC \ddagger	6.262 \pm 1.129	2.098 \pm 0.637	15.775 \pm 11.054	30.536 \pm 11.592	17.731	14.203
KL-Div.	2.764 \pm 0.736	0.746 \pm 0.429	0.277 \pm 0.403	4.973 \pm 2.248	2.409	2.649
KL-Div. \dagger	0.800 \pm 0.103	1.316 \pm 0.077	1.403 \pm 0.913	-1.552 \pm 1.821	0.425	0.405
Uncert. \dagger	0.121 \pm 0.119	-0.012 \pm 0.256	1.245 \pm 0.700	0.285 \pm 0.133	-0.292	0.399
Random	-0.048 \pm 0.167	0.671 \pm 0.542	1.329 \pm 0.512	2.189 \pm 1.764	-0.832	0.387
Uncert. \mathfrak{j}	0.397 \pm 0.031	0.312 \pm 0.090	1.060 \pm 0.408	0.287 \pm 0.093	0.512	0.384
Uncert.	-1.728 \pm 0.662	0.190 \pm 0.470	1.224 \pm 0.536	-0.974 \pm 2.384	-1.706	0.335
Rank \dagger	0.202 \pm 0.192	0.974 \pm 0.041	2.298 \pm 1.714	-0.790 \pm 0.663	-0.083	0.308
Rank \mathfrak{j}	-0.015 \pm 0.186	0.989 \pm 0.490	0.043 \pm 0.189	-3.264 \pm 2.220	0.513	0.074
Rank	0.337 \pm 0.091	0.246 \pm 0.433	1.594 \pm 1.021	-3.591 \pm 1.582	0.040	-0.312
Prob.	-2.784 \pm 0.997	0.475 \pm 0.982	0.657 \pm 0.299	-10.662 \pm 5.205	2.079	-1.990

Table 40: Acquisition performance on MIMIC Symile, presenting results for AUPRC strategies. For each metric, strategies are sorted by their descending $G_{\text{full}} \uparrow$ values. Oracle strategies are marked with \ddagger , upper-bound heuristics with \dagger and unimodal baselines with \mathfrak{j} . Here, ECG is imputed by Lab.

Strategy	Fracture	Enl. Card.	Consolidation	Atelectasis	Edema	Mean
AUPRC \ddagger	7.894 \pm 1.207	7.935 \pm 0.606	7.801 \pm 1.620	3.681	13.663 \pm 0.667	9.827
AUROC \ddagger	7.885 \pm 1.211	6.954 \pm 0.470	6.615 \pm 1.262	3.288	13.463 \pm 1.022	8.990
KL-Div.	-1.014 \pm 0.482	1.979 \pm 1.044	0.596 \pm 0.626	0.331	3.890 \pm 0.009	1.408
Random	0.667 \pm 1.260	0.750 \pm 0.531	0.520 \pm 0.275	0.946	0.091 \pm 0.283	0.585
Prob. \mathfrak{j}	0.398 \pm 0.120	0.796 \pm 0.109	0.747 \pm 0.126	0.861	0.424 \pm 0.202	0.581
KL-Div. \dagger	-0.038 \pm 1.091	0.843 \pm 0.368	-0.530 \pm 0.679	0.175	0.815 \pm 0.157	0.501
Rank \dagger	0.172 \pm 0.009	0.532 \pm 0.379	1.309 \pm 0.247	0.635	-0.719 \pm 0.197	0.354
Uncert.	0.079 \pm 0.427	2.413 \pm 0.318	1.197 \pm 0.340	0.817	-0.565 \pm 0.214	0.324
Uncert. \mathfrak{j}	0.398 \pm 0.120	0.641 \pm 0.487	0.114 \pm 0.434	-0.013	0.097 \pm 0.015	0.265
Uncert. \dagger	0.480 \pm 0.166	0.645 \pm 0.089	0.762 \pm 0.322	0.205	0.039 \pm 0.013	0.240
Rank	-3.557 \pm 1.533	0.231 \pm 0.154	-0.653 \pm 0.806	0.206	0.003 \pm 0.267	-0.331
Prob.	-0.291 \pm 0.867	2.492 \pm 0.270	1.173 \pm 0.256	1.229	-3.963 \pm 0.175	-0.348

Strategy	Cardiomegaly	Lung Lesion	Lung Opacity	Pneumonia	Pneumothorax	Mean
AUPRC \ddagger	5.680 \pm 1.134	3.483 \pm 1.480	7.752	29.069 \pm 4.831	11.309	9.827
AUROC \ddagger	5.751 \pm 1.190	3.462 \pm 1.498	7.124	27.891 \pm 4.714	7.471	8.990
KL-Div.	2.195 \pm 0.603	0.565 \pm 0.242	0.762	4.430 \pm 1.624	0.343	1.408
Random	-0.098 \pm 0.129	1.243 \pm 0.713	0.239	1.417 \pm 0.819	0.076	0.585
Prob. \mathfrak{j}	0.038 \pm 0.225	1.274 \pm 0.637	0.945	-0.603 \pm 1.027	0.936	0.581
KL-Div. \dagger	0.840 \pm 0.151	1.316 \pm 0.130	0.423	0.558 \pm 0.955	0.607	0.501
Rank \dagger	0.341 \pm 0.150	1.125 \pm 0.278	0.399	-0.106 \pm 0.270	-0.148	0.354
Uncert.	-1.266 \pm 0.476	0.223 \pm 0.360	0.606	-0.563 \pm 1.118	0.304	0.324
Uncert. \mathfrak{j}	0.267 \pm 0.041	0.055 \pm 0.237	-0.024	0.178 \pm 0.051	0.936	0.265
Uncert. \dagger	0.037 \pm 0.123	-0.790 \pm 0.744	0.221	0.157 \pm 0.074	0.648	0.240
Rank	0.218 \pm 0.086	1.061 \pm 1.227	0.155	-1.583 \pm 0.600	0.613	-0.331
Prob.	-2.197 \pm 0.763	0.887 \pm 0.999	0.932	-4.773 \pm 1.949	1.029	-0.348

Table 41: Acquisition performance on MIMIC Symile, presenting results for AUROC strategies. For each metric, strategies are sorted by their descending $G_{\text{full}} \uparrow$ values. Oracle strategies are marked with \ddagger , upper-bound heuristics with \dagger and unimodal baselines with \jmath . Here, ECG is imputed by Image and Lab.

Strategy	Fracture	Enl. Card.	Consolidation	Atelectasis	Edema	Mean
AUROC \ddagger	2.634 \pm 0.819	4.500 \pm 1.001	3.062 \pm 0.288	4.806 \pm 0.645	2.415 \pm 0.090	4.486
AUPRC \ddagger	2.598 \pm 0.804	4.389 \pm 0.975	2.936 \pm 0.270	4.581 \pm 0.609	2.261 \pm 0.082	4.364
KL-Div. \dagger	1.145 \pm 0.450	1.172 \pm 0.141	0.774 \pm 0.037	0.821 \pm 0.061	0.897 \pm 0.006	0.839
KL-Div.	1.120 \pm 0.452	1.200 \pm 0.150	0.771 \pm 0.037	0.812 \pm 0.065	0.894 \pm 0.006	0.838
Rank \dagger	1.120 \pm 0.318	1.107 \pm 0.131	0.858 \pm 0.021	0.776 \pm 0.057	0.916 \pm 0.007	0.836
Uncert.	1.063 \pm 0.392	0.820 \pm 0.140	0.638 \pm 0.072	0.358 \pm 0.070	0.673 \pm 0.013	0.551
Uncert. \jmath	0.785 \pm 0.249	0.509 \pm 0.088	0.499 \pm 0.058	0.468 \pm 0.062	0.604 \pm 0.009	0.544
Uncert. \dagger	1.047 \pm 0.381	0.787 \pm 0.136	0.632 \pm 0.069	0.338 \pm 0.071	0.675 \pm 0.013	0.537
Rank	0.126 \pm 0.141	0.517 \pm 0.086	0.489 \pm 0.027	0.507 \pm 0.059	0.504 \pm 0.009	0.473
Prob. \jmath	0.097 \pm 0.243	0.594 \pm 0.105	0.528 \pm 0.047	0.435 \pm 0.077	0.556 \pm 0.012	0.466
Prob.	0.933 \pm 0.302	0.676 \pm 0.106	0.508 \pm 0.038	0.111 \pm 0.120	0.349 \pm 0.014	0.438
Random	0.487 \pm 0.212	0.363 \pm 0.126	0.463 \pm 0.043	0.118 \pm 0.177	0.458 \pm 0.013	0.427

Strategy	Cardiomegaly	Lung Lesion	Lung Opacity	Pneumonia	Pneumothorax	Mean
AUROC \ddagger	2.675 \pm 0.236	3.710 \pm 0.511	7.949 \pm 2.090	4.600 \pm 0.301	8.512 \pm 1.512	4.486
AUPRC \ddagger	2.558 \pm 0.225	3.571 \pm 0.497	7.620 \pm 2.027	4.248 \pm 0.277	8.875 \pm 1.550	4.364
KL-Div. \dagger	0.897 \pm 0.010	0.549 \pm 0.239	0.504 \pm 0.303	0.902 \pm 0.021	0.724 \pm 0.092	0.839
KL-Div.	0.865 \pm 0.013	0.617 \pm 0.239	0.474 \pm 0.345	0.927 \pm 0.022	0.704 \pm 0.090	0.838
Rank \dagger	0.951 \pm 0.011	0.578 \pm 0.154	0.661 \pm 0.122	0.912 \pm 0.025	0.485 \pm 0.086	0.836
Uncert.	0.205 \pm 0.029	0.496 \pm 0.283	0.436 \pm 0.127	0.701 \pm 0.034	0.121 \pm 0.074	0.551
Uncert. \jmath	0.324 \pm 0.015	0.517 \pm 0.183	0.569 \pm 0.102	0.575 \pm 0.036	0.592 \pm 0.127	0.544
Uncert. \dagger	0.214 \pm 0.031	0.460 \pm 0.273	0.414 \pm 0.121	0.696 \pm 0.035	0.107 \pm 0.073	0.537
Rank	0.469 \pm 0.018	0.458 \pm 0.105	0.886 \pm 0.236	0.483 \pm 0.030	0.287 \pm 0.206	0.473
Prob. \jmath	0.654 \pm 0.014	0.348 \pm 0.250	0.256 \pm 0.120	0.604 \pm 0.017	0.591 \pm 0.127	0.466
Prob.	0.188 \pm 0.025	0.518 \pm 0.303	0.125 \pm 0.121	0.178 \pm 0.041	0.789 \pm 0.051	0.438
Random	0.486 \pm 0.023	0.736 \pm 0.238	0.351 \pm 0.077	0.420 \pm 0.038	0.392 \pm 0.071	0.427

Table 42: Acquisition performance on MIMIC Symile, presenting results for AUPRC strategies. For each metric, strategies are sorted by their descending $G_{\text{full}} \uparrow$ values. Oracle strategies are marked with \ddagger , upper-bound heuristics with \dagger and unimodal baselines with \jmath . Here, ECG is imputed by Image and Lab.

Strategy	Fracture	Enl. Card.	Consolidation	Atelectasis	Edema	Mean
AUPRC \ddagger	1.578 \pm 0.119	3.454 \pm 0.465	3.604 \pm 0.479	3.295 \pm 0.414	2.989 \pm 0.181	3.703
AUROC \ddagger	1.586 \pm 0.119	3.216 \pm 0.435	3.447 \pm 0.450	3.358 \pm 0.427	2.886 \pm 0.172	3.449
KL-Div. \dagger	0.634 \pm 0.094	1.070 \pm 0.078	0.807 \pm 0.038	0.702 \pm 0.052	0.904 \pm 0.017	0.814
KL-Div.	0.621 \pm 0.092	1.087 \pm 0.082	0.815 \pm 0.041	0.702 \pm 0.061	0.903 \pm 0.017	0.812
Rank \dagger	0.782 \pm 0.060	1.014 \pm 0.057	0.873 \pm 0.054	0.707 \pm 0.076	0.923 \pm 0.019	0.800
Prob. \jmath	0.435 \pm 0.052	0.502 \pm 0.063	0.684 \pm 0.050	0.499 \pm 0.081	0.660 \pm 0.015	0.585
Uncert. \jmath	0.456 \pm 0.053	0.596 \pm 0.072	0.377 \pm 0.054	0.287 \pm 0.026	0.521 \pm 0.017	0.444
Uncert.	0.572 \pm 0.081	0.851 \pm 0.087	0.533 \pm 0.061	0.188 \pm 0.056	0.602 \pm 0.018	0.441
Uncert. \dagger	0.565 \pm 0.081	0.826 \pm 0.085	0.531 \pm 0.060	0.175 \pm 0.056	0.601 \pm 0.018	0.431
Rank	0.182 \pm 0.091	0.481 \pm 0.066	0.422 \pm 0.074	0.514 \pm 0.052	0.469 \pm 0.015	0.430
Random	0.374 \pm 0.078	0.367 \pm 0.062	0.432 \pm 0.083	-0.072 \pm 0.281	0.430 \pm 0.021	0.347
Prob.	0.577 \pm 0.055	0.687 \pm 0.059	0.484 \pm 0.052	-0.037 \pm 0.152	0.382 \pm 0.026	0.336

Strategy	Cardiomegaly	Lung Lesion	Lung Opacity	Pneumonia	Pneumothorax	Mean
AUPRC \ddagger	2.445 \pm 0.148	2.303 \pm 0.239	4.150 \pm 0.421	5.900 \pm 0.609	7.316 \pm 0.974	3.703
AUROC \ddagger	2.374 \pm 0.128	2.362 \pm 0.252	4.235 \pm 0.437	5.714 \pm 0.594	5.316 \pm 0.704	3.449
KL-Div. \dagger	0.856 \pm 0.016	0.749 \pm 0.133	0.746 \pm 0.062	0.952 \pm 0.058	0.714 \pm 0.062	0.814
KL-Div.	0.832 \pm 0.018	0.772 \pm 0.124	0.707 \pm 0.056	0.978 \pm 0.061	0.707 \pm 0.067	0.812
Rank \dagger	0.938 \pm 0.014	0.690 \pm 0.094	0.702 \pm 0.072	0.914 \pm 0.049	0.461 \pm 0.074	0.800
Prob. \jmath	0.674 \pm 0.014	0.517 \pm 0.139	0.403 \pm 0.072	0.655 \pm 0.032	0.821 \pm 0.050	0.585
Uncert. \jmath	0.279 \pm 0.017	0.272 \pm 0.065	0.400 \pm 0.050	0.436 \pm 0.036	0.820 \pm 0.050	0.444
Uncert.	0.154 \pm 0.029	0.123 \pm 0.086	0.334 \pm 0.062	0.603 \pm 0.059	0.445 \pm 0.061	0.441
Uncert. \dagger	0.161 \pm 0.031	0.098 \pm 0.098	0.321 \pm 0.066	0.598 \pm 0.057	0.438 \pm 0.061	0.431
Rank	0.426 \pm 0.015	0.559 \pm 0.123	0.463 \pm 0.081	0.378 \pm 0.055	0.401 \pm 0.059	0.430
Random	0.435 \pm 0.016	0.368 \pm 0.178	0.362 \pm 0.119	0.325 \pm 0.048	0.447 \pm 0.078	0.347
Prob.	0.137 \pm 0.036	-0.030 \pm 0.151	0.176 \pm 0.123	0.112 \pm 0.108	0.877 \pm 0.029	0.336

F Results for MIMIC HAIM

Table 43: Acquisition performance on MIMIC HAIM, presenting results for AUROC strategies. Acquisition strategies are sorted by their descending mean. Oracle strategies are marked with ‡, upper-bound heuristics with † and unimodal baselines with ¡.

Strategy	Fracture	Enl. Card.	Consolidation	Atelectasis	Edema	Mean
AUROC ‡	5.121 ±1.873	6.802 ±2.953	4.228 ±1.374	5.862 ±0.933	3.435 ±0.792	4.602
AUPRC ‡	5.110 ±1.829	6.498 ±2.803	4.099 ±1.321	5.730 ±0.915	3.224 ±0.737	4.456
Rank †	0.853 ±0.107	0.684 ±0.056	0.706 ±0.034	0.676 ±0.087	0.714 ±0.041	0.723
KL-Div. †	0.842 ±0.154	0.558 ±0.187	0.673 ±0.054	0.518 ±0.093	0.708 ±0.025	0.608
Uncert.	0.022 ±0.463	0.647 ±0.108	0.880 ±0.241	0.503 ±0.123	0.493 ±0.056	0.554
Uncert. †	0.429 ±0.264	0.647 ±0.107	0.729 ±0.099	0.332 ±0.116	0.555 ±0.057	0.538
Random	1.005 ±0.367	0.143 ±0.289	0.470 ±0.045	0.546 ±0.096	0.510 ±0.025	0.526
Prob.	0.318 ±0.280	0.657 ±0.105	0.761 ±0.133	0.620 ±0.082	0.578 ±0.051	0.494
KL-Div	0.827 ±0.213	0.561 ±0.142	0.488 ±0.053	0.505 ±0.109	0.459 ±0.074	0.465
Prob. ¡	0.244 ±0.302	0.615 ±0.116	0.550 ±0.045	0.641 ±0.065	0.580 ±0.042	0.457
Uncert. ¡	0.492 ±0.209	0.598 ±0.038	0.486 ±0.061	0.244 ±0.163	0.525 ±0.032	0.452
Rank	0.530 ±0.685	-0.048 ±0.305	0.311 ±0.079	0.429 ±0.150	0.485 ±0.032	0.391

Strategy	Cardiomegaly	Lung Lesion	Lung Opacity	Pneumonia	Pneumothorax	Mean
AUROC ‡	4.246 ±0.416	1.912 ±0.205	5.429 ±1.539	2.864 ±0.716	6.119 ±2.055	4.602
AUPRC ‡	4.112 ±0.389	1.956 ±0.208	5.277 ±1.502	2.721 ±0.684	5.833 ±1.959	4.456
Rank †	0.756 ±0.027	0.751 ±0.166	0.898 ±0.051	0.738 ±0.022	0.455 ±0.155	0.723
KL-Div. †	0.609 ±0.059	0.674 ±0.148	0.801 ±0.086	0.775 ±0.019	-0.083 ±0.370	0.608
Uncert.	0.561 ±0.042	0.744 ±0.146	0.541 ±0.050	0.587 ±0.013	0.558 ±0.102	0.554
Uncert. †	0.554 ±0.047	0.638 ±0.131	0.330 ±0.127	0.720 ±0.019	0.446 ±0.110	0.538
Random	0.482 ±0.022	0.703 ±0.129	0.534 ±0.038	0.553 ±0.009	0.319 ±0.136	0.526
Prob.	0.618 ±0.041	0.601 ±0.048	0.636 ±0.066	0.591 ±0.023	-0.435 ±0.322	0.494
KL-Div	0.385 ±0.058	0.362 ±0.161	0.418 ±0.109	0.499 ±0.046	0.140 ±0.290	0.465
Prob. ¡	0.619 ±0.043	0.508 ±0.086	0.754 ±0.050	0.575 ±0.025	-0.513 ±0.421	0.457
Uncert. ¡	0.460 ±0.038	0.511 ±0.063	0.396 ±0.095	0.539 ±0.023	0.272 ±0.185	0.452
Rank	0.305 ±0.061	0.422 ±0.157	0.306 ±0.194	0.519 ±0.044	0.653 ±0.050	0.391

Table 44: Acquisition performance on MIMIC HAIM, presenting results for AUPRC strategies. Acquisition strategies are sorted by their descending mean. Oracle strategies are marked with ‡, upper-bound heuristics with † and unimodal baselines with ¡.

Strategy	Fracture	Enl. Card.	Consolidation	Atelectasis	Edema	Mean
AUPRC ‡	1.490 ±0.249	3.181 ±0.283	3.084 ±0.331	2.738 ±0.363	2.782 ±0.349	3.087
AUROC ‡	1.486 ±0.249	3.086 ±0.269	3.009 ±0.315	2.739 ±0.357	2.719 ±0.332	2.982
Rank †	1.014 ±0.085	0.721 ±0.068	0.541 ±0.112	0.958 ±0.097	0.769 ±0.031	0.754
Prob. ¡	0.480 ±0.112	0.713 ±0.046	0.755 ±0.054	0.589 ±0.053	0.752 ±0.017	0.701
Prob.	0.584 ±0.111	0.672 ±0.041	0.807 ±0.075	0.480 ±0.018	0.754 ±0.017	0.686
KL-Div. †	0.967 ±0.098	0.652 ±0.076	0.435 ±0.167	0.847 ±0.065	0.717 ±0.030	0.662
Uncert. †	0.842 ±0.068	0.592 ±0.081	0.605 ±0.047	0.425 ±0.084	0.611 ±0.057	0.587
Uncert.	0.799 ±0.056	0.540 ±0.082	0.680 ±0.071	0.353 ±0.047	0.584 ±0.030	0.570
Random	0.941 ±0.107	0.404 ±0.060	0.455 ±0.057	0.452 ±0.180	0.546 ±0.024	0.561
KL-Div	0.889 ±0.097	0.578 ±0.054	0.301 ±0.163	0.655 ±0.110	0.518 ±0.030	0.516
Uncert. ¡	0.920 ±0.131	0.556 ±0.082	0.409 ±0.085	0.365 ±0.011	0.487 ±0.053	0.479
Rank	0.890 ±0.120	0.337 ±0.081	0.247 ±0.115	0.706 ±0.052	0.474 ±0.023	0.456

Strategy	Cardiomegaly	Lung Lesion	Lung Opacity	Pneumonia	Pneumothorax	Mean
AUPRC ‡	4.751 ±0.276	1.878 ±0.237	2.730 ±0.219	3.910 ±0.892	4.329 ±0.483	3.087
AUROC ‡	4.663 ±0.260	1.791 ±0.257	2.772 ±0.227	3.693 ±0.836	3.860 ±0.397	2.982
Rank †	0.636 ±0.071	0.725 ±0.153	0.861 ±0.144	0.683 ±0.035	0.630 ±0.042	0.754
Prob. ¡	0.795 ±0.076	0.806 ±0.109	0.855 ±0.043	0.725 ±0.021	0.536 ±0.033	0.701
Prob.	0.808 ±0.057	0.764 ±0.115	0.737 ±0.030	0.736 ±0.025	0.518 ±0.040	0.686
KL-Div. †	0.374 ±0.137	0.688 ±0.130	0.660 ±0.196	0.699 ±0.035	0.575 ±0.039	0.662
Uncert. †	0.599 ±0.059	0.430 ±0.127	0.505 ±0.173	0.732 ±0.031	0.530 ±0.043	0.587
Uncert.	0.641 ±0.052	0.450 ±0.120	0.561 ±0.092	0.621 ±0.030	0.468 ±0.030	0.570
Random	0.504 ±0.042	0.606 ±0.151	0.572 ±0.086	0.569 ±0.022	0.556 ±0.022	0.561
KL-Div	0.248 ±0.124	0.573 ±0.133	0.413 ±0.218	0.399 ±0.089	0.588 ±0.043	0.516
Uncert. ¡	0.372 ±0.063	0.274 ±0.111	0.359 ±0.220	0.496 ±0.042	0.550 ±0.036	0.479
Rank	0.167 ±0.117	0.216 ±0.119	0.494 ±0.147	0.490 ±0.079	0.538 ±0.024	0.456

Table 45: Acquisition performance on MIMIC HAIM, presenting results for AUROC strategies. Acquisition strategies are sorted by their descending mean. Oracle strategies are marked with ‡, upper-bound heuristics with † and unimodal baselines with j. Here, Image is imputed by Lab.

Strategy	Fracture	Enl. Card.	Consolidation	Atelectasis	Edema	Mean
AUROC ‡	4.447 ± 3.050	3.381 ± 1.055	2.055 ± 0.185	6.068 ± 1.280	1.710 ± 0.036	3.810
AUPRC ‡	4.300 ± 2.905	3.286 ± 1.040	2.016 ± 0.189	5.980 ± 1.275	1.592 ± 0.033	3.692
Rank †	0.902 ± 0.059	0.704 ± 0.044	0.667 ± 0.035	0.575 ± 0.139	0.698 ± 0.010	0.671
Uncert.	0.710 ± 0.087	0.730 ± 0.091	0.548 ± 0.029	0.597 ± 0.215	0.587 ± 0.012	0.625
Uncert. †	0.908 ± 0.185	0.768 ± 0.035	0.641 ± 0.022	0.301 ± 0.207	0.709 ± 0.008	0.610
Random	1.112 ± 0.371	0.483 ± 0.041	0.509 ± 0.015	0.556 ± 0.138	0.542 ± 0.008	0.582
Rank	1.530 ± 0.782	0.045 ± 0.280	0.418 ± 0.037	0.203 ± 0.164	0.450 ± 0.021	0.497
KL-Div. †	1.002 ± 0.142	0.425 ± 0.184	0.623 ± 0.061	0.299 ± 0.113	0.687 ± 0.022	0.476
Prob.	0.514 ± 0.051	0.773 ± 0.153	0.560 ± 0.026	0.768 ± 0.113	0.590 ± 0.010	0.445
Uncert. j	0.512 ± 0.247	0.635 ± 0.040	0.491 ± 0.032	0.086 ± 0.287	0.587 ± 0.015	0.438
KL-Div	0.686 ± 0.060	0.579 ± 0.031	0.463 ± 0.054	0.412 ± 0.085	0.539 ± 0.022	0.416
Prob. j	0.109 ± 0.371	0.759 ± 0.146	0.533 ± 0.026	0.739 ± 0.095	0.592 ± 0.010	0.392

Strategy	Cardiomegaly	Lung Lesion	Lung Opacity	Pneumonia	Pneumothorax	Mean
AUROC ‡	3.257 ± 0.286	2.139 ± 0.317	3.951 ± 0.558	1.968 ± 0.068	9.124 ± 3.961	3.810
AUPRC ‡	3.207 ± 0.286	2.124 ± 0.312	3.854 ± 0.564	1.870 ± 0.071	8.693 ± 3.777	3.692
Rank †	0.671 ± 0.017	0.808 ± 0.318	0.898 ± 0.066	0.711 ± 0.015	0.081 ± 0.265	0.671
Uncert.	0.620 ± 0.047	0.668 ± 0.165	0.581 ± 0.057	0.591 ± 0.015	0.613 ± 0.206	0.625
Uncert. †	0.558 ± 0.042	0.625 ± 0.057	0.456 ± 0.097	0.734 ± 0.020	0.400 ± 0.221	0.610
Random	0.482 ± 0.030	0.941 ± 0.176	0.518 ± 0.049	0.558 ± 0.010	0.119 ± 0.262	0.582
Rank	0.233 ± 0.093	0.339 ± 0.349	0.468 ± 0.090	0.498 ± 0.017	0.783 ± 0.075	0.497
KL-Div. †	0.440 ± 0.063	0.714 ± 0.312	0.734 ± 0.096	0.775 ± 0.021	-0.936 ± 0.646	0.476
Prob.	0.698 ± 0.059	0.544 ± 0.099	0.693 ± 0.063	0.600 ± 0.020	-1.295 ± 0.522	0.445
Uncert. j	0.434 ± 0.052	0.568 ± 0.074	0.394 ± 0.109	0.557 ± 0.023	0.114 ± 0.373	0.438
KL-Div	0.321 ± 0.083	0.458 ± 0.273	0.342 ± 0.129	0.552 ± 0.027	-0.187 ± 0.576	0.416
Prob. j	0.693 ± 0.057	0.541 ± 0.162	0.790 ± 0.054	0.589 ± 0.018	-1.427 ± 0.750	0.392

Table 46: Acquisition performance on MIMIC HAIM, presenting results for AUPRC strategies. Acquisition strategies are sorted by their descending mean. Oracle strategies are marked with ‡, upper-bound heuristics with † and unimodal baselines with j. Here, Image is imputed by Lab.

Strategy	Fracture	Enl. Card.	Consolidation	Atelectasis	Edema	Mean
AUPRC ‡	1.490 ± 0.249	3.177 ± 0.420	3.038 ± 0.399	2.586	1.812 ± 0.037	2.790
AUROC ‡	1.486 ± 0.249	3.107 ± 0.401	2.976 ± 0.381	2.585	1.800 ± 0.035	2.757
Rank †	1.014 ± 0.085	0.632 ± 0.084	0.498 ± 0.128	0.773	0.685 ± 0.019	0.706
Prob. j	0.480 ± 0.112	0.714 ± 0.071	0.749 ± 0.063	0.483	0.715 ± 0.011	0.686
Prob.	0.584 ± 0.111	0.674 ± 0.058	0.796 ± 0.087	0.455	0.710 ± 0.011	0.662
Uncert. †	0.842 ± 0.068	0.790 ± 0.040	0.624 ± 0.054	0.575	0.776 ± 0.014	0.660
Uncert.	0.799 ± 0.056	0.683 ± 0.085	0.700 ± 0.081	0.263	0.665 ± 0.022	0.615
Random	0.941 ± 0.107	0.429 ± 0.088	0.464 ± 0.067	0.590	0.595 ± 0.012	0.615
KL-Div. †	0.967 ± 0.098	0.523 ± 0.091	0.372 ± 0.195	0.717	0.664 ± 0.033	0.579
Uncert. j	0.920 ± 0.131	0.700 ± 0.096	0.448 ± 0.096	0.387	0.651 ± 0.025	0.553
KL-Div	0.889 ± 0.097	0.540 ± 0.066	0.260 ± 0.194	0.456	0.586 ± 0.031	0.478
Rank	0.890 ± 0.120	0.288 ± 0.118	0.229 ± 0.139	0.650	0.459 ± 0.026	0.416

Strategy	Cardiomegaly	Lung Lesion	Lung Opacity	Pneumonia	Pneumothorax	Mean
AUPRC ‡	4.700 ± 0.289	1.725 ± 0.306	2.830 ± 0.264	2.510 ± 0.170	4.037 ± 0.525	2.790
AUROC ‡	4.648 ± 0.297	1.734 ± 0.314	2.880 ± 0.274	2.387 ± 0.154	3.966 ± 0.508	2.757
Rank †	0.463 ± 0.068	0.834 ± 0.425	0.903 ± 0.193	0.661 ± 0.030	0.601 ± 0.047	0.706
Prob. j	0.944 ± 0.092	0.671 ± 0.071	0.850 ± 0.058	0.732 ± 0.022	0.523 ± 0.031	0.686
Prob.	0.920 ± 0.072	0.556 ± 0.160	0.718 ± 0.033	0.725 ± 0.030	0.485 ± 0.043	0.662
Uncert. †	0.490 ± 0.057	0.666 ± 0.066	0.495 ± 0.235	0.726 ± 0.038	0.615 ± 0.050	0.660
Uncert.	0.655 ± 0.077	0.656 ± 0.200	0.574 ± 0.124	0.638 ± 0.037	0.519 ± 0.034	0.615
Random	0.462 ± 0.059	0.958 ± 0.269	0.576 ± 0.117	0.580 ± 0.019	0.553 ± 0.031	0.615
KL-Div. †	0.054 ± 0.147	0.651 ± 0.392	0.621 ± 0.266	0.731 ± 0.039	0.493 ± 0.045	0.579
Uncert. j	0.293 ± 0.089	0.529 ± 0.084	0.416 ± 0.296	0.544 ± 0.042	0.643 ± 0.024	0.553
KL-Div	0.064 ± 0.176	0.384 ± 0.277	0.385 ± 0.295	0.540 ± 0.044	0.680 ± 0.038	0.478
Rank	-0.025 ± 0.160	0.216 ± 0.282	0.456 ± 0.198	0.478 ± 0.034	0.518 ± 0.025	0.416

Table 47: Acquisition performance on MIMIC HAIM, presenting results for AUROC strategies. Acquisition strategies are sorted by their descending mean. Oracle strategies are marked with ‡, upper-bound heuristics with † and unimodal baselines with ¡. Here, Lab is imputed by Image.

Strategy	Fracture	Enl. Card.	Consolidation	Atelectasis	Edema	Mean
AUROC ‡	6.244 ± 0.851	12.503 ± 7.484	11.469 ± 3.810	5.604 ± 1.451	5.899 ± 1.530	6.851
AUPRC ‡	6.459 ± 1.274	11.851 ± 7.101	11.044 ± 3.674	5.418 ± 1.392	5.555 ± 1.406	6.617
Rank †	0.773 ± 0.299	0.649 ± 0.136	0.836 ± 0.030	0.802 ± 0.076	0.736 ± 0.102	0.796
KL-Div. †	0.575 ± 0.311	0.780 ± 0.402	0.842 ± 0.049	0.792 ± 0.088	0.737 ± 0.054	0.770
Prob.	-0.010 ± 0.798	0.463 ± 0.079	1.433 ± 0.393	0.435 ± 0.086	0.560 ± 0.129	0.551
KL-Div	1.063 ± 0.606	0.531 ± 0.397	0.572 ± 0.156	0.622 ± 0.223	0.345 ± 0.175	0.519
Prob. ¡	0.470 ± 0.594	0.375 ± 0.158	0.608 ± 0.200	0.519 ± 0.069	0.563 ± 0.105	0.511
Uncert.	-1.124 ± 0.961	0.508 ± 0.248	1.986 ± 0.840	0.385 ± 0.063	0.359 ± 0.123	0.492
Uncert. ¡	0.460 ± 0.449	0.535 ± 0.076	0.467 ± 0.283	0.441 ± 0.053	0.438 ± 0.063	0.458
Random	0.826 ± 0.879	-0.425 ± 0.748	0.337 ± 0.193	0.534 ± 0.143	0.464 ± 0.056	0.435
Uncert. †	-0.370 ± 0.158	0.445 ± 0.274	1.020 ± 0.440	0.371 ± 0.065	0.334 ± 0.084	0.416
Rank	-1.136 ± 0.350	-0.202 ± 0.707	-0.044 ± 0.241	0.712 ± 0.244	0.535 ± 0.072	0.180

Strategy	Cardiomegaly	Lung Lesion	Lung Opacity	Pneumonia	Pneumothorax	Mean
AUROC ‡	5.483 ± 0.647	1.730 ± 0.268	9.123 ± 5.217	7.345 ± 3.084	3.113 ± 0.375	6.851
AUPRC ‡	5.244 ± 0.606	1.821 ± 0.296	8.835 ± 5.093	6.974 ± 2.986	2.973 ± 0.359	6.617
Rank †	0.861 ± 0.023	0.706 ± 0.194	0.896 ± 0.088	0.873 ± 0.035	0.830 ± 0.017	0.796
KL-Div. †	0.821 ± 0.038	0.641 ± 0.142	0.969 ± 0.173	0.774 ± 0.071	0.771 ± 0.016	0.770
Prob.	0.518 ± 0.032	0.646 ± 0.037	0.492 ± 0.164	0.543 ± 0.113	0.425 ± 0.017	0.551
KL-Div	0.465 ± 0.074	0.286 ± 0.213	0.608 ± 0.194	0.233 ± 0.147	0.467 ± 0.028	0.519
Prob. ¡	0.526 ± 0.049	0.482 ± 0.103	0.664 ± 0.114	0.508 ± 0.151	0.400 ± 0.018	0.511
Uncert.	0.487 ± 0.070	0.805 ± 0.241	0.441 ± 0.090	0.570 ± 0.037	0.503 ± 0.028	0.492
Uncert. ¡	0.492 ± 0.057	0.466 ± 0.100	0.401 ± 0.220	0.454 ± 0.058	0.430 ± 0.020	0.458
Random	0.482 ± 0.033	0.512 ± 0.145	0.575 ± 0.056	0.530 ± 0.018	0.519 ± 0.024	0.435
Uncert. †	0.550 ± 0.096	0.648 ± 0.244	0.017 ± 0.360	0.652 ± 0.013	0.492 ± 0.038	0.416
Rank	0.395 ± 0.065	0.489 ± 0.114	-0.098 ± 0.659	0.626 ± 0.318	0.522 ± 0.033	0.180

Table 48: Acquisition performance on MIMIC HAIM, presenting results for AUPRC strategies. Acquisition strategies are sorted by their descending mean. Oracle strategies are marked with ‡, upper-bound heuristics with † and unimodal baselines with ¡. Here, Lab is imputed by Image.

Strategy	Fracture	Enl. Card.	Consolidation	Atelectasis	Edema	Mean
AUPRC ‡	—	3.188 ± 0.307	3.312 ± 0.007	2.814 ± 0.615	4.169 ± 0.490	4.011
AUROC ‡	—	3.047 ± 0.278	3.175 ± 0.105	2.815 ± 0.605	4.031 ± 0.474	3.751
Rank †	—	0.881 ± 0.081	0.758 ± 0.195	1.051 ± 0.050	0.889 ± 0.035	0.811
KL-Div. †	—	0.884 ± 0.047	0.749 ± 0.053	0.912 ± 0.012	0.792 ± 0.043	0.776
Prob. ¡	—	0.712 ± 0.031	0.782 ± 0.104	0.642 ± 0.002	0.806 ± 0.028	0.726
Prob.	—	0.668 ± 0.054	0.858 ± 0.163	0.492 ± 0.022	0.816 ± 0.022	0.723
KL-Div	—	0.647 ± 0.098	0.508 ± 0.078	0.755 ± 0.079	0.419 ± 0.032	0.489
Rank	—	0.424 ± 0.082	0.335 ± 0.044	0.734 ± 0.076	0.495 ± 0.042	0.485
Random	—	0.361 ± 0.069	0.406 ± 0.089	0.383 ± 0.287	0.478 ± 0.045	0.472
Uncert. †	—	0.237 ± 0.075	0.508 ± 0.005	0.350 ± 0.067	0.376 ± 0.071	0.467
Uncert.	—	0.282 ± 0.094	0.580 ± 0.160	0.398 ± 0.022	0.469 ± 0.034	0.461
Uncert. ¡	—	0.298 ± 0.039	0.214 ± 0.113	0.354 ± 0.001	0.254 ± 0.039	0.294

Strategy	Cardiomegaly	Lung Lesion	Lung Opacity	Pneumonia	Pneumothorax	Mean
AUPRC ‡	4.828 ± 0.574	1.969 ± 0.352	2.430 ± 0.426	8.578 ± 2.467	4.816 ± 0.981	4.011
AUROC ‡	4.685 ± 0.513	1.825 ± 0.393	2.448 ± 0.414	8.047 ± 2.348	3.683 ± 0.691	3.751
Rank †	0.895 ± 0.034	0.660 ± 0.093	0.735 ± 0.039	0.756 ± 0.125	0.678 ± 0.081	0.811
KL-Div. †	0.854 ± 0.056	0.711 ± 0.032	0.776 ± 0.034	0.595 ± 0.055	0.712 ± 0.014	0.776
Prob. ¡	0.571 ± 0.058	0.887 ± 0.166	0.870 ± 0.029	0.703 ± 0.060	0.559 ± 0.076	0.726
Prob.	0.640 ± 0.029	0.889 ± 0.138	0.794 ± 0.073	0.773 ± 0.051	0.574 ± 0.078	0.723
KL-Div	0.524 ± 0.084	0.687 ± 0.135	0.495 ± 0.131	-0.069 ± 0.185	0.434 ± 0.051	0.489
Rank	0.455 ± 0.084	0.216 ± 0.127	0.607 ± 0.038	0.533 ± 0.382	0.570 ± 0.049	0.485
Random	0.568 ± 0.050	0.395 ± 0.110	0.561 ± 0.044	0.535 ± 0.077	0.560 ± 0.029	0.472
Uncert. †	0.762 ± 0.089	0.289 ± 0.175	0.537 ± 0.099	0.752 ± 0.052	0.389 ± 0.036	0.467
Uncert.	0.621 ± 0.069	0.326 ± 0.134	0.523 ± 0.042	0.566 ± 0.018	0.381 ± 0.036	0.461
Uncert. ¡	0.489 ± 0.062	0.121 ± 0.130	0.187 ± 0.017	0.333 ± 0.042	0.396 ± 0.034	0.294